UNITED STATES DEPARTMENT OF THE INTERIOR

GEOLOGICAL SURVEY

The stable isotope geochemistry of acid-sulfate alteration and vein forming alunite

by

Robert O. Rye[1]
Philip M. Bethke[2]
Michael D. Wasserman[1]

Open-File Report 91-257

1) Denver, CO 80225
2) Reston, VA 22092

ABSTRACT

Acid-sulfate wall-rock alteration, characterized by the assemblage alunite+kaolinite+quartz±pyrite, results from base-leaching by fluids concentrated in H_2SO_4. Requisite amounts of H_2SO_4 can be generated by different mechanisms in 3 principal geological environments: 1) by atmospheric oxidation of sulfides in the *supergene* environment, 2) by atmospheric oxidation at the water table in the *steam-heated* environment, of H_2S released by deeper, boiling fluids, and 3) by the disproportionation of magmatic SO_2 to H_2S and H_2SO_4 during condensation of a magmatic vapor plume at intermediate depths in *magmatic-hydrothermal* environments in silicic and andesitic volcanic terrains. In addition, coarse vein alunite may form in a *magmatic-steam* environment from rapid release of a SO_2-rich magmatic vapor phase at high temperature and low pressure or from the oxidation of a more reduced magmatic vapor by entrained atmospheric oxygen in the carapace of a volcanic edifice.

Alunite [$KAl_3(SO_4)_2(OH)_6$] contains four stable isotope sites and complete analyses (δD, $\delta^{18}O_{SO_4}$, $\delta^{18}O_{OH}$, and $\delta^{34}S$) are now possible. Except for $\delta^{18}O_{OH}$ in *magmatic-hydrothermal* alunites, primary values are usually retained. In cooperation with many colleagues, over 500 measurements have been made on nearly 200 samples of alunite and associated minerals from 20 localities and 55 additional analyses have been taken from the literature. These complete stable isotope analyses permit recognition of environments of formation and provide information on origins of components, processes (including rates), physical-chemical environments, and temperatures of formation.

Supergene acid-sulfate alteration may form over any sulfide zone when it is raised above the water table by tectonics or exposed by erosion. It may overprint earlier acid-sulfate assemblages, particularly the *magmatic-hydrothermal* assemblages which are pyrite-rich such as at El Salvador, Chile; Rodalquilar, Spain and Goldfield, Nevada. *Supergene* alunite has $\delta^{34}S$ virtually identical to precursor sulfides unless bacteriogenic reduction of aqueous sulfate takes place in standing pools of water. δD values will be close to that of local meteoric water unless extensive evaporation occurs, and δD-$\delta^{18}O_{OH}$ of *supergene* alunites from a range of latitudes fall in a broad zone parallel to the *meteoric water line* much the way δD and $\delta^{18}O$ values of associated halloysite/kaolinite fall near the *kaolinite line* of Savin and Epstein (1970). $\delta^{18}O_{SO_4}$ values are kinetically controlled and will reflect the hydrogeochemistry of the environment. $\Delta^{18}O_{SO_4\text{-}OH}$ values are grossly out of equilibrium and negative values are usually definitive of a *supergene* origin.

In *steam-heated* environments, such as those at the Tolfa district, Italy and Marysvale, Utah, and numerous modern geothermal systems, acid-sulfate alteration zones are characterized by pronounced vertical zoning. Such acid-sulfate alteration may occur over adularia-sericite type base- and precious-metal ore deposits such as at Buckskin, Nevada. Initial $\delta^{18}O_{SO_4}$ and $\delta^{34}S$ values are kinetically controlled, but $\delta^{18}O_{SO_4}$ values usually reach equilibrium with fluids, and even $\delta^{34}S$ values may reflect partial exchange with H_2S where the residence time of aqueous sulfate are sufficient. Most alunites of *steam-heated* origin have $\delta^{34}S$ the same as precursor H_2S (and as related sulfides, if present) and δD the same as local meteoric water. In the samples analyzed, $\delta^{18}O_{SO_4}$ and $\delta^{18}O_{OH}$ appear to reflect a close approach to equilibrium with the fluid, and $\Delta^{18}O_{SO_4\text{-}OH}$ values give depositional temperatures of 90° to 160°C. The $\delta^{18}O_{SO_4}$ and $\delta^{18}O_{OH}$ values reflect the degree of exchange of the meteoric fluids with wall rock. Coeval kaolinites typically have $\delta^{18}O_{SO_4}$ and δD to the left of the *kaolinite line.*

Magmatic-hydrothermal acid-sulfate environments in near-surface epithermal deposits such as Summitville, Colorado; Julcani, Peru and Red Mountain, Lake City, Colorado are characterized by vertical aspect and horizontal zoning, the presence of coeval pyrite and possibly PO_4 analogs of alunite, and zunyite, and later gold, pyrite and enargite. Acid-sulfate alteration assemblages also occur as late stages in the porphyry-copper deposit at El Salvador, Chile. In the examples studied, *magmatic-hydrothermal* alunites have δD and initial $\delta^{18}O_{OH}$ close to values for magmatic water. $\delta^{34}S$ values are 16 to 28 ‰ larger than those for associated pyrite, reflecting equilibrium between aqueous H_2S and SO_4 formed by the disproportionation of magmatically derived SO_2. $\delta^{18}O_{SO4}$ values are 10 to 15 ‰ and vary systematically with $\delta^{34}S$ reflecting variations in temperature and/or H_2S/SO_4 fluid ratios. Further variation of $\delta^{18}O_{SO4}$ may result if SO_2 condenses in mixed magmatic-meteoric water fluids. $\Delta^{18}O_{SO4\text{-}OH}$ values of *magmatic-hydrothermal* alunites are generally unsuitable for temperature determinations because of retrograde exchange in the OH site but $\Delta^{34}S_{alun\text{-}py}$ values provide reliable temperature estimates.

Magmatic-steam environments appear to occur over a range of depths and are characterized by monomineralic veins of coarse alunite in variably alunitized and kaolinized wall rocks containing minor pyrite. Alunite formed in the *magmatic-steam* environment can usually be recognized by $\delta^{34}S$ near $\delta^{34}S_{\Sigma S}$ and δD and $\delta^{18}O_{SO4}$ near magmatic values. *Magmatic-steam* alunite differs from *magmatic-hydrothermal* alunite by having $\delta^{34}S$ close to $\delta^{34}S_{\Sigma S}$ of the system. $\Delta^{18}O_{SO4\text{-}OH}$ values of most *magmatic-steam* alunite give temperatures ranging from 90 to 200°C but, for reasons which are not understood, calculated $\delta^{18}O_{H2O}$ values are often too low for presumed precipitation from a magmatic vapor phase. *Magmatic-steam* environments may occur over porphyry type mineralization as Red Mountain, CO and Alunite Ridge, UT and over adularia-sericite type deposits as at Cactus, CA.

INTRODUCTION

Acid-sulfate alteration is a sub-set of advanced-argillic alteration, distinguished from it by the presence of alunite in the assemblage: alunite + kaolinite + quartz ± pyrite (Hemley and Jones, 1964; Meyer and Hemley, 1967). Acid-sulfate alteration can develop by several different mechanisms in different geologic environments. Because the products are the same, and in many cases the gross geologic setting is similar, a certain amount of confusion has existed in identifying the origin of a given acid-sulfate alteration zone. This has occasionally led to inappropriate extrapolation of processes known to occur in one type of acid-sulfate environment to another; for instance the application of well-studied processes in the surficial parts of geothermal systems, such as those in the Taupo Volcanic Zone in New Zealand, to the interpretation of alteration and ore-forming processes in the acid-sulfate type of epithermal deposits of Heald et al., 1987 (or high-sulfidation deposits of Hedenquist, 1987) such as Summitville, Colorado. The ability to distinguish between the several environments is of more than academic interest because mineralization - particularly precious metal mineralization - often accompanies acid-sulfate alteration, and the spatial and genetic relationships between mineralization and alteration are different for different environments. In many instances careful consideration of the geologic, mineralogic and geochemical attributes of a given acid-sulfate system will provide a sufficient basis for distinction, but sometimes this is not the case, or is not possible, and additional criteria would be useful.

Drawing on earlier studies by Field (1966), Schoen and Rye (1970), Jensen et al. (1971), Ohmoto (1972), Marumo et al. (1982), and Ohmoto and Lasaga (1982), Bethke (1984) proposed that the stable isotope systematics of alunite and kaolinite and associated sulfides in the several acid-sulfate environments, if known, might provide a set of criteria useful in making such distinctions, a concept further developed by Hayba et al. (1985). The present cooperative study was begun shortly thereafter to establish the isotope systematics, and evaluate their utility in identifying and elucidating the several origins of acid-sulfate alteration. A critical part of this effort required the development of techniques for the routine separation of alunite and subsequent stable isotope analyses (Wasserman et al., 1990) and the determination of the alunite-water ^{18}O and D fractionations (Stoffregen et al., 1989). In the analytical effort we build on the work of Field (1966) who first analyzed the $\delta^{34}S$ of alunite, Cunningham et al. (1984) who added δD analyses, and Pickthorn and O'Neil (1985) who did pioneering work on the technique for analysis of $\delta^{18}O_{OH}$ in alunite. In this paper we present over 500 determinations on over 200 samples from 20 localities. These determinations include the first analyses of $\delta^{18}O$ in both the SO_4 and OH radicals in alunite, as well as the first complete (δD, $\delta^{18}O_{SO4}$, $\delta^{18}O_{OH}$ and $\delta^{34}S$) stable isotope data on individual alunites, the $\delta^{34}S$ data on associated pyrite and the δD and $\delta^{18}O$ data on associated kaolinite. High quality data on some isotopes in 55 samples from 7 localities have been previously reported for some of the examples. These are presented with our data and used in our interpretations. All stable isotope data used in this study are listed in the Table 1.

Our approach has been to undertake detailed stable isotope studies on well-studied examples of acid-sulfate alteration formed in each of the environments. Many of these studies have been undertaken as parts of broader studies in cooperation with various colleagues. These detailed isotope studies have been supplemented by analyses of only a few samples from several localities, and in some cases by published data. As it turns out, the stable isotope systematics are substantially more complex than suggested by Bethke (1984), but they do provide a useful basis for distinguishing between the various origins of acid-sulfate alteration. Of greater significance, the very complexity of the stable isotope systematics has provided a number of insights into alteration and/or mineralization processes in each of the environments, and has provided isotopic documentation of concepts inferred from other studies. Further, this study has identified a number of new questions about hydrothermal and supergene processes and laid the basis for their future investigation.

This paper is organized to first examine the pertinent aspects of the several environments of acid-sulfate alteration and alunite formation, followed by the principles and predicted stable isotope systematics in each. Next, the stable isotope data for several geologically well documented deposits from each environment are presented as examples and evaluated, followed by reconnaissance data on samples from several mining districts and predictions about the origin of the acid-sulfate alteration they represent. Finally, the criteria for distinguishing among alteration zones formed in the various environments are summarized along with some insights provided by stable isotope systematics on processes of their formation.

This paper is principally concerned with the examination of the stable isotope systematics of acid-sulfate alteration and their interpretation of processes operating in the various acid-sulfate environments and is not meant to be a comprehensive or definitive treatise on acid-sulfate alteration. In addition, the geologic framework required to interpret the stable isotope data varies widely for the various areas that we have chosen to study. Some of these deposits are currently being studied in sufficient detail to improve the interpretation of their stable isotope systematics and our understanding of the processes of acid-sulfate alteration. Stable isotope studies coupled with appropriate geologic and geochemical investigations of additional areas of acid-sulfate alteration should be a fruitful area of research for some time to come.

ACKNOWLEDGMENTS

As indicated above, this study has been conducted in cooperation with a number of colleagues engaged in more comprehensive studies of several of the examples chosen for investigation, particularly mineralized areas. Antonio Arribas, Jr., currently studying the Rodalquilar district in Spain as part his Ph. D. program, and Jeff Deen, who recently completed a Ph. D. dissertation on Julcani, Peru each conducted the stable isotope portion of his research in Rye's laboratory, and provided a number of analyses herein reported, in addition to those related to his thesis studies. Each provided geological and mineralogical information and insights that were critical to the interpretation of the stable isotope data. Roger Stoffregen, whose recently published study of the Summitville, Colorado Cu-Au-Ag deposit (Stoffregen, 1987) provided the mineralogical and paragenetic basis for the interpretation of that deposit, supplied samples and cooperated in the interpretation of the stable isotope data for Summitville. Dana Bove worked out the complex paragenesis of acid-sulfate alteration in the Red Mountain district near Lake City, Colorado, and supplied samples based on that paragenesis. In addition, a number of other colleagues supplied samples from various localities. Foremost among these was Cy Field who supplied all the

samples from Tolfa, Italy and samples from El Salvador, Chile; Santa Rita, New Mexico; and Mineral Park, Arizona. Rich Fifarek supplied most of the samples on Round Mountain, Nevada. Peter Vikre and Roger Ashley provided samples and shared their knowledge of several districts in Nevada as noted at appropriate places in the text. CoCa Mines permitted access to their Cactus, California gold deposit and Jim Brady shared his knowledge of the district and guided the sampling of the deposit.

The stable isotope analysis of all four sites in alunite is a formidable task. Considerable effort was expended in developing mineralogical and chemical separation techniques as well as isotope analytical methods. A summary of the methodology is currently being prepared for publication. The development of these techniques was undertaken by Wasserman with the assistance of Rye on isotope analyses and Arribas and Bethke on mineralogical separation and J. A. Goss and Bethke on the chemical separation of sulfate from alunite. A number of analyses were made by Carol Gent.

In addition to those colleagues whose contributions to this study have been cited above, a number of others have contributed suggestions, information and other support. These include C.G. Cunningham, P.B. Barton, Jr., J.J. Hemley, B.R. Berger, R.W. Henley, T.J. Casadevall, T.M. Gerlach, and M.F. Coolbaugh. We are indebted to B.R. Berger, and T.J. Casadevall, and A.H. Hofstra for in-depth reviews of earlier versions of this paper.

ENVIRONMENTS OF ACID-SULFATE ALTERATION AND ALUNITE FORMATION

As shown by the experimental studies of Hemley et al. (1969) and the thermochemical assessment by Knight (1977), acid-sulfate alteration is a product of extreme base-leaching by fluids relatively concentrated in H_2SO_4 at temperatures below approximately 400°C. Its occurrence indicates extreme conditions of very low pH and redox conditions sufficiently oxidizing that sulfate ion (or SO_2 gas) are important sulfur species.

Requisite amounts of H_2SO_4 to produce acid-sulfate alteration may be generated by different mechanisms in three environments of interest in ore deposits. We here denote these environments as: *supergene, steam-heated,* and *magmatic-hydrothermal.* In addition, coarse vein alunite may precipitate directly from a vapor phase in what we here denote as the *magmatic-steam* environment. With the obvious exception of the supergene, each of the above environments is typically related to felsic to intermediate magmatism, some more intimately than others. Figures 1a and 1b (modified from Henley and Ellis, 1983), show, schematically, the spatial relations of the various environments, except the supergene, to one another, to the paleo-surface, and to magmatism in two different volcanic terrains. Figure 1a represents the relative positions of magmatic-hydrothermal, steam-heated and magmatic-steam environments closely related in space to a volcanic edifice. It is drawn to represent the relations in a calc-alkaline stratovolcano typical of Pacific Rim volcanism, but it also serves, in a general way, to show the relationships in a silicic volcanic dome, a typical host for acid-sulfate alteration in continental terrains. Figure 1b represents a mineralized, near-neutral-pH hydrothermal system in a silicic volcanic terrain, and was constructed to show the general features of geothermal systems, such as Wairakei, in the Taupo volcanic zone in New Zealand. Note that Figure 1a-b is not intended to represent all possible relations between environments nor all volcanic terrains that host acid-sulfate alteration. Precious- or base-metal mineralization may or may not accompany, or be related to acid-sulfate alteration in each of the environments depicted, and not necessarily in the relative positions shown.

Supergene environment

Supergene acid-sulfate alteration is a product of the weathering of sulfide-rich deposits. Resulting assemblages contain, in addition to alunite, disordered kaolinite, halloysite or, occasionally, allophane as well as iron oxide minerals, such as hematite, goethite, and jarosite. Typically, the alteration occurs as topographically-contolled blankets that often underlie gossans. Where protore mineralization is vein-controlled, the alteration may occur as curtains running down structure for vertical distances up to a hundred meters or more. When accompanied by supergene enrichment, the alteration is typically associated with copper sulfide minerals such as chalcocite, digenite or djurleite, or a suite of cupric minerals such as azurite, malachite, chrysacolla, turquoise, etc. Supergene alunite typically occurs as disseminations in the argillized wall rock and as thin, cryptocrystalline veinlets that cut both argillic zones and, occasionally, unaltered wall rock or protore.

The sulfuric acid required for acid-sulfate alteration is produced in the supergene environment, by the oxidation of sulfide minerals, typically pyrite. The oxidation of pyrite is a complex process as discussed later in the Principles section, but a representative summary reaction to produce a hydrous iron oxide phase may be written:

$$2FeS_2 + 7\,H_2O + 15/2\,O_2 = Fe_2O_3{\bullet}3H_2O + 4H_2SO_4 \qquad (1)$$

Because the textures, mineralogy, and frequently the form of supergene acid-sulfate alteration zones are often similar to those formed in steam-heated environments overlying and marginal to deeply-circulating hydrothermal systems (see next section), the distinction between the two is sometimes difficult to make. The presence of a gossan and subjacent secondary enrichment are unique characteristics of supergene systems. Potassium-Argon age determinations on the alunite may be a reliable indicator of a supergene origin where the corresponding hypogene mineralization is sufficiently old, and can also be dated.

Steam-heated environment

Steam-heated environments occur in the upper portions of hydrothermal systems. Much of our knowledge of the environment comes from studies of acid-sulfate alteration in active geothermal systems (c.f. Ellis and Mahon, 1977). Acid-sulfate alteration zones produced by steam-heated waters may or may not overlie mineralization deposited at deeper levels in the system (c.f. Henley and Ellis, 1983, and Henley, 1985). As noted above, typically the mineralogical characteristics and form of acid-sulfate alteration zones produced by steam-heated waters are similar to those produced by supergene processes, and the distinction is often difficult to make. As opposed to the supergene environment, in steam-heated waters sulfuric acid is produced by the oxidation, at and above the water table, of H_2S distilled off the underlying hydrothermal system. Again, the oxidation of H_2S in such systems is complex and not completely understood (c.f. Schoen, et al., 1974), but it can be described by the summary reaction:

$$H_2S + 2O_2 = H_2SO_4 \qquad (2)$$

Attributes, not necessarily universal, of fossil steam-heated environments include the presence of extensive sinter (often at a distance from the acid-sulfate alteration), a vertical zonation downward from alunite through kaolinite to an argillic or propylitic alteration assemblage, control by paleo-topography, and an age coincident with underlying mineralization, if such occurs and can be dated. The absence of a “protore” sufficient to supply the requisite sulfuric acid by weathering, and lack of secondary enrichment may be useful criteria in distinguishing steam-heated from supergene environments. Note, however, that secondary sulfide phases may also be produced by the downward encroachment of overlying steam-heated waters on sulfide mineralization, as described by Plumlee and Rye (1989), and their presence is not necessarily definitive of a supergene origin.

Magmatic-hydrothermal environment

Broadly speaking, the magmatic-hydrothermal environment includes all hydrothermal systems that are driven by magmatic heat and have significant magmatic components in their hydrothermal fluids. The magmatic-hydrothermal acid-sulfate environment, as used here, is closely drawn to include that in which deposits denoted as "Acid-Sulfate" by Heald et al., (1987), "High-Sulfidation" by Hedenquist (1987), and, perhaps most appropriately,"Kaolinite-Alunite" systems by Berger and Henley (1989) are formed. We include the enargite-bearing massive sulfide deposits, described by Sillitoe (1983), in this group although we have not studied any material from them. Acid-sulfate alteration in magmatic-hydrothermal environments is generally fracture-controlled, and alteration zoning is outward from the vein. In this environment base-leaching may be so intense that even aluminum is removed, leaving a core of sugary silica surrounded by successive zones of quartz-alunite, quartz-kaolinite and argillic alteration which grades into propylitized wall rock. Because magmatic-hydrothermal acid-sulfate alteration often develops in nearly coeval, coarsely porphyritic volcanic plugs or domes, the silica core often contains voids produced by the leaching of phenocrysts (typically alkali feldspar) giving rise to the term "vuggy silica". Disseminated pyrite is a common accompaniment, particularly in silica-rich zones. Pyrophyllite and, occasionally, diaspore may also occur in the alteration assemblage, particularly in the deeper levels of the deposit. The presence of the mineral zunyite, and high PO_4 contents of alunite appear to be unique attributes of acid-sulfate alteration assemblages produced in magmatic-hydrothermal environments. In the quartz-alunite zone, alunite typically occurs as aggregates of bladed or lath-like crystals up to 250μ long replacing alkali-feldspar phenocrysts and as lath-shaped crystals intergrown with quartz in the groundmass. The acid-sulfate alteration is typically succeeded by an ore assemblage including pyrite + enargite/luzonite ± covellite which, at depth, may grade into an assemblage of predominantly tetrahedrite/tennantite and chalcopyrite. Native sulfur is commonly present. Some magmatic-hydrothermal acid-sulfate zones, such as Red Mountain near Lake City, Colorado contain little or no precious or base metal mineralization. Several workers (e.g., Sillitoe, 1973, 1983, Wallace, 1979, Sillitoe and Bonham, 1984, and Bove et al., 1990) have pointed out that some magmatic-hydrothermal acid-sulfate systems are known to overlie deeper porphyry-Cu or porphyry-Mo environments.

In magmatic-hydrothermal acid-sulfate systems sulfuric acid is produced by the disproportionation of SO_2 on decreasing temperature according to the reaction:

$$4SO_2 + 4H_2O = 3H_2SO_4 + H_2S \qquad (3)$$

SO_2 disproportionation becomes important at temperatures below about 400°C, depending on P_{H_2O}, with increasing amounts of H_2SO_4 and H_2S being produced as temperature decreases. The SO_2 is derived from a magma and transported in a vapor plume consisting predominantly of water (c.f. Henley and McNabb, 1978), and disproportionation probably begins in the plume. Acid-sulfate wall-rock alteration is interpreted to commence when the vapor plume begins to condense. In some systems, such as Julcani, Peru (discussed in the Examples section), the condensed liquid is essentially of totally magmatic origin. In other systems, such as Summitville, Colorado (also discussed in the Examples section), the condensate appears to be a mixture of magmatic and meteoric water, either because the vapor plume condenses into, and mixes with, the surrounding meteoric water, or because meteoric water was drawn into, and mixed with, the vapor plume deep in the system and during its ascent.

Somewhat surprisingly, a number of magmatic-hydrothermal acid-sulfate deposits have been interpreted as being of steam-heated origin. However, the occurrence of vuggy silica cores, large amounts of pyrite in the alteration assemblage, the coarse crystallinity of the alunite - often replacing feldspar phenocrysts, the occurrence in near-vertical tabular or pod-like masses, and the association with an ore mineral assemblage containing covellite and enargite/luzonite are field characteristics unique to shallow magmatic-hydrothermal acid-sulfate deposits.

Magmatic-steam environment

Because the magmatic-steam environment is dominated by a vapor phase of magmatic origin, it could be considered a subset of the magmatic-hydrothermal environment. However, its products and mechanisms are quite different, and its stable isotope systematics differ significantly (and definitively) from those of magmatic-hydrothermal deposits; it is best considered separately. Alunite produced by magmatic-steam systems appears to have grown from the vapor phase (Cunningham, et al., 1984) and occurs in coarsely crystalline veins, up to tens of meters wide. The wall rock alteration around these veins can be tens of meters thick or only narrow and weak selvages with little or no pyrite on their margins. Only very small amounts of quartz and hematite occur with alunite in the veins. The type occurrence is the vein alunite deposits at Alunite Ridge, 10 km southwest of Marysvale, Utah described by Callaghan (1973) and Cunningham et al. (1984). We are not aware of descriptions of other alunite occurrences that have been ascribed to such an origin, but we interpret two of the examples, discussed later, to include alunite formed from magmatic steam. Such occurrences may be more common than suspected. The genesis of alunite veins of this type is not well understood, but the stable isotope data, discussed later, essentially require that : 1) virtually all the sulfur in the system was present as SO_2 released from magma at high temperatures and low pressures without reduction during ascent, or 2) essentially all the sulfur in the fluid was oxidized by entrainment of atmospheric oxygen during its ascent. Both options require release from a magmatic reservoir at fairly shallow depth.

Relationships between environments

Figure 1a represents the relative positions of magmatic-hydrothermal, steam-heated and magmatic-steam environments closely related in time and space to stratovolcanic volcanism typical of the Pacific Rim. These relations apply equally to a silicic volcanic dome in a continental terrain. The magmatic-hydrothermal environment develops at depth some distance above a magma chamber at the point where a magmatic vapor plume containing H_2O, H_2S and SO_2 begins to condense. Although not shown, it might overlie deeper porphyry-type mineralization. Magmatic-hydrothermal acid-sulfate alteration results from the attack on the wallrocks by sulfuric acid produced by the disproportionation of SO_2. The H_2S in the fluid continues to rise, and upon reaching the water table, is oxidized to sulfuric acid which attacks the wall rock to produce a surficial zone of steam-heated acid-sulfate alteration. Such steam-heated alteration zones may be expected to develop over all magmatic-hydrothermal acid-sulfate systems. If the stratovolcano contains a crater lake it may become strongly acid, as at Poas volcano in Costa Rica (Brantley et al., 1987). Although drawn vertically separated, the steam-heated waters may encroach on the zone of magmatic-hydrothermal acid-sulfate alteration, particularly late in the life of the hydrothermal system, producing alunite veins cutting earlier magmatic-hydrothermal alteration.

A magmatic-steam environment is shown marginal to the magmatic-hydrothermal environment, but no necessary spatial relationship is implied. Presumably such zones may develop at various times in the volcanic-hydrothermal cycle and could occur with, but precede or post date, either the magmatic-hydrothermal or steam-heated environments. The magmatic-steam environment might also overlie deeper porphyry-type or adularia-sericite type mineralization.

Figure 1b represents a mineralized, near-neutral pH hydrothermal system typical of those with a deep heat source in a silicic volcanic terrain. The system is driven by a magmatic heat source at considerable depth. Again, although not shown, porphyry-type mineralization may occur close to the magmatic hearth. Mineralization which may occur in the upper part of the system is of the adularia-sericite type. An overlying zone of steam-heated acid sulfate alteration may develop near the surface by the oxidation of H_2S distilled off the underlying hydrothermal system. The superjacent, low pH waters may mix along the top or the margins of the underlying near-neutral waters, and during the waning stages of the system, the acid-sulfate waters may descend into the ore zone and overprint the adularia-sericite assemblage. Systems such as these are often only weakly mineralized or not mineralized at all. Many active geothermal systems such as those in the Taupo volcanic zone in New Zealand and Yellowstone Park in Wyoming are of this type.

PRINCIPLES OF STABLE ISOTOPE GEOCHEMISTRY AND PREDICTED STABLE ISOTOPE COMPOSITIONS FOR VARIOUS ACID-SULFATE AND ALUNITE-FORMING ENVIRONMENTS

Alunite [$KAl_3(SO_4)_2(OH)_6$] contains four stable isotope sites, more than any other common mineral except crystallographically similar jarosite [$KFe_3(SO_4)_2(OH)_6$]. The various sites provide different information about the formation of the mineral, and stable isotope analyses (δD, $\delta^{18}O_{SO4}$, $\delta^{18}O_{OH}$, and $\delta^{34}S$) of each, especially when accompanied by stable isotope analyses on coexisting minerals, can provide information on origins of components, processes (including rates), physical-chemical environments, and temperatures of formation. Of particular interest, because of the possibility for a single mineral isotope geothermometer, is the occurrence of oxygen in both SO_4 and OH sites. In addition, because alunite is a potassium-bearing mineral it has proven useful for geochronology - an attribute sometimes useful in the interpretation of the stable isotope data. Sufficient knowledge exists of isotopic fractionation factors and kinetics of relevant processes to predict the stable isotopic compositions of alunite and associated minerals for each acid-sulfate and alunite-forming environment, given certain assumptions about the physical-chemical environment and composition of fluids, degree of equilibrium between fluids and minerals, and preservation of primary isotope compositions.

Assumptions

Every stable isotope study requires assumptions about equilibrium/disequilibrium, temperature, fluid compositions, fractionation factors, and degree of retention of primary compositions. In this section theoretical stable isotopic compositions of minerals were calculated by assuming arbitrary fluid compositions in various alunite-forming environments, and by making certain assumptions about temperature, fractionation factors, and degree of approach to equilibrium. The assumed temperatures and fluid compositions and calculated mineral compositions are indicated on Figures 2-5 and are typical of those for Tertiary epithermal deposits of the western U.S. The following isotope fractionation factors were used: kaolinite-water oxygen (Savin and Lee, 1988); kaolinite-water hydrogen (Liu and Epstein, 1984); sulfate/alunite-H_2S/pyrite sulfur (Ohmoto and Rye, 1979); alunite SO_4 and alunite OH-water oxygen and alunite OH-water hydrogen in the temperature range 250°-400°C (Stoffregen et al., 1989); alunite-water hydrogen at low temperatures (Bird et al., 1989). Hydronium ion (H_3O^+)is known to substitute for alkalis in low temperature alunites. The effect of hydronium on isotope systematics needs to be investigated further. However, studies by Alpers et al. (in press) indicate that hydronium has only minor effect on the δD analysis of alunites.

Extensive chemical substitution occurs in each of the atomic sites in alunite leading to a large number of minerals in the alunite group (Botinelly, 1976). Except for the substitution of sodium in the potassium site (Stoffregen and Cygan, 1990) and of ferric iron in the aluminum site (Brophy, et al., 1962) the phase relations between the minerals of the alunite groups are virtually unknown. The effect of chemical variations in alunite on isotopic fractionation have not been considered in this study. Experimental studies by Stoffregen et al. (1989) indicate that the substitution of sodium for potassium has negligible effect on isotopic fractionation. The substitution of ferric iron in the aluminum site, however has a strong effect on hydrogen isotope fractionations (Alpers et al., in press). We have ignored the effects of ferric iron substitution because XRD characterization studies have suggested only minor ferric iron substitution in the samples studies. Similarly, other substitutions in alunite appear to very limited and their effects have also been ignored.

Quartz usually forms with alunite in acid-sulfate environments. The $\delta^{18}O$ values of quartz coexisting with alunite in the magmatic-hydrothermal acid-sulfate alteration zones at Summitville, Colorado, have been investigated by Rye et al. (1990). We have not pursued similar $\delta^{18}O$ analyses of quartz in this study for the following reasons: 1) the ^{18}O fractionations between quartz and sulfate in alunite are small and do not vary significantly with temperature, 2) quartz often precipitates over a larger portion of the paragenesis than does alunite and it is virtually impossible to sample only coeval quartz and alunite, and 3) it is often impossible to separate hydrothermal from primary igneous quartz in volcanic rocks.

Kinetic Considerations

Kinetic factors play an important role in the stable isotope systematics of alunite and acid-sulfate alteration. To a very large extent they form the isotopic basis for distinguishing between environments of acid-sulfate alteration, and they provide important insights into attendant processes. Exchange rates for sulfur isotopes between aqueous sulfur species and for oxygen isotopes between sulfate and H_2O are kinetically inhibited, but reach a maximum for a given temperature at the low pH of alunite formation (Chiba et al., 1981; Ohmoto and Lasaga, 1982). Sulfur and oxygen isotopic equilibrium between sulfate and water is probably readily obtained in most magmatic-hydrothermal environments and at least oxygen isotopic equilibrium is obtained in most steam-heated environments. However, complete kinetic control of isotopic compositions of sulfate is likely in the supergene environment. Hydrogen and oxygen isotope equilibrium for OH between alunite and fluids is likely during the precipitation of the mineral in all environments.

Retention of primary isotope compositions in alunite

Most hydrothermal minerals retain their isotopic compositions after deposition unless recyrstallized. Our studies suggest that retrograde isotope exchange between alunite and later fluids does not normally occur in hydrothermal environments except, in some instances, for the OH site. A recent study by Stoffregen et al. (1990) indicates that nearly complete D exchange between fine-grained alunites (<2-5 microns) and water will occur in less than 10^4 years at 25° C. Because the D fractionation between alunite and water is very small, significant changes in δD of the alunite will occur only if a water of different δD is involved. Modification of original $\delta^{18}O_{OH}$ values in alunite by retrograde exchange can be important because the alunite OH-water oxygen isotope fractionation changes significantly with temperature. Some alunites, especially those from supergene and some steam-heated environments, are very fine-grained, but we have not yet identified any example of post-depositional isotope exchange between the OH site and water except in the magmatic-hydrothermal environment. There, our studies indicate that the OH site in alunites *is* subject to post-depositional exchange even though the grain size of the alunite may range up to greater than 100 microns. We have seen no evidence of such exchange in magmatic-steam alunites whose grain sizes range from millimeters to centimeters.

Predicted δD, $\delta^{18}O_{SO4}$, $\delta^{18}O_{OH}$ and $\delta^{34}S$ systematics of supergene alunite.

The predicted δD - $\delta^{18}O_{SO4}$ - $\delta^{18}O_{OH}$ and $\delta^{34}S$ systematics of supergene alunites for an arbitrary set of fluid compositions are shown in Figure 2a-b The initial δD and $\delta^{18}O_{OH}$ values of supergene alunite are controlled by equilibrium exchange and reflect the temperature and δD_{H2O} and $\delta^{18}O_{H2O}$ of the parent fluid. On the other hand, the $\delta^{34}S$ and $\delta^{18}O_{SO4}$ values of supergene alunite are kinetically controlled and depend on the hydrogeochemical and biogeochemical environment of oxidation of precursor sulfides.

$\delta^{34}S$-$\delta^{18}O_{SO4}$-δD systematics: Field (1966) observed that sulfur undergoes essentially zero fractionation during supergene oxidation of sulfides and the formation of sulfate minerals. Laboratory studies of both chemical and microbially-mediated pyrite oxidation have confirmed that only small sulfide-sulfate fractionations are produced during oxidation of solid sulfides (Nakai and Jensen, 1964; Kaplan and Rittenberg, 1964; Lewis and Krouse, 1969). Large fractionations may occur during the oxidation of aqueous sulfide species (Kaplan and Rafter, 1958; Kaplan and Rittenberg, 1964), but this situation probably seldom applies to supergene oxidation of sulfide-rich deposits. Except where bacteriogenic reduction of sulfate occurs in standing pools of water, the $\delta^{34}S$ values of supergene sulfate will be similar to those of the precursor sulfides as indicated in Figure 2a.

Caution is required when selecting precursor sulfide minerals for comparison with supergene alunites, because late-stage sulfides associated with the collapse of hydrothermal systems in shallow ore deposits may be the first to be oxidized and may have $\delta^{34}S$ values that are substantially different from those of the remaining main-stage minerals (Plumlee and Rye, 1989).

The $\delta^{18}O_{SO4}$ values of supergene sulfates are not as easy to predict. The oxidation of sulfides is a complex process that is not completely understood. However, Lloyd (1968), Taylor et al. (1984) and van Everdingen and Krouse (1985) show that the $\delta^{18}O_{SO4}$ derived from the oxidation of pyrite is basically the result of two kinetically-controlled summary reactions. The first reaction is the oxidation of pyrite by oxygen:

$$FeS_2 + 7/2O_2 + H_2O = Fe^{2+} + 2SO_4^{=} + 2H^+ \qquad (4)$$

where 87.5% of the sulfate's oxygen is contributed by molecular atmospheric oxygen, and the remaining 12.5% is derived from water. The second summary reaction is the oxidation of pyrite by ferric iron:

$$FeS_2 + 14Fe^{3+} + 8H_2O = 15Fe^{2+} + 2SO_4^{=} + 16H^+ \qquad (5)$$

where 100% of the oxygen in the sulfate is derived from water. The $\delta^{18}O$ of sulfate produced by reaction (4) is governed largely by the constant $\delta^{18}O$ value (23‰) of atmospheric oxygen and will vary only slightly with the $\delta^{18}O$ of the local water whereas the $\delta^{18}O$ of sulfate produced by reaction (5) is governed completely by the $\delta^{18}O$ of local meteoric water. Because of the large difference between the isotopic composition of atmospheric oxygen and surface water at all latitudes, a considerable range of $\delta^{18}O_{SO4}$, indicated by the shaded area in Figures 2a and 2b, can result during the oxidation of pyrite, depending on which reaction is dominant An important reference field (Figure 2b) for possible δD-$\delta^{18}O_{SO4}$ values for supergene alunite is herein denoted as the *supergene alunite sulfate field* (SASF) and is defined by the following: 1) the minimum kinetic fractionation (4‰) between sulfate and water observed for reaction (5) (Taylor et al., 1984), 2) the maximum value for the combined kinetic fractionations between sulfate and atmospheric oxygen and sulfate and water of a given composition resulting from reaction (4) (van Everdingen and Krouse, 1985), and 3) the small low-temperature fractionation of hydrogen between alunite and water (Bird et al., 1989). The position of the field may change slightly as more precise values for the fractionation of oxygen isotopes between aqueous sulfate and alunite during the precipitation of alunite become available; alunites may have $\delta^{18}O_{SO4}$ values several permil larger than the aqueous sulfate, judging from the 3.5 ‰ fractionation observed between aqueous sulfate and gypsum in evaporites (Holser et al., 1979). Low-temperature aqueous sulfate will not have δD-$\delta^{18}O_{SO4}$ values to the right of the SASF unless it undergoes redox recycling in the presence of reducing bacteria, or unless it undergoes exchange with water in low pH solutions. Either possibility would require long-standing pools of low pH waters, a condition that is probably seldom attained in the supergene environment. Such conditions have been observed, however, for acid playa lakes in Australia (Alpers et al., in press). There, based on extrapolation of the experimental data of Stoffregen et al. (1989), the $\delta^{18}O_{SO4}$ values for alunite are close to isotopic equilibrium with local meteoric water.

Taylor et al. (1984) observed that maximum fractionations occur for reactions (4) and (5) during microbially-mediated reactions. Therefore, the $\delta^{18}O_{SO4}$ value of supergene alunite will depend on the hydrogeochemistry which controls the role of bacteria during sulfide oxidation. Presumably, the largest fractionations during microbially-mediated reactions will occur in alternating wet/dry environments and the smallest in flooded, anaerobic environments. Thus the $\delta^{18}O_{SO4}$ of alunites can be used to indicate the hydrogeochemical history during supergene oxidation. For example, large $\delta^{18}O_{SO4}$ values may indicate maximum fractionations during oxidation in alternating wet/dry environments while small $\delta^{18}O_{SO4}$ values may indicate minimum fractionations under continually flooded conditions (Taylor et al., 1984).

δD–$\delta^{18}O_{OH}$ Systematics: The δD and $\delta^{18}O_{OH}$ values of supergene alunite are controlled by equilibrium exchange and reflect the temperature, δD_{H2O}, and $\delta^{18}O_{H2O}$ of

the parent fluid. Thus, using the extrapolated fractionation factors of Stoffregen et al., (1989), the $\delta^{18}O_{OH}$ values of supergene alunite can be used to place important constraints on the temperature and composition of supergene fluids. The δD-$\delta^{18}O_{OH}$ values of supergene alunites may be expected to plot in a band parallel to the *meteoric water line* (MWL) much the same way as do δD-$\delta^{18}O$ values of supergene kaolinite. Oxidation reactions are strongly exothermic so supergene alteration probably takes place over a range of temperatures. An important reference zone (Figure 2b) for possible δD-$\delta^{18}O_{OH}$ values for supergene alunites is herein referred to as the *supergene alunite OH zone* (SAOZ) and is defined by the compositions of alunite in equilibrium with meteoric water between 20° and 80°C. Since the $\delta^{18}O_{SO4}$ of low-temperature alunites formed in the supergene environment is kinetically controlled, $\delta^{18}O_{OH}$ will normally be out of equilibrium with $\delta^{18}O_{SO4}$. In fact, unique to the supergene environment, $\delta^{18}O_{OH}$ values can be larger than $\delta^{18}O_{SO4}$ values.

Alunite formed by supergene oxidation will have δD values similar to that of local groundwater (Bird et al., 1989) as indicated in Figure 2b. In some cases, however, the water may be enriched in D as a result of evaporation or may be different as a result of climatic changes. Also, it is conceivable that in zones of intense hydrolytic alteration the δD of the supergene fluid can be buffered by the hydrous minerals and therefore be enriched in D, but this has not been demonstrated. Associated kaolinites and halloysites will have δD values approximately 30 ‰ lower than ambient meteoric water and δD and $\delta^{18}O$ values close to the *kaolinite line* of Savin and Epstein (1970; Lawrence and Taylor, 1971; Marumo et al., 1982; Savin and Lee, 1988).

Predicted δD, $\delta^{18}O_{SO4}$, $\delta^{18}O_{OH}$ and $\delta^{34}S$ systematics of steam-heated alunites

Steam-heated alunites and associated kaolinites probably form at and above the water table over the approximate temperature range of 90 to 150°C in waters acidified by atmospheric oxidation of H_2S distilled off of underlying hydrothermal fluid. Predicted $\delta^{34}S$-$\delta^{18}O_{SO4}$-$\delta^{18}O_{OH}$ and δD-$\delta^{18}O_{SO4}$-$\delta^{18}O_{OH}$ systematics of steam-heated alunites for a given set of conditions are shown in Figure 3a-b.

$\delta^{34}S$-$\delta^{18}O$ systematics: The $\delta^{34}S$ of alunite will normally be the same as the H_2S boiled off of the hydrothermal fluid, as indicated in Figure 3a. However, at the temperatures of the steam-heated environment, and given enough time, aqueous SO_4 may exchange with the H_2S resulting in larger $\delta^{34}S$ values, as suggested by the data from Marysvale, Utah discussed later.

Values of $\delta^{18}O_{OH}$ probably always reflect equilibrium with the fluid, and the expected range of values for alunite in equilibrium with a fluid of an arbitrarily chosen $\delta^{18}O_{H2O}$ at 90 and 150° C is indicated on Figure 3a. Prediction of the $\delta^{18}O_{SO4}$ of steam-heated alunite is more difficult, and is dependent on the assumptions made with respect to the ratio of air to water oxygen involved in the oxidation, the $\delta^{18}O_{H2O}$ of the fluid, the temperature of oxidation, and the degree of exchange of the sulfate oxygen with the fluid. If oxidation involves largely air oxygen ($\delta^{18}O = 23‰$) and exchange with fluid does not occur, the original $\delta^{18}O_{SO4}$ values can be quite large. However, our data on the steam-heated systems reported in this study suggest that equilibrium between sulfate oxygen and fluid is usually closely approached. As indicated above, values of $\delta^{18}O_{OH}$ probably always reflect equilibrium with the fluid. Our data indicate that temperatures calculated based on the variation of $\Delta^{18}O_{SO4-OH}$ with temperature almost uniformly fall in the range 90 - 160°C, the expected range for steam-heated environments, requiring that $\delta^{18}O_{SO4}$ also closely approach equilibrium values with the fluid. One of the distinguishing characteristics of the steam-heated environment is near-equilibrium $\Delta^{18}O_{SO4-OH}$ values that give reasonable depositional temperatures. The fact that in some steam-heated environments oxygen in the sulfate site appears to have equilibrated with the water, whereas the sulfur did not exchange with the H_2S (c.f. later section on Tolfa, Italy) is in agreement with the comparison between the experimentally determined exchange rates for oxygen isotope exchange between sulfate and water (Lloyd, 1968), and for sulfur isotope exchange between aqueous sulfate and sulfide (Ohmoto and Lasaga, 1982). The fact that in some systems both sulfur and sulfate oxygen appear to have undergone considerable isotopic exchange (c.f. later section on Marysvale, Utah) suggests that the steam-heated environment is in the temperature-pH range wherein significant amounts of oxygen and even sulfur isotopic exchange can occur in geologically reasonable times. The degree to which equilibrium between aqueous sulfate and fluid and aqueous sulfate and H_2S is normally approached in the steam-heated environments remains an uncertainty that needs to be evaluated by detailed study of individual deposits. In fact, the degree of approach to $^{18}O_{SO4}$ and ^{34}S equilibrium with water and H_2S is probably related to the integrated time-temperature history of the alunite and is a fruitful area for research.

δD-$\delta^{18}O$ systematics: Steam-heated alunites should have δD similar to that of the paleo-groundwater as indicated in Figure 3b. $\delta^{18}O_{SO4}$ and $\delta^{18}O_{OH}$ values associated with a given δD value will depend on temperature and the degree to which the paleo-groundwater has exchanged ^{18}O with the country rocks. Alunites formed from unexchanged waters as represented by the high δD example in Figure 3b will have δD-$\delta^{18}O_{OH}$ to the left of the SAOZ and δD-$\delta^{18}O_{SO4}$ within the SASF. Alunites formed from exchanged waters represented by the low δD example in Figure 3b will have most δD-$\delta^{18}O_{SO4}$ values to the right of the SASF while the position of δD-$\delta^{18}O_{OH}$ values relative to the SAOZ will depend on degree of ^{18}O exchange of the water. δD - $\delta^{18}O$ values for associated kaolinites will normally be to the left of the kaolinite line (Marumo et al., 1982). Compare the position of these mineral fields with those for supergene alunite and kaolinite. The difference in orientation of the alunite and kaolinite fields in Figure 3b is due to the difference in temperature dependence of mineral-water hydrogen isotope fractionations which are very small for alunite.

Predicted δD, $\delta^{18}O_{SO4}$, $\delta^{18}O_{OH}$ and $\delta^{34}S$ systematics of magmatic-hydrothermal alunites

Predicted δD-$\delta^{18}O_{SO4}$-$\delta^{18}O_{OH}$ and $\delta^{34}S$-$\delta^{18}O_{SO4}$-$\delta^{18}O_{OH}$ systematics of magmatic hydrothermal alunites for assumed isotopic compositions of fluids and physical-chemical conditions are shown in Figure 4a-b. Magmatic-hydrothermal alunites derive their sulfate from sulfuric acid formed by the disproportionation of SO_2 derived from a magma. At the temperature and pH of this environment, equilibrium conditions in the fluids are likely and the $\delta^{34}S$ of alunite and associated pyrite will reflect the H_2S/SO_4 and temperature of the fluid. As indicated in the discussion of the magmatic-hydrothermal environment, disproportionation may take place in magmatic or mixed magmatic-meteoric water. Both situations are discussed below.

$\delta^{34}S$-$\delta^{18}O$ systematics: In Figure 4a-b the darkest shading of the alunite SO_4 field indicates compositions of alunites deposited from purely magmatic water over the range of H_2S/SO_4 and temperatures typical of magmatic fluids. Gradational shadings show displacement of compositions with increasing proportions of exchanged, ^{18}O-depleted, meteoric water. Referring to Figure 4a, for a magmatic-water dominated fluid of given H_2S/SO_4 as temperature decreases, the $\delta^{34}S$ of pyrite will decrease (shown schematically by an arrow), the $\delta^{34}S$ of alunite will increase, and $\delta^{18}O$ in both SO_4 and OH sites will increase. The $\delta^{34}S$ of pyrite and alunite also will be functions of the H_2S/SO_4 of the fluid which will be controlled by the redox state of the system (c.f. Whitney, 1984 and 1988). With decreasing temperature, the $\delta^{18}O$ and $\delta^{34}S$ will co-vary and track a line defined by the initial and final H_2S/SO_4. In Figure 4a H_2S/SO_4 ratios of 1 and 8 are used, along with temperatures of 400 and 200°C, to define the darkly shaded field containing all $\delta^{34}S$-$\delta^{18}O_{SO4}$ values for alunites formed over that temperature and H_2S/SO_4 range for predominantly magmatic waters. The open field offset to lower $\delta^{18}O$ values represents all values of $\delta^{34}S$ and $\delta^{18}O_{OH}$ of the same alunites, reflecting the difference in fractionation factors for oxygen between the SO_4 and OH sites and water. The effect of mixing with meteoric water (indicated for SO_4 by the lighter shading) is to decrease $\delta^{18}O$ of both SO_4 and OH sites by an amount dependent on the $\delta^{18}O_{H2O}$ and degree of involvement of

meteoric water. The effect of mixing on the composition of the OH site is identical to that for SO_4, but is not shown on Figure 4a to avoid overcrowding.

δD-$\delta^{18}O$ systematics: In Figure 4b the fields for δD, and $\delta^{18}O$ in both SO_4 and OH sites, for alunite in equilibrium with arbitrarily chosen magmatic and meteoric waters, are shown for temperatures between 400 and 200°C. Over the temperature interval of most magmatic-hydrothermal alunite formation, the D and ^{18}O fractionations between water and alunite are small enough that the δD and initial $\delta^{18}O_{OH}$ values of the alunite will closely reflect the values for the water in the fluid. Our studies of magmatic-hydrothermal systems indicate that associated kaolinites (not shown to avoid overcrowding on the diagram) almost always reflect a greater degree of mixing with exchanged meteoric water along the margins of the alteration zone with substantially lower δD, but somewhat similar $\delta^{18}O$ values to adjacent alunites (see examples from Red Mountain and Summitville discussed later).

Predicted δD, $\delta^{18}O_{SO4}$, $\delta^{18}O_{OH}$ and $\delta^{34}S$ systematics of magmatic-steam alunites

The principles of δD, $\delta^{18}O_{SO4}$, $\delta^{18}O_{OH}$ and $\delta^{34}S$ systematics in magmatic-steam alunites are similar to those for steam-heated alunites and are shown in Figure 5a-b. Magmatic-steam alunite, however, appears to form directly from an SO_2-rich magmatic vapor by mechanisms as yet incompletely understood (Cunningham et al., 1984), and in some cases probably at higher temperatures. The paucity of pyrite, or other sulfides, in deposits of this type require that the sulfur must be carried essentially entirely as SO_2 , derived either from high temperature - low pressure release from a magma, or from near-surface oxidation by atmospheric O_2, as in the carapace of a volcanic edifice. Because in either circumstance oxidation to sulfate is essentially quantitative, the $\delta^{34}S$ of the alunite will be close to that of the bulk sulfur in the magma. At high temperatures the oxygen in the sulfate will equilibrate with the magmatic-steam in all cases and $\delta^{18}O_{SO4}$ values will be similar to those for magmatic-hydrothermal alunites. We would expect the $\delta^{18}O_{OH}$ values to be in equilibrium with, or to reflect retrograde exchange with, the fluids such that $\Delta^{18}O_{SO4\text{-}OH}$ values yield depositional temperatures or higher. However, for reasons that are not clear, $\delta^{18}O_{OH}$ values of some magmatic-steam alunites show evidence of equilibration with fluids having low $\delta^{18}O_{H2O}$ values, with the result that their $\Delta^{18}O_{SO4\text{-}OH}$ values of give lower than presumed depositional temperatures. Magmatic-steam alunites can be distinguished from steam-heated alunites by δD values in the magmatic range (except when local meteoric waters have δD values in the primary magmatic range).

EXAMPLES

The following examples are given as representative of the various environments of acid-sulfate alteration and, in some cases, of the overprinting or crosscutting of one type of acid-sulfate alteration by another. Several of these examples are from areas that have been the object of detailed published studies or current investigations with various colleagues with more detailed papers in preparation. Only a brief description is given of each area; for more detail the reader is referred to the pertinent references. As above, the data are shown on paired isotope plots that summarize the δD, $\delta^{18}O_{SO4}$, $\delta^{18}O_{OH}$ and $\delta^{34}S$ systematics of alunite, the δD and $\delta^{18}O$ systematics of associated kaolinite/halloysite, the $\delta^{34}S$ of sulfides and sometimes the δD_{H2O} and $\delta^{18}O_{H2O}$ of parent fluids calculated from the mineral data. All stable isotope data are also listed in Table 1. Techniques used for isotope analyses of alunite are discussed by Wasserman et al. (1990). Analytical precision (1σ) is ±2‰ for δD, ±0.1‰ for $\delta^{18}O_{SO4}$, ±0.2‰ for $\delta^{18}O_{OH}$, ±0.1‰ for $\delta^{34}S$ and ±0.3 for $\Delta^{18}O_{SO4\text{-}OH}$ which corresponds to a temperature uncertainty of ±20°C at low temperatures (~100°C) and ±50°C at high temperatures (~ 400°C).

Stable isotope systematics of alunite and halloysite from Creede, Colorado: an example of supergene acid-sulfate alteration over adularia-sericite type silver-base metal mineralization

The epithermal Ag-Pb-Zn vein deposits at Creede have been described in a number of recent publications (c.f. Steven and Eaton, 1975, Barton et al., 1977, Bethke and Rye 1979, Rye et al., 1989). Small amounts of alunite occur in narrow veins in the upper parts of the ore bodies in the southern part of the district. These alunites have been dated between 3.1 and 4.8 Ma (Lanphere, written communication, 1986) versus 25 Ma for the main-stage mineralization (Bethke et al., 1976). Alunite formation appears to have coincided with the relative lowering of the water table during regional uplift of the Rocky Mountains (Taylor 1975). Halloysite also occurs principally as vein fillings in the upper part of the ore body. At no place have the alunite and halloysite been observed to occur together, but the halloysites are presumed to also be of supergene origin. Stable isotope data are presented in Figure 6a-b. The $\delta^{18}O_{OH}$ values of the alunite fall within the SAOZ and suggest temperatures between 80° and 40°C, which seem consistent with supergene oxidation processes that involve strong exothermic reactions. The halloysites at Creede plot somewhat to the left of the *kaolinite line* (Figure 6b) indicating temperatures somewhat higher than 17°C but, in contrast to alunite, the fractionation factors for kaolinite-water are too ambiguous to permit useful temperature estimates (Savin and Lee, 1988). The halloysites and alunite have wide range of δD values (-79 to -99‰ and -82 to -117‰, respectively). The values for halloysites and alunites are not consistent with precipitation from the same fluid. Furthermore, the δD values for the both alunite and halloysite imply surface water compositions heavier than expected for the Creede area (Bethke and Rye, 1979; Rye et al., 1988). Possibly these δD systematics reflect changes in surface water compositions due to evaporation and/or climatic or seasonal variations over an approximate 2 million years.

Stable isotope systematics of alunite at Round Mountain, Nevada: an example of supergene acid-sulfate alteration over adularia-sericite type gold mineralization

Alunite occurs in the upper parts of the Round Mountain gold deposit as veinlets up to 5 centimeters in thickness often accompanied by jarosite, limonite, quartz and manganese oxides (Ferguson, 1921; Tingley and Berger, 1985; Sander, 1988). Round Mountain alunites formed between 16.3 and 9.1 Ma, mainly between 12.4 and 9.1 Ma; main stage gold mineralization has been dated at 25.9 to 26.6 Ma (Sander, 1988). Ferguson considered the alunite to be of supergene origin but Tingley and Berger pointed out that it could represent a later hypogene (presumably steam-heated) hydrothermal event. The alunite fills NE-trending fractures parallel to the regional block faulting and the age range of the alunites corresponds to that of the period of uplift in this part of Nevada (Tingley and Berger, 1985; Sander, 1988). The stable isotope data on alunite shown in Figure 7a-b are typical of supergene environments. The $\delta^{34}S$ values of the precursor sulfides at Round Mountain are large, resulting in large $\delta^{34}S$ values of the supergene alunites. The $\delta^{18}O_{OH}$ values are consistent with formation from unexchanged meteoric waters in the temperature range of 20° to 80 °C. $\Delta^{18}O_{SO4-OH}$ fractionations vary widely and show both positive and negative values. The narrow range of δD values over 3.5 to 7 million years indicates remarkably constant local climatic conditions perhaps controlled by presence of large lakes in the area (B.R. Berger, personal comm., 1991). The combination of smaller range of δD values and larger range of $\delta^{18}O_{SO4}$ values than for Creede alunites may indicate that oxidation of sulfides at Round Mountain occurred in a more flooded environment that allowed for less evaporation. Samples in this study are the same ones analyzed in our laboratory and presented by Fifarek and Gerike (1990).

Stable isotope systematics of supergene alunites and halloysites from the weathering zones of various ore deposits and sulfide occurrences at different latitudes

The stable isotopic composition of supergene alunites and associated halloysite/kaolinites from various types of ore deposits that occur over a range of latitudes and $\delta^{34}S$ of precursor sulfides are shown in Figure 8a-b. The alunites from the porphyry copper deposits at Santa Rita, NM and Mineral Park, AZ are the same samples described by Field (1966). The alunites from the gold deposits at Mount Leyshon and Kidston, Australia are the same samples used by Bird et al. (1989). The alunites from Creede, CO and the gold deposit at Round Mountain, NV are those shown above. The alunites from Rodalquilar are the stage 2 alunites shown in Figure 17a-b. The alunites at Riaza, Spain are from black shale and are currently under investigation by A. Arribas and R.O. Rye. The alunite in most of these occurrences have been demonstrated to be supergene by K-Ar dating. The $\delta^{34}S$ values of the supergene alunites from all localities are within the range observed for precursor sulfides or within a few permil of them. The δD-$\delta^{18}O_{OH}$ values for all supergene alunites lie within the SAOZ and the δD-$\delta^{18}O_{SO4}$ values for all supergene alunites except some of those from Riaza lie within the SASF. Riaza is currently being investigated in detail with A. Arribas. It is a special case involving bacteriogenic reduction of sulfate in a lake that permits the enrichment of residual sulfate in both ^{34}S and ^{18}O as shown in Figure 8a. The δD-$\delta^{18}O$ values of halloysites from Creede and Riaza and supergene kaolinites from Rodalquilar fall close to, but to the left of, the *kaolinite line*.

Stable isotope systematics of alunites and kaolinites from the Tolfa District, Latium, Italy: an example of steam-heated acid-sulfate alteration with unequilibrated SO_4-H_2S

The Tolfa district, approximately 60 kilometers northwest of Rome, has been mined for alunite since the mid-Fifteenth Century and for base metals since Roman times. Today kaolinite is mined for the cement industry. The district, described by Lombardi and Mattias (1979), coincides with a 25 km^2 Pliocene-Pleistocene silicic volcanic complex that overlies a lithologically variable Cretaceous-Oligocene flysch sequence capped by an erosional remnant of an interbedded continental and marine Pliocene sedimentary section including evaporites. The volcanic rocks are extensively altered, and small base-metal deposits occur in the sedimentary basement rocks. Alunite often occurs as nearly pure earthy masses in veins up to two meters wide. Field and Lombardi (1972) reported sulfur isotope data from these deposits and the actual samples used by them in their study were given to us by Cy Field. They favored a supergene origin because of extensive oxidation of sulfides at some areas, the presence of halloysite with alunite, and the fact that alunite is observed replacing sulfide. They admitted, however, that the geologic evidence did not permit discrimination between a supergene origin and an origin involving the oxidation of H_2S (our steam-heated environment). Some supergene alunite undoubtedly occurs in the Tolfa district, especially where it is associated with halloysite. However, as kaolinite and dickite are more abundant than halloysite it is likely that most of the alunite formed in a steam-heated environment.

Our stable isotope data on alunite, along with the sulfur data of Field and Lombardi (1972) and hydrogen and oxygen isotope data of Lombardi and Sheppard (1977) for associated kaolinites are presented in Figure 9a-b. These data clearly establish a steam-heated origin for most of the samples. The $\delta^{34}S$ values are within the range of pyrite observed in the altered volcanics. The large $\delta^{34}S$ values for both pyrite and alunite probably reflect the contribution of sulfur from the basement sediments (Field and Lombardi, 1972). Most $\delta^{18}O_{SO4}$ values are to the right of the SASF and all $\delta^{18}O_{OH}$ values plot outside the SAOZ. With one exception, the $\Delta^{18}O_{SO4\text{-}OH}$ values give temperatures in the range of 80 to 180 °C. When these temperatures are used to calculate the δD_{H2O} and $\delta^{18}O_{H2O}$ of the fluids from the $\delta^{18}O_{SO4}/\delta^{18}O_{OH}$ data, all but two of the values fall close to the meteoric water line and to the value for modern spring water in the area. Since the composition of meteoric water is such an important reference it can be argued: a) that most of the fluids were unexchanged meteoric waters, b) that aqueous sulfate was close to ^{18}O equilibrium with the fluids and, c) that substantial retrograde exchange in the OH site did not occur. The one sample whose fluid plots to the left of the meteoric water line must reflect ^{18}O disequilibrium between aqueous sulfate and water or a poor analysis. Finally, the isotopic compositions of kaolinites are substantially removed from the *kaolinite line* and are consistent with a steam-heated origin within the temperature range defined by the alunite isotope data. It is noteworthy that the data imply that, in most cases, dissolved sulfate reached ^{18}O but not ^{34}S equilibrium with the fluid. Reference to Ohmoto and Lasaga's (1982) data for sulfur isotope exchange rates for aqueous sulfur species implies that the residence time for aqueous sulfate was less than a few hundred days.

Stable isotope systematics of replacement alunites surrounding the Central mining area, Marysvale, Utah: an example of steam-heated acid-sulfate alteration with equilibrated SO_4 - H_2S

The replacement alunite deposits at Marysvale, Utah, have most recently been described by Callaghan (1973) and Cunningham et al. (1984). The alunite replaces intermediate composition volcanic rocks in several hydrothermally altered areas, roughly circular in plan and up to 3 km diameter clustered around the 23 Ma Central Intrusive. K/Ar ages of alunite are coincident with that of the Central Intrusive which hosts the uranium deposits of the Central mining area (Steven et al., 1979). In each area the alteration is zoned vertically from a flooded silica cap down through a hematite zone, then a jarosite zone, into an alunite zone, and finally into a propylitic zone. The alunite zone is ringed laterally by a kaolinite zone (Cunningham et al., 1984). From this geologic evidence it is clear that the alunite formed in a steam-heated environment of a fossil geothermal system. The stable isotope data of alunite from six different replacement deposits are shown in Figure 10a-b. The $\delta^{34}S$ values for alunites are much larger than those of all of the pyrites in the underlying propylitic zone, but it is not certain that these minerals formed at the same time. The sulfur isotope data may represent: 1) different sources of sulfur for the alunite and pyrite as proposed by Cunningham et al. (1984), or 2) near-equilibrium exchange of the sulfate with the H_2S in the system. The latter possibility is the most likely. $\Delta^{18}O_{SO4\text{-}OH}$ values are very consistent and give temperatures ranging from 90° to 160°C. Independent temperature information on these samples is not available, but the temperatures are reasonable for alunite formation in steam-heated environments. The calculated temperatures imply that both $\delta^{18}O_{SO4}$ and $\delta^{18}O_{OH}$ values of the alunites were in equilibrium with exchanged meteoric waters. $\delta^{18}O_{H2O}$ values calculated from the $\Delta^{18}O_{SO4\text{-}OH}$ range from -7 to 0‰. The individual hydrothermal systems were evidently rock-dominated and alteration fluids were exchanged meteoric water. The approach to sulfur as well as oxygen isotopic equilibrium between sulfate and fluid indicates that the integrated time-temperature regime of the hydrothermal systems was greater than for the Tolfa district. Note (Figure 10b) that the δD values of Marysvale alunite are reasonable for compositions of meteoric water in the area, that the $\delta^{18}O_{SO4}$ - δD values of alunite fall to the right of the SASF and that most of the $\delta^{18}O_{OH}$ - δD values fall outside the SAOZ.

Stable isotope systematics alunite and kaolinite in the Julcani district, Peru: an example of of magmatic-hydrothermal acid-sulfate alteration in a nearly pure magmatic water system

The Julcani district contains zoned Ag-Cu-Pb±W±Bi±Au veins associated with a Miocene dacitic dome complex that developed on a thick section of Paleozoic sediments (Petersen et al., 1977; Deen et al.,1987, 1988). Mineralization occurred within 0.5 m.y. of latest dome formation and was interrupted by emplacement of an anhydrite-bearing dacite dike. Pre-ore acid-sulfate alteration in the center of the district produced zones with vuggy silica cores and successive alunite+quartz+pyrite and kaolinite+quartz+pyrite envelopes that extend downward at least 400 m (Deen et al., 1988). The acid-sulfate alteration was followed by the emplacement of radiating swarms of tourmaline-pyrite breccia dikes cemented by quartz containing saline fluid inclusions. Several centers of mineralization developed in reactivated regional structures following the emplacement of an anhydrite-free dacite dike in a fracture most likely related to an underlying intrusion. The ore fluids can be shown by hydrogen and oxygen isotope evidence to have been derived from a magma that had a composition similar to the magmas that produced the earlier biotite-bearing dacitic domes, and mineralization can be shown to be largely the result of mixing of the magmatic fluids of δD ~-50 ‰ with isotopically light meteoric water of δD ~-140 ‰ (Deen et al., 1987; 1988). Calculated δD_{H2O}-$\delta^{18}O_{H2O}$ values for fluids in equilibrium with alunite, as shown in Figure 11a-b, are nearly identical to those values calculated for fluids in equilibrium with the igneous biotites and to those measured from inclusion fluids in vein minerals (Deen 1990). Associated wall rock kaolinites have lower δD values but similar $\delta^{18}O$ indicating that the kaolinites formed where magmatic fluids were diluted by highly exchanged meteoric water. Late-stage vein kaolinite has a δD of -90‰ reflecting even more meteoric water involvement. Temperatures calculated from sulfur isotope fractionation between coeval pyrite and alunite range from 210° to 263°C with a mean of 242°C. $\delta^{34}S$ values of alunite and pyrite in the acid-sulfate alteration are similar to those for barite and sulfide minerals in the vein mineralization, respectively. This indicates that $\delta^{34}S_{\Sigma S}$ (~5 ‰) and H_2S/SO_4 (~6:1) was similar for both pre-ore acid-sulfate alteration and mineralization. The one $\Delta^{18}O_{SO4-OH}$ value gives an unreasonably high temperature of 560°C indicating that OH in alunite exchanged with the fluid as the deposit cooled.

Stable isotope systematics of alunite and kaolinite in the Summitville, Colorado Cu-Au-Ag deposit: an example of magmatic-hydrothermal acid-sulfate alteration in a mixed magmatic-meteoric water system

The acid-sulfate alteration at the Summitville, Colorado, Au-Cu-Ag deposit has been described by Steven and Ratté (1960) and its genesis recently discussed by Stoffregen (1987). At Summitville, irregular pipes and lenticular pods of vuggy silica, some of which are developed vertically over 300 meters and reach thickness of up to 70 meters, are enclosed sequentially by zones of quartz-alunite, quartz-kaolinite and clay alteration. Mineralization occurred in the vuggy silica zones subsequent to the acid-sulfate alteration. A more comprehensive interpretation of the stable isotope data by Rye et al. (1990) is summarized here. Stable isotope data are presented in Figure 12a-b. Temperatures measured from sulfur isotope fractionations of coeval alunite and pyrite permit calculation of fluid compositions and reconstruction of a geothermal gradient. The large $\delta^{34}S$ values for the alunites support Stoffregen's (1987) conclusion that the acid-sulfate alteration resulted from the attack on the wall rocks by H_2SO_4 derived from the disproportionation of SO_2. The large δD and $\delta^{18}O_{SO4}$ values support the derivation of the SO_2 from a magma. However, the range of these values is larger than for Julcani (shown above) and the lowest δD values correlate with the lowest $\delta^{18}O_{SO4}$ values indicating that the disproportionation of some of the SO_2 occurred in mixtures of magmatic and meteoric water. H_2S/SO_4 of fluids during both acid-sulfate alteration and later mineralization was about 4±2 and $\delta^{34}S_{\Sigma S}$ was about 2±2 ‰. The positive correlation between $\delta^{34}S$ and $\delta^{18}O_{SO4}$ of alunite, evident in Figure 12a reflects a temperature range of alunite formation of about 400 to 200 °C. All $\delta^{18}O_{OH}$ values are larger than fluid $\delta^{18}O_{H2O}$ calculated from $\delta^{18}O_{SO4}$, and all $\Delta^{18}O_{SO4-OH}$ values give temperatures that are higher than depositional temperatures determined by alunite-pyrite sulfur isotope fractionations. Furthermore, $\Delta^{18}O_{SO4-OH}$ values show an inverse correlation with temperatures of deposition. These results indicate retrograde exchange between fluid and OH in alunite as the deposit cooled (c.f. Figure 19). The low δD values of the wall- rock kaolinites from the quartz-kaolinite zone indicate that contemporaneous kaolinite formation was related to even greater dilution of the low pH magmatic fluids by low-δD meteoric water. δD values for vein kaolinites accompanying subsequent enargite-covellite mineralization are substantially lower than those for earlier wall rock kaolinites indicating that the later mineralizing fluids were dominated by exchanged meteoric water.

Stable isotope systematics of the vein alunite deposits at Alunite Ridge southwest of Marysvale, Utah: the classic example of magmatic-steam alunite

The vein alunite deposits of Alunite Ridge have been described by Callaghan (1973) and their origin discussed by Cunningham et al. (1984). They occur in the Tushar Range about 15 km southwest of the replacement alunite deposits, but are not related to them in origin. This type of alunite deposit is rare and those along Alunite Ridge are the largest, purest, most coarsely crystalline veins of alunite in the U.S. Alunite Ridge is located at the center of a radial fracture pattern interpreted to have resulted from the forceful injection of an underlying stock believed to contain porphyry-type mineralization (Beaty et al., 1986). The veins, which contain virtually no coeval quartz, pyrite or kaolinite formed 14 m.y. ago as open-space fillings in extension fractures as much as 20 m wide and 100 m deep. They are hosted by volcanic rocks that are pervasively alunitized adjacent to the veins and kaolinitized away from them and contain small amounts of pyrite. Fluid-inclusion evidence indicates that the alunite formed from low-density vapor (Cunningham et al., 1984). From the descriptions of Callaghan, (1973), Cunningham et al., (1984) and Beaty et al. (1986) the alunites at Alunite Ridge may have formed at depths of as much as a kilometer, although the geologic evidence does not provide tight constraints.

The stable isotope data are summarized in Figure 13a-b. The δD values are nearly constant and indicate a large magmatic component in the fluids. These values are substantially larger than those for the replacement alunites near the Central mining district (see above). The $\delta^{34}S$ values of the alunite are very tightly clustered near 0‰. They must represent quantitative oxidation of the sulfur in the system because they are the same as the bulk sulfur in the fluids, believed to have been derived from the underlying stock, responsible for the nearby Deer Trail Mountain manto deposits (Cunningham et al., 1984; Beaty et al., 1986). The $\delta^{18}O_{SO4}$ values are also tightly clustered and typical of magmatic sulfates. The $\delta^{18}O_{OH}$ values are in the lower part of the range observed for magmatic-hydrothermal alunites. The above isotope systematics are what would be predicted for alunite formed from a vapor phase released at high temperature and low pressure from a silicic magma chamber. However, the $\delta^{18}O_{OH}$ are too light by 3 to 4‰ relative to $\delta^{18}O_{SO4}$ to represent equilibrium values for alunites formed from a magmatic vapor phase. Furthermore, $\Delta^{18}O_{SO4\text{-}OH}$ values give unreasonably low temperatures ranging from 200° to 40 °C for the presumed deep origin. The large grain size of the alunite and the tightness of the vein structure effectively rule out the possibility that the low values resulted from post-depositional exchange with isotopically lighter fluids. At a presumed depth of a kilometer it is hard to image oxidation of the sulfur in the fluid by atmospheric oxygen. Since pyrite is present in only small amounts in the alunitized wall rocks, and not at all in the alunite veins, it seems unlikely that oxidation of SO_2 to aqueous sulfate occurred by disproportionation of SO_2 during vein-filling. However, it is possible that disproportionation of SO_2 did occur in the adjacent wall rocks. Clearly, there is much we do not understand about the oxidation processes or the precipitation mechanism of alunite at Alunite Ridge. Perhaps the $\delta^{18}O_{SO4}$ values reflect equilibration of the SO_2 with the fluid at higher temperatures below the level of deposition while the $\delta^{18}O_{OH}$ values reflect a decrease in the $\delta^{18}O_{H2O}$ of the fluids at the time and temperature of formation. Such a situation is perhaps possible in a dynamic vapor transport system, but would seem to require at least some SO_3 or SO_4 and a high SO_2/H_2O ratio in the vapor. A better understanding of transport and precipitation mechanisms of alunite in magmatic vapor environments is required to evaluate such an interpretation and detailed study of the Alunite Ridge deposits should be a fruitful area of research. In any event, at this time it seems most probable that, the quantitative oxidation of sulfur in the Alunite Ridge system was due to the release of the vapor plume from the magma at sufficiently high temperatures and low pressures that SO_2 was by far the dominant sulfur species, and that transport and deposition of alunite was rapid enough to prevent reduction of SO_2 on cooling. Most of the $\delta^{34}S$ data are from Cunningham et al. (1984). The $\delta^{18}O_{SO4}$, $\delta^{18}O_{OH}$, and δD data are from the same samples used by Cunningham et al. (1984).

Stable isotope systematics of alunites and kaolinites of the Cactus gold deposit, California : an example of acid-sulfate alteration overlying adularia-sericite type mineralization

The Cactus gold deposit is an example of acid-sulfate alteration overlying, in part, an adularia-sericite type base- and precious-metal vein system. Approximately 100,000 ounces of gold were produced between 1934 and 1952, primarily by underground exploitation of the adularia-sericite veins (Troxel and Morton, 1962). Theses by Jordon (1941) and Smith (1941) provide early descriptions of the geology and ore deposits, with emphasis on the deep vein ores. The deposit is currently under production by Coca Mines, developing proven reserves of approximately 370,000 ounces of gold in the acid-sulfate zone by open pit operations. The district is situated in the western Mojave desert about 15 kilometers south of the Garlock fault and about 35 kilometers northeast of its intersection with the San Andreas fault. The deposit occurs in the Middle Buttes volcanic complex, an early Miocene quartz latitic to rhyolitic dome field. The geology and alteration of the complex has been studied recently by Bottaro (1987). The age of volcanism has not been determined, but nearly identical rocks at Soledad Mountain about 3 kilometers east of the Middle Buttes complex were erupted from 21.5 to 16.9 Ma (McCusker, 1982). Bottaro (1987) reports a K/Ar age on fine-grained alunite of 18.4 Ma, suggesting that the alteration is roughly coincident with volcanism. The highest gold values occur near the alunite-dominant zone. Alunite occurs in several forms: 1) as very fine-grained, blanket-like, but structurally controlled, bodies, often intermixed with kaolinite, 2) as coarse veins and veinlets cutting alunitized and kaolinitized wall rock, and 3) as coarse vein- and volcanic-breccia-filling without significant amounts of kaolinite. The latter occurrence does not appear to be related to mineralization.

The study of the Cactus deposit is in preliminary stages and interpretations are tentative. The stable isotope data on alunite, pyrite and kaolinite are summarized in Figure 14a-b. On textural and morphological grounds we anticipated that the data for coarse alunites would reflect a magmatic-steam origin while the data for the other alunites would reflect a steam-heated origin. However, the alunite data from each of the three occurrences noted above fall on a trend that suggests a common origin and indicates that they are probably of mixed magmatic-steam and exchanged steam-heated or possibly magmatic-hydrothermal origin. The δD values of alunites are significantly larger than those of kaolinite and suggest that the alunite fluids contained a magmatic component and mixed with meteoric waters. The calculated $\delta^{18}O_{H2O}$ values for the alunite fluids indicate a significant meteoric component. The $\delta^{34}S$ values of alunite are larger than the one value obtained for pyrite but are still much smaller than expected for values from magmatic-hydrothermal acid-sulfate alteration where the aqueous sulfate is derived from disproportionation of SO_2. The $\delta^{34}S$ values show an inverse correlation with both $\delta^{18}O_{SO4}$ and $\delta^{18}O_{OH}$ and, although not plotted, barite isotope data fall on the projection of the trend to lower values. The $\Delta^{18}O_{SO4-OH}$ values give temperatures ranging from 110 to 150°C which are reasonable for such a shallow environment. In contrast to the magmatic-steam deposits of Alunite Ridge, the alteration at Cactus appears to have taken place near the ground surface, and the near quantitative oxidation of sulfur species in the hydrothermal system at Cactus may have involved entrained atmospheric oxygen. The correlation of $\delta^{34}S$ and $\delta^{18}O$ values observed in Figure 14a may reflect the mixing of aqueous sulfate derived from the oxidation of SO_2 and H_2S in the fluid at the surface with aqueous sulfate that at least partially equilibrated with H_2S in the fluid at depth. Detailed studies of the deposit currently underway should greatly clarify our interpretation of the stable isotope systematics.

Stable isotope systematics of alunites from Red Mountain, Lake City, Colorado: an example of magmatic-hydrothermal acid-sulfate alteration cut by later magmatic-steam alunite

The alunite deposit at Red Mountain, Lake City, Colorado has recently been described, and its origin discussed, by Bove et al. (1988, 1990). Stable isotope data are summarized in Figure 15a-b. The deposit, which is one of the largest in the U.S., consists of two roughly conical centers with roots extending more than 250 meters beneath the surface. Alunite+quartz+pyrite rock changes outward into argillized and propylitized dacitic volcanics and downward through argillic, sericitic, and potassic zones in dacite intrusions. The acid-sulfate alteration does not appear to be accompanied by gold-enargite mineralization, but drilling indicates a molydenum-bearing porphyry system at depth. Detailed mineralogic studies within the quartz-alunite zone indicate at least 4 stages of alunite deposition. The earliest stage (stage 1) is characterized by replacement of feldspar phenocrysts by very fine-grained alunite±quartz and the development of some pyrite, quartz, and alunite in the groundmass. Stage 1 alunite underwent extensive dissolution prior to the precipitation of stage 2. Stage 2 is characterized by multiple generations of void-and microfracture-filling alunite with minor quartz and pyrite. Stage 3 comprises alunite ± minor quartz veins up to 5 cm thick which are concentrated in areas of hydrothermal brecciation. Stage 4 has very limited distribution and is characterized by smaller veins of almost pure coarse, banded alunite. The geologic and mineralogic relations and stable isotope data indicate that stage 1 and 2 alunite are of magmatic hydrothermal origin and stage 3 and 4 alunite of magmatic-steam origin.

Sulfur isotope data on coeval alunite and pyrite have been interpreted (Bove et al., 1990) to indicate bulk $\delta^{34}S$ of ~0‰ and temperatures of ~400° and ~200°C and H_2S/SO_4 ~1 and ~8, for stage 1 and 2 fluids, respectively. Calculations based on the $\delta^{18}O_{SO4}$ values indicate the $\delta^{18}O_{H2O}$ of fluid was ~4‰ for stages 1 and 2. The large $\delta^{34}S$ values for stage 1 and 2 sulfates indicate they were derived from the disproportionation of SO_2. The δD values (-66 to -81‰) of the alunite indicate derivation from magmatic fluids, especially when compared with those for kaolinite (-124 to -135‰) on the margins of the deposit and sericite (-105 to -120‰) at depth (Bove et al., 1990). $\delta^{18}O_{OH}$ values for a given stage are remarkably consistent. $\Delta^{18}O_{SO4\text{-}OH}$ values of both stage 1 and stage 2 alunites range from about 4.5 to 8.3‰ and give temperatures ranging from 100 to 370°C. The cause of the large variation of $\Delta^{18}O_{SO4\text{-}OH}$ values for a given stage is not understood, but may be related to the dissolution of stage 1 alunite. $\delta^{18}O_{OH}$ of stage 1 and 2 alunites are fairly uniform over a range of $\delta^{18}O_{SO4}$ values. The difference between average $\delta^{18}O_{OH}$ for stages 1 and 2 is about the same as the change in the $\Delta^{18}O_{alunite(OH)\text{-}water}$ between 400 and 200°C. This suggests that the trend of $\delta^{18}O_{SO4}$-$\delta^{34}S$ values may reflect not continually decreasing temperature, but, the mixing of stage 2 sulfate with unequilibrated aqueous sulfate derived from the dissolution of stage 1 alunite. The $\delta^{18}O_{OH}$ values were fixed during deposition by equilibrium exchange with fluids at ~200 °C.

The stable isotope systematics of stage 3 and 4 alunites from Lake City, Colorado are similar to those for Alunite Ridge near Marysvale, Utah and virtually identical to those for Cactus. The $\delta^{34}S$ values of stage 3 and 4 alunites are close to the 0 ‰ value for bulk sulfur in the magmatic system at Red Mountain as defined by sulfur isotope data on stage 1 and 2 and on disseminated pyrite in the sericitic alteration related to the deep porphyry system. As in stages 1 and 2, the large δD values of the alunites require a magmatic origin for the fluids. The $\Delta^{18}O_{SO4\text{-}OH}$ values for stage 3 and 4 alunites yield temperatures 80° to 150°C. We interpret the Red Mountain system to have evolved from magmatic-hydrothermal to a magmatic-steam system. This interpretation is consistent with the monomineralic nature of stage 3 and 4 alunites and the association of stage 3 alunites with hydrothermally brecciated parts of the area.

Stable isotope systematics alunite and kaolinite at El Salvador, Chile: an example of magmatic-hydrothermal acid-sulfate alteration associated with porphyry type mineralization and later supergene acid-sulfate alteration

The geology and geochemistry of the El Salvador porphyry copper deposit have been described in a series of classic studies (Gustafson and Hunt, 1975; Field and Gustafson, 1976; Sheppard and Gustafson, 1976). The deposit formed at the culmination of volcanic and hydrothermal activity that ended about 41 Ma. Advanced argillic alteration assemblages containing alunite and, where preserved, pyrite are strongly developed at high elevations in post ore pebble dikes. These alunites have K-Ar dates of about 39 Ma and are considered to be nearly contemporaneous with the latest intrusive event (Gustafson and Hunt, 1975). The stable isotope data are summarized in Figure 16a-b. The large $\delta^{34}S$ values of the hypogene alunite and magmatic δD values (Sheppard and Gustafson, 1976) indicate that the sulfate was derived from disproportionation of magmatically derived SO_2. The two $\Delta^{18}O_{SO4-OH}$ values give temperature of 400 to 590°C compared to a maximum temperature of about 420° C calculated from the minimum $\Delta^{34}S_{alunite-pyrite}$ of Field and Gustafson (1976). This, plus the fact that the temperatures are close to or above the upper stability of alunite, suggests that retrograde exchange occurred in the OH site. At these temperatures, D and ^{18}O fractionations between alunite and water are small so that primary δD-$\delta^{18}O_{OH}$ values are very close to δD_{H2O}-$\delta^{18}O_{H2O}$ of the fluid. Fluid compositions so calculated are similar to those calculated by Sheppard and Gustafson (1976) for some of the earlier vein alteration assemblages.

Alunite also occurs in supergene enrichment zones that formed the commercial ore body and has been dated at about 36 Ma (Gustafson and Hunt, 1975). These alunites exhibit typical supergene isotope systematics as do supergene kaolinites reported by Sheppard and Gustafson (1976). The δD values of these alunites are in the range of the 36 Ma meteoric waters calculated by Sheppard and Gustafson (1976), consistent with the near 0 permil fractionation of hydrogen between alunite and water at low temperatures (Bird et al., 1989). However, the $\delta^{34}S$ values of some of the supergene samples are substantially larger than precursor sulfides and may indicate enrichment of supergene fluids in ^{34}S (along with ^{18}O) as a result of bacteriogenic reduction of sulfate in standing pools of water. The $\delta^{34}S$ of values of sulfides and alunite are from Field and Gustafson (1976). The δD and $\delta^{18}O_{SO4}$ and $\delta^{18}O_{OH}$ data in this study are from the same samples. The δD and $\delta^{18}O$ of kaolinite are from Sheppard and Gustafson (1976).

Stable isotope systematics of alunites and kaolinites from the Rodalquilar gold-alunite deposit, Almeria, Spain: an example of magmatic-hydrothermal acid-sulfate alteration with later supergene acid-sulfate alteration

The Rodalquilar gold-alunite deposit (Almeria, S.E. Spain) has recently been studied by Rytuba et al. (1988) and Arribas et al. (1989). Au - Ag bearing chalcedony veins fill ring and radial fractures associated with a Miocene caldera. Mineralization is associated with a central zone of acid-sulfate alteration (stage 1 alunite) that extends several hundred meters below the surface and contains cores of vuggy silica. K/Ar ages of stage 1 alunites and associated illites average 10.8 Ma. This central zone is surrounded by younger, barren alunite-jarosite veins (stage 2 alunite). Most of these veins are shallow, but barren veins of alunite have also been recognized at deeper levels. Stable isotope data are summarized in Figure 17a-b. Stage 1 alunite formed in a magmatic-hydrothermal environment. Sulfur isotope data on coexisting pyrite and alunite give temperatures ranging from 220° to 370° C. $\Delta^{18}O_{SO4-OH}$ values of stage 1 alunites give temperatures ranging from 350° to 550 °C indicating substantial retrograde exchange in the OH site. The large $\delta^{34}S$ values for the stage 1 alunite and pyrite reflect the large $\delta^{34}S_{\Sigma S}$ value for the hydrothermal system (typical of Miocene hydrothermal systems in the southern coastal regions of Spain). δD values of alunite range from -15 to -26 ‰. These values are larger than those considered typical of magmatic waters and reflect the proximity of the area to the ocean and possible involvement of sea water in the magmatic system. δD values of two samples of stage 1 wall rock kaolinites are -36 and -39 ‰; slightly lower than those for adjacent alunites and consistent with the involvement of highly exchanged meteoric water in the formation of the kaolinite.

Stage 2 alunites have been dated at about 3.5 Ma (A. Arribas written comm., 1990) and the stable isotopic data are diagnostic of a supergene origin. $\delta^{34}S$ values are slightly larger than but overlap the range of values for pyrite in the mineralized zone. $\delta^{18}O_{OH}$ values fall within the SAOZ and the $\Delta^{18}O_{SO4-OH}$ values are negative. Also, the δD-$\delta^{18}O_{SO4}$ values lie within the SASF. In addition, δD values of coeval stage 2 kaolinites range from -41 to -72 ‰. The -61 to -72‰ supergene kaolinites are compatible with formation from present day meteoric water compositions. However, the δD values of the -41‰ supergene kaolinite and all of the supergene alunites indicate formation from waters isotopically heavier than present day meteoric water. Causes of these differences are currently being investigated by A. Arribas.

Stable isotope systematics of alunite in the Buckskin National and Goldfield deposits and pervasive alunite alteration in western Virginia Range: examples of diverse types of acid-sulfate alteration in Miocene volcanic rocks in Nevada

Figure 18a-b summarizes the isotope data on alunite from acid-sulfate alteration associated with three major Miocene hydrothermal centers in Nevada: the magmatic-hydrothermal and later supergene alteration in the Goldfield district, the pervasive magmatic-hydrothermal quartz-alunite alteration in the Virginia Range, and the steam-heated alteration at the Buckskin deposit in the National district. These areas have recently been studied by Peter Vikre and colleagues and he supplied all of the samples except those from Goldfield which were supplied by Roger Ashley. The data are grouped together because only a few samples were analyzed from each district, and because the data are from diverse acid-sulfate environments each of which has well defined stable isotope systematics.

The Goldfield district has produced over 4 million ounces of gold from altered Miocene volcanic rocks. The district has been described by Ransome (1909), Albers and Stewart (1972) and Ashley (1974) and has been the subject of stable isotope studies by Jensen et al. (1971), dating studies by Ashley and Silberman (1976), and fluid inclusion and stable isotope studies by Vikre (1989a). The ore zones and alteration assemblages at Goldfield are similar to those at Summitville with Au+Cu±Ag ores occurring in vuggy silica, with envelopes of intense kaolinite-alunite alteration. Jensen et al. (1971) demonstrated the presence of both hypogene and supergene alunite at Goldfield on the basis of $\delta^{34}S$ data. Ashley and Silberman (1976) dated the hypogene alunites at about 20 Ma, nearly coeval with the host volcanics, and the supergene alunites at about 10 Ma. The alunite of both origins are clearly identified from our isotope data in Figure 18a-b. The large $\delta^{34}S$ of the single sample (R9-25) of hypogene alunite is consistent with values observed by Jensen et al. (1971) and Vikre (1989a) and is typical of alunites formed in magmatic-hydrothermal environments from the disproportionation of SO_2. The low $\delta^{18}O_{SO4}$ and δD indicates that the disproportionation of SO_2 occurred in predominantly meteoric waters. The $\Delta^{18}O_{SO4\text{-}OH}$ value gives a temperature of 230 °C in the range of fluid inclusion filling temperatures and pyrite-alunite sulfur isotope temperatures for the Sandstorm-Kendell deposit 3 kilometers northwest of the sample location (Vikre, 1989a). The low $\delta^{34}S$ values of two samples of later alunite are in the range of values for precursor sulfides and are consistent with formation in a supergene environment. The δD-$\delta^{18}O_{OH}$ values for these samples plot within the SAOZ and their $\Delta^{18}O_{SO4\text{-}OH}$ values are negative, almost certainly indicating a supergene origin. The δD values of the secondary alunite are larger than that for the magmatic hydrothermal alunite, indicating either extensive evaporation of meteoric water or a regional increase in the δD of meteoric water over the interval 21 to 10 Ma. The presence of large lakes in the area during the interval 17 to 5 Ma suggest that the first possibility is more likely (B.R. Berger, personal comm., 1991).

Widely distributed, pervasive quartz-alunite alteration of lower to middle Miocene volcanic rocks in the western part of the Virginia Range adjacent to and north of Virginia City, Nevada, has recently been discussed by Vikre (1989b). Recent dating of alunites indicates two age groups of 14 to 17 and 9 to 10 Ma for the alteration throughout the Virginia Range (Vikre et al., 1988). In the Virginia City area, the 14-17 Ma quartz-alunite alteration is earlier than the lode mineralization which produced the famous bonanza ores of the Comstock mining district. In the Ramsey mining district to the north, however, precious-metal mineralization was apparently coeval with 9.3 Ma quartz-alunite alteration. In other parts of the Virginia Range, alunite alteration occurs without apparent metallic mineralization. With the exception of the 10.0 Ma quartz-alunite occurrence from Long Valley, 22 Km north of Virginia City, the alunites in the pervasively altered volcanics in the western Virginia Range have large $\delta^{34}S$ values and are magmatic-hydrothermal in origin. The wide range of $\delta^{18}O_{SO4}$ values and the low δD values for these alunites indicate that much of the disproportionation of SO_2 took place in meteoric water. The stable isotope systematics for the Long Valley alunite are much different from the others and suggest a steam-heated origin for the quartz-alunite alteration at that locality. Our analyses are of the same samples used by Vikre et al. (1988) for dating the alteration in the Virginia Range.

The National district has been well documented by the comprehensive studies by Vikre (Vikre, 1985 and 1987). A 75-meter thick quartz+alunite+pyrite zone underlies an ~75-meter thick zone of cinnabar-bearing chalcedonic sinter. The quartz+alunite+pyrite zone grades downward into a quartz+kaolinite+pyrite zone. These zones overlie base- and precious-metal veins of the adularia-sericite type with kaolinite-dominated alteration selvages adjacent to the vein. K/Ar dating of alunite and vein-related muscovite yield concordant ~15 Ma ages. The stable isotope data indicate a steam-heated origin consistent with the geologic and geochronologic data. $\delta^{34}S$ values of the two alunites analyzed fall in the upper range of values for associated pyrite. $\delta^{18}O_{SO4}$ values fall to the right of the SASF and would be in equilibrium (at 100°C) with exchanged meteoric water of $\delta^{18}O$ = ~-3.5‰. Kaolinite data from the quartz+kaolinite+pyrite zone beneath the quartz+alunite+pyrite zone are from Vikre (1987) and fall to the left of the kaolinite line as predicted. The $\Delta^{18}O_{SO4\text{-}OH}$ values give a temperature of range 80° to 90 °C.

EQUILIBRIUM AND KINETIC PROCESSES AND RETENTION OF PRIMARY STABLE ISOTOPE VALUES IN ALUNITE

The stable isotope systematics of alunite reflect a combination of equilibrium and kinetic processes that operate on four isotope exchange reactions:

$$2KAl_3(SO_4)_2(OH)_9 + 9D_2O = 2KAl_3(SO_4)_2(OD)_9 + 9H_2O \qquad (6)$$

$$2KAl_3(SO_4)_2(O^{16}H)_9 + 9H_2O^{18} = 2KAl_3(SO_4)_2(O^{18}H)_9 + 9H_2O^{16} \qquad (7)$$

$$S^{32}O_{4(aq)} + H_2S^{34}{}_{(aq)} = S^{34}O_{4(aq)} + H_2S^{32}{}_{(aq)} \qquad (8)$$

$$SO_4{}^{16}{}_{(aq)} + 4H_2O^{18} = SO_4{}^{18}{}_{(aq)} + 4H_2O^{16} \qquad (9)$$

The degree to which these exchange reactions approach equilibrium, and the degree to which primary isotope values are preserved, varies for different environments and provides the isotopic basis for distinguishing between them. This is illustrated in Figures 19a-b and 20a-b where isotope fractionations noted for each alunite-forming environment are compared to the equilibrium values predicted from the appropriate experimental isotope fractionation curve.

Alunites from all environments probably precipitate in hydrogen and OH oxygen isotopic equilibrium with the parent fluid. However, these isotopes are also the most susceptible to post-depositional exchange between alunite and later fluids. Experimental studies have shown that fine-grained alunites are susceptible to hydrogen isotope (and by implication oxygen isotope) OH exchange at low temperatures (Stoffregen et al., 1990). We have not found examples of such low temperature exchange in our studies. Our data do indicate that OH oxygen (and by implication hydrogen) in coarser alunites is susceptible to retrograde exchange during the cooling of high-temperature fluids in magmatic-hydrothermal environments. Since ^{18}O fractionation between OH-site in alunite and water is significant, retrograde exchange has an important effect on the $\Delta^{18}O_{SO4\text{-}OH}$ of magmatic-hydrothermal alunites during the cooling of high-temperature fluids. However, since the deuterium fractionation between alunite-water is small at all geologic temperatures, retrograde exchange will not change the δD values of magmatic-hydrothermal alunite unless the composition of the fluid changes. Such changes in δD have not been documented in our examples. (However, low temperature kaolinite-water hydrogen isotope fractionations are larger than those for alunite-water and fine-grained high-temperature kaolinites may be susceptible to δD decreases as large as 30 ‰ as the hydrothermal system cools (Kharaka and O'Neil, 1978)).

Fields for $\Delta^{18}O_{SO4\text{-}OH}$ values of alunites from steam-heated, magmatic-steam and supergene environments and data points from the magmatic-hydrothermal Summitville deposit are plotted versus measured or estimated temperatures of formation in Figure 19a, and against $\Delta^{18}O_{SO4\text{-}OH}$ values predicted from equilibrium fractionation curves calculated for those temperatures in Figure 19b. The $\Delta^{18}O_{SO4\text{-}OH}$ values of magmatic-hydrothermal alunites from Summitville (and all other magmatic-hydrothermal deposits, although not plotted) give temperatures that are lower than predicted from the depositional temperatures calculated from $\delta^{34}S_{alun\text{-}py}$ values.. Significant increase in $\delta^{18}O_{OH}$ values of alunites during cooling of the deposit is well documented from the study of the Summitville deposit (Rye et al., 1990). There the $\Delta^{18}O_{SO4\text{-}OH}$ values of alunite vary as a function of depositional temperature as calculated from alunite-pyrite sulfur isotope fractionations; alunites formed at the highest temperatures have the smallest $\Delta^{18}O_{SO4\text{-}OH}$ values (Rye et al., 1990). The temperature at which retrograde exchange in the OH site is complete probably varies with the grain-size of primary alunites and the cooling history of the system.

$\Delta^{18}O_{SO4\text{-}OH}$ values serve as valuable geothermometer for steam-heated environments and provide a tool for detailed studies of individual steam-heated deposits. Calculated temperatures from all steam-heated systems studied range from 90 to 160°C. The $\Delta^{18}O_{SO4\text{-}OH}$ values of alunites from shallow magmatic-steam environments (Cactus and Red Mountain, Lake City) also give reasonable depositional temperatures ranging 90 to 150°C. However, some $\Delta^{18}O_{SO4\text{-}OH}$ values from Alunite Ridge near Marysvale, presumably formed at deeper levels, are larger than we would expect from the presumed high temperatures of deposition. Although it appears that magmatic-steam alunites precipitated from steam derived directly from a magma, the composition, sulfur speciation, and reactions between sulfur species leading to sulfate, and the precipitation mechanism of alunite are not well understood. These alunites appear to precipitate from fluids in which the sulfate and water are not always in equilibrium. This disequilibrium presents important clues into the nature of the magmatic-steam environment.

$\Delta^{18}O_{SO4\text{-}OH}$ values of supegene alunites will almost always be in disequilibrium, and if negative, indicate that the alunite formed in a supergene environment or exchanged with low temperature ground water. $\delta^{18}O_{OH}$ values will always reflect equilibrium with the last fluid of equilibration and, along with δD values of alunite, can be used to determine the isotopic composition of the supergene fluids.

Sulfur isotope exchange between sulfate and sulfide in solution is kinetically inhibited because of the large valence difference between reduced and oxidized sulfur species. Sulfur isotope equilibrium between aqueous sulfur species is obtained only at the integrated time-temperatures present in the magmatic-hydrothermal environment (Fig 20a). Consequently, sulfur isotope equilibrium between alunite and pyrite is a distinguishing characteristic of the magmatic-hydrothermal environment and $\Delta^{34}S_{alun\text{-}py}$ values are an excellent geothermometer that can be used to determine the thermal structure and history of magmatic-hydrothermal acid-sulfate alteration. In all of the magmatic-hydrothermal deposits studied, temperatures calculated from alunite-pyrite fractionations give reasonable temperatures, and at Summitville and Julcani such calculated temperatures are consistent with fluid inclusion measurements.

In the steam-heated environment, an approach to sulfur isotopic equilibrium may be achieved between aqueous sulfur species where residence times of aqueous sulfate are fairly long. However, alunites in most steam-heated, and all magmatic-steam and supergene, environments are characterized by $\delta^{34}S$ values that indicate a lack of exchange between aqueous sulfate and sulfide. This is illustrated in Figure 20a where the sulfur isotope fractionation between alunite and pyrite or alunite and H_2S in the system are plotted versus against predicted fractionations based on measured or presumed depositional temperatures.

The low-pH environments of alunite formation promote oxygen isotope exchange between aqueous sulfate and water in the fluid. This is illustrated in Figure 20b where the ^{18}O fractionation between aqueous sulfate and water indicated by the $\delta^{18}O_{SO4}$ data on alunites from various environments are plotted versus predicted equilibrium values of

$\Delta^{18}O_{SO4\text{-}H2O}$ for those environments based on measured or presumed depositional temperatures. Disequilibrium between parent aqueous sulfate and water has not been observed in the isotope data of alunites from the magmatic-hydrothermal, magmatic-steam or steam-heated environments. Even in low-temperature sedimentary environments oxygen isotopic equilibrium between aqueous sulfate and water has been observed in standing pools of low-pH waters (Alpers et al., in press). Supergene alunites, however, are distinguished by $\delta^{18}O_{SO4}$ values not in equilibrium with parent fluids. The actual $\delta^{18}O_{SO4}$ values of supergene alunites are controlled by kinetic factors that reflect the hydrogeochemical environment of aqueous sulfate formation and detailed studies of the $\delta^{18}O_{SO4}$ of supergene alunites should reveal a great deal about processes operating in that environment.

SUMMARY AND CONCLUSIONS

SUPERGENE acid-sulfate assemblages may form over any sulfide mineralized zone (particularly those that are pyrite-rich) when it is raised above the water table by tectonics or exposed by erosion. Obviously, supergene assemblages may overprint other acid-sulfate assemblages, particularly magmatic-hydrothermal assemblages which are pyrite-rich. Supergene alunite can often be recognized by K-Ar dating. The stable isotope data can provide diagnostic indicators of supergene origin. Negative $\Delta^{18}O_{SO4\text{-}OH}$ values are usually definitive of a supergene origin. $\delta^{34}S$ values of alunite will be close to those of precursor sulfides. δD - $\delta^{18}O_{SO4}$ values will fall within the *supergene alunite sulfate field* (SASF). δD values will be near that of local meteoric water during weathering. $\delta^{18}O_{OH}$ - δD values will fall within the *supergene alunite OH zone* (SAOZ) while coeval kaolinites or halloysites will have δD and $\delta^{18}O$ values near the kaolinite line. Rare exceptions may occur when the meteoric waters have been evaporated leading to enrichment in δD values or standing pools of water permit exchange of sulfate with low-pH waters and or bacteriogenic reduction of sulfate leading to enrichment in both ^{34}S and ^{18}O. Although only suggested in this study stable isotope data are powerful indicators of the hydrogeochemical environments of supergene acid-sulfate formation at specific localities.

STEAM-HEATED acid-sulfate alteration zones form near the water table by the attack of sulfuric acid formed from the oxidation, in the vadose zone, of H_2S derived from the degassing of underlying hydrothermal fluids. They are characterized by pronounced vertical zoning in paleogeothermal environments. Initial $\delta^{18}O_{SO4}$ and $\delta^{34}S$ values are kinetically controlled, but $\delta^{18}O_{SO4}$ usually reaches equilibrium with water and even $\delta^{34}S$ values may approach equilibrium with H_2S. The steam-heated assemblage can be recognized isotopically by $\delta^{34}S$ that is the same as precursor H_2S (and as related sulfides, if present), possibly large $\delta^{18}O_{SO4}$, and δD the same as meteoric water. Coeval kaolinites will have $\delta^{18}O$ and δD to the left of the *kaolinite line*. Steam-heated alunites appear to have $\Delta^{18}O_{SO4\text{-}OH}$ values that give reasonable depositional temperatures (90-160 °C).

MAGMATIC-HYDROTHERMAL acid-sulfate assemblages in near-surface epithermal environments such as the examples shown for Summitville, Julcani, Red Mountain at Lake City, and Rodalquilar result from the disproportionation of magmatic SO_2 in magmatic or mixed magmatic-meteoric fluid. Such assemblages, which are characterized by horizontal zoning, also occur as late stages in the porphyry-copper deposit at El Salvador. Alunite in such assemblages is characterized by large $\delta^{34}S$ values (relative to coeval sulfides) which vary with changes in temperature and the H_2S/SO_4 ratio. $\delta^{34}S$ values of coexisting alunite and pyrite can be used to define the thermal history of the acid-sulfate alteration and to trace changes in H_2S/SO_4 ratio of the fluids. The magmatic-derived SO_2 may disproportionate into magmatic or meteoric hydrothermal fluid or mixtures thereof as reflected by the $\delta^{18}O_{SO4}$ and δD values of alunite. Coeval kaolinites which occur outward of the alunite usually have similar $\delta^{18}O$ but lower δD than alunites, reflecting increased dilution of magmatic fluids by meteoric water. Magmatic-hydrothermal alunites have $\Delta^{18}O_{SO4\text{-}OH}$

smaller than equilibrium values because of retrograde exchange between the OH site and the fluids. The degree of retrograde exchange depends on the initial temperature of deposition. At low temperatures of formation, the $\Delta^{18}O_{SO4-OH}$ values will be close to equilibrium. Magmatic-hydrothermal environments may be overprinted by later steam-heated, magmatic-steam, or supergene environments.

MAGMATIC-STEAM acid sulfate alteration is characterized by monomineralic veins of alunite often with limited alteration and pyrite in adjacent wall rock. The origin of this type of alunite is not well understood. It appears to have formed at shallow levels at the Cactus deposit in California and at Red Mountain near Lake City, Colorado, and at apparently deeper levels in the Alunite Ridge deposits near Marysvale, Utah. These alunites appear to be related to the rapid, high-temperature, low-pressure release of SO_2-rich fluid from a magma at deep levels. At shallow levels they may be related to the oxidation of H_2S and or SO_2 in a volcanic edifice that permits atmospheric oxygen to mix with high-temperature magmatic steam. The formation of magmatic-steam alunite differs from that of magmatic-hydrothermal alunite in that precipitation occurs directly from dry steam instead of during condensation. Its formation differs from that of steam-heated alunite in that precipitation occurs during the expansion of steam rather than during condensation in shallow water. Magmatic-steam alunite has been presumed to overlie porphyry-type mineralization at Alunite Ridge, and adularia-sericite mineralization at Cactus and to develop subsequent to magmatic-hydrothermal acid-sulfate alteration at Red Mountain, Lake City. δD values reflect a magmatic water component, and $\delta^{34}S$ has the value of the bulk sulfur in the system. $\Delta^{18}O_{SO4-OH}$ values of most magmatic-steam alunites give reasonable temperatures of deposition, but for reasons not yet clear, the values of $\delta^{18}O_{OH}$ and $\delta^{18}O_{SO4}$ are anomalously low for their presumed magmatic vapor origin.

REFERENCES

Albers, J.P. and Stewart, J.H., 1972, Geology and mineral deposits of Esmeralda County, Nevada: Nevada Bur. Mines Geology Bull. 78, 80. p.

Alpers, C.N., Rye, R.O., Nordstrom, D. K., White, D.L., and King, Bi-Shia, Chemical, crystallographic, and isotopic properties of alunite and jarosite from acid hyersaline Australian lakes: Chem. Geol. (in Press).

Arribas, A. Jr., Rytuba, J.J., Rye, R.O., Cunningham, C.G., Podwysocki, M.H., Kelly, W.C., and Arribas, A. Sr, McKee, E.H., Smith, J.G., 1989, Preliminary study of the ore deposits and hydrothermal alteration in the Rodalquilar caldera complex southeastern Spain: U.S. Geol. Surv. Open-File Report 89-327, 39 p.

Ashley, R.P., 1974, Goldfield mining district, in Guidebook to the geology of four Tertiary volcanic centers in central Nevada: Nevada Bureau of Mines and Geology Report 19, p. 49-66.

Ashley, R.P. and Silberman, M.L., 1976, Direct dating of mineralization at Goldfield, Nevada, by potassium-argon and fission-track methods: Econ. Geol., v. 71, p. 904-921.

Barton, P. B., Jr., Bethke, P.M., and Roedder, E., 1977, Environment of ore deposition in the Creede mining district, San Juan Mountain, Colorado: Part III. Progress toward interpretation of the chemistry of the ore forming fluid for the OH vein: Econ. Geol., v. 72, p. 1-24.

Beaty, D.W., Cunningham, C.G., Rye, R.O., Steven, T.A., and Gonzalez-Urien, E., 1986, Geology and geochemistry of the Deer Trail Pb-Zn-Ag-Cu manto deposits, Marysvale district, west-central Utah: Econ. Geol., v. 81, p. 1932-1952.

Berger, B.R. and Henley, R.W., 1989, Advances in the understanding of epithermal gold-silver deposits, with special reference to the western United States: Econ. Geol. Monograph 6, p. 405-423.

Bethke, P.M., 1984, Controls on base-and precious-metal mineralization in deeper epithermal environments: U.S. Geol. Surv. Open-File Report 84-890, 40 p.

Bethke, P.M., Barton., P.B., Jr., Lanphere, M.A., and Steven, T.A., 1976, Environment of ore deposition in the Creede mining district, San Juan Mountains, Colorado: Part II. Age of mineralization: Econ. Geol., v. 71, p. 1006-1011.

Bethke, P.M. and Rye, R.O., 1979, Environment of ore deposition in the Creede mining district, San Juan Mountains, Colorado: Part IV. Source of fluids from oxygen, hydrogen and carbon isotope studies: Econ. Geol., v. 74, p. 1832-1851.

Bird, M.I., Andrew, A.S., Chivas, A.R., and Lock, D., 1989, An isotopic study of surficial alunite in Australia 1: Hydrogen and sulphur isotopes: Geochim. Cosmochim. Acta v. 53, p. 3223-3237.

Botinelly, T., 1976, A review of the minerals of the alunite-jarosite, beudantite and plumbogummite groups: Journal of Research of the U.S.Geological Survey, v. 4, p. 213-216

Bottaro, J.L., 1987, Geology of the Middle Buttes volcanic complex, Mojave district, Kern, County, California: Unpub. MSc. thesis, San Jose State University, 94 p.

Bove, D., Hon, K., and Rye, R.O., 1988, Evolution of the Red Mountain alunite deposits, Lake City, Colo (abst.): Geological Society of America Abstracts with Programs, v. 20, p. A353.

Bove, D., Rye, R.O., and Hon, K., 1990, Evolution of the Red Mountain alunite deposits, Lake City, Colo: U.S. Geol. Surv. Open-File Report 90-0235, 29 p.

Brantley, S.L., Borgia, A., Rowe, G., Fernandez, J.F., and Reynolds, J.R., 1987, Paos volcano crater lake acts as a condenser for acid metal-rich brines: Nature, v.330, p. 470-472.

Brophy, G.P., Scott, E.S., and Snellgrove, R.A., 1962, Sulfate studies II. Solid solution between alunite and jarosite: Am. Min., v. 78, p. 73-90.

Callaghan, E., 1973, Mineral resource potential of Piute County, Utah and adjoining area: Utah Geol. Mineralog. Surv. Bull., 102, 135 p.

Chiba, H., Kusakabe, M., Hirano, S., Matsuo, S., and Somiya, S, 1981, Oxygen isotope fractionation factors between anhydrite and water from 100 to 500°C: Earth Planet. Sci. Lett., v. 53, p. 55-62.

Craig, H., 1961, Isotopic variations in meteoric waters: Science, v. 133, p. 1702-1703.

Cunningham, C.G., Rye, R.O., Steven, T.A., and Mehnert, H.H., 1984, Origins and exploration significance of replacement and vein-type alunite deposits in the Marysvale volcanic field, west central Utah: Econ. Geol., v. 79, p. 50-71.

Deen, J.A., 1990, Hydrothermal ore deposition related to high-level igneous activity: A stable-isotope study of the Julcani mining district, Peru: Unpub. Ph.D. thesis, University of Colorado, 246 p..

Deen, J.A., Drexler, J.W., Rye, R.O., and Munoz, J.L., 1987, A magmatic fluid origin for the Julcani district, Peru: stable isotope evidence (abst.): Geological Society of America Abstracts with Programs, v. 19, p. 638.

Deen, J.A., Rye, R.O., and Drexler, J.W., 1988, Polymineralic mineralization related to magma evolution and magmatic-meteoric fluid mixing, Julcani district, Peru (abst.): Geological Society of America Abstracts with Programs, v. 19, p. A351.

Ellis, A.J. and Mahon, W.A.J., 1977, Geochemistry and geothermal systems: Academic Press, New York, 392 p.

Ferguson, H.G., 1921, The Round Mountain district, Nevada: U.S. Geological Survey Bull., 725-I, p. 383-406.

Field, C.W., 1966, Sulfur isotopic method for discriminating between sulfates of hypogene and supergene origin: Econ. Geol., v. 61, p. 1428-1435.

Field, C.W. and Gustafson, L.B., 1976, Sulfur isotopes in the porphyry copper deposit at El Salvador, Chile: Econ. Geol., v. 71, p. 1533-1548.

Field, C.W. and Lombardi, Gianni, 1972, Sulfur isotopic evidence for the supergene origin of alunite deposits: Mineralium Deposita, v. 7, p. 113-125.

Fifarek, R.H. and Gerike, G.N., 1990, gold deposition and remobilization at Round Mountain, Nevada (abst.): Geology and ore deposits of the Great Basin Reno-Sparks, Nevada 1990, Great Basin Symposium Program with Abstracts, Nevada Bureau of Mines Geology, Reno, p. 125.

Gustafson, L.B. and Hunt, J.P., 1975, The porphyry copper deposit at El Salvador, Chile: Econ. Geol., v. 70, p. 857-912.

Hayba, D.O., Bethke, P.M., Heald, P.W., and Foley, N.K.,1985, Geologic, mineralogic, and geochemical characteristics of volcanic-hosted epithermal precious-metal deposits, in Berger, B.R. and Bethke, P.M. (eds.), Geology and geochemistry of epithermal systems: Rev. in Econ. Geol., v. 2, p. 129-167.

Heald, P.W., Foley, N.K., and Hayba, D.O, 1987, Comparative anatomy of volcanic-hosted epithermal deposits: Acid-sulfate and adularia-sulfate types: Econ. Geol., v. 82, p. 1-25.

Hedenquist, J.W., 1987, Mineralization associated with volcanic-related hydrothermal systems in the circum-pacific Basin *in* Horn, M.K., ed., Transactions of the Fourth Circum-Pacific Energy and Mineral Resources Conferences: Singapore, p. 513-524.

Hemley, J.J., Hostetler, P.B., Gude, A. J., and Mountjoy, W.T., 1969, Some stability relations of alunite: Econ Geol., v. 64, p. 599-612.

Hemley, J.J. and Jones, W.R., 1964, Chemical aspects of hydrothermal alteration with emphasis on hydrogen metasomatism: Econ. Geol. v. 59, p. 538-569.

Henley, R.W., 1985, The geothermal framework for epithermal deposits: in Berger, B.R. and Bethke, P.M. (eds.), Geology and geochemistry of epithermal systems: Rev. in Econ. Geol., v. 2, p. 1-24.

Henley, R.W. and Ellis, A.J., 1983, Geothermal systems ancient and modern: a geochemical review: Earth-Science Reviews, v. 19, p. 1-50.

Henley, R.W. and McNabb, A., 1978, Magmatic vapor plumes and ground-water interaction in porphyry copper emplacement: Econ. Geol., v. 73, p. 1-20.

Holser, W.T., Kaplan, I.R., Sakai, H., and Zak, I., 1970, Isotope geochemistry of oxygen in the sedimentary sulfate cycle. Chem. Geol., v., 25, p. 1-17.

Jensen, M.L., Ashley, R.P., and Albers, J.P., 1971, Primary and secondary sulfates at Goldfield: Econ. Geol., v. 66, p. 618-626.

Jordan, J.T., 1941, Geology of the Cactus mines, Rosamond, Kern County, California: Unpub. M.Sc. thesis, California Inst. of Technology, 30 p.

Kaplan, I.R. and Rafter T.A., 1958, Fractionation of stable isotopes of sulfur by thiobacilli: Science, v 127, p. 517.

Kaplan, I.R. and Rittenburg, 1964, Microbiological fractionation of sulfur isotopes: J. Gen. Microgiology, v.34, p. 195-121.

Kharaka, Y.K. and O'Neil, J.R., 1976, Hydrogen isotope exchange between clay minerals and water: Geochim. et Cosmochim. Acta, v. 40, p. 241-246.

Knight, J.E., 1977, A thermochemical study of alunite, enargite, luzonite and tennantite deposits: Econ. Geol. v.,72, p. 1321-1336.

Lawrence, J.R., and Taylor, H.P., 1971, Deuterium and oxygen-correlation: clay minerals and hydroxides in Quaternary soils compared to meteoric waters: Geochim. Cosmochim. Acta, v. 35, p. 993-1003.

Lewis, J.S. and Krouse, H.R., 1969, Isotopic composition of sulfur and sulfate produced by oxidation of FeS_2: Earth Planet. Sci. Lett. v. 5, p. 425-453.

Liu, K.-K. and Epstein, S., 1984, The hydrogen isotope fractionation between kaolinite and water: Isotope. Geoscience., v. 2, p. 335-350.

Lloyd, R.M., 1968, Oxygen isotope behavior in the sulfate-water system: Jour. Geophys. Research, v. 73, p. 6099-6110.

Lombardi, Gianni and Mattias, Pierpaolo, 1979, Petrology and mineralogy of the kaolin and alunite mineralizations of Latium (Italy): Geologica Rom., v. 18, p. 157-214.

Lombardi, Gianni and Sheppard, S.M.F., 1977, Petrographic and isotopic studies of the altered acid volcanics of the Tolfa-Cerite area, Italy: the genesis of the clays: Clay Minerals, v. 12, p. 147-161.

Marumo, K., Matsuhisa, Y., and Nagasawa, K., 1982, Hydrogen and oxygen-isotopic compositions of kaolin minerals in Japan; in Van Olphan, H. and Veniale, F. (eds.) Developments in Sedimentalogy 35, International Clay conference, 1981, Elsevier, p. 315-320.

McCusker, R.T., 1982, Geology of the Soledad Mountain volcanic complex, Mojave Desert, California: Unpub. M.Sc. thesis, San Jose State University, 113 p.

Meyer, C.A. and Hemley, J.J., 1967, Wall rock alteration: in Barnes, H.L. (ed.), Geochemistry of hydrothermal ore deposits, Holt Rinehart, and Winston, New York, p. 166-235.

Nakai, N. and Jensen, M.L., 1964, The kinetic isotope effect in the bacterial reduction and oxidation of sulfur: Geochim. Cosmochim. Acta, v. 28, 1893-1912.

Ohmoto, H., 1972, systematics of sulfur and carbon isotopes in hydrothermal ore deposits: Econ Geol., v. 67, p. 551-578.

Ohmoto, H. and Lasaga, A.C., 1982, Kinetics of reactions between aqueous sulfates and sulfides in hydrothermal systems: Geochim. Cosmochim Acta, v. 46, p. 1727-1746.

Ohmoto, H. and Rye, R.O., 1979, Isotopes of sulfur and carbon, in Barnes, H.L. (ed.), Geochemistry of hydrothermal ore deposits, Holt Rinehart, and Winston, New York, p. 509-567.

Petersen, U., Noble, D.C., Arenas, M.J., and Goodell, P.C., 1977, Geology of the Julcani mining district, Peru: Econ. Geol., v. 72, p. 931-949.

Pickthorn, W. J. and O'Neil, J.R., 1985, ^{18}O relations in alunite mineral: potential single-mineral thermometer (abst.): Geological Society of America Abstracts with Programs, v. 17, p. 686.

Plumlee, G.S. and Rye R.O., 1989, Mineralization in the waning Creede epithermal system and similar behavior in other systems: U.S. Geol. Survey Open-File Report 89-95, 29 p.

Ransome, F.L., 1909, Geology and ore deposits of Goldfield, Nevada: U.S. Geol. Survey Prof. Paper 66, 258 p.

Rye, R.O., Bethke, P.M., and Wasserman, M.D., 1989, Diverse origins of alunite and acid sulfate alteration: stable isotope systematics: U.S. Geol. Surv. Open-File Report 89-5, 33 p.

Rye, R.O., Plumlee, G.S., Bethke, P.M., and Barton, P.B., 1988, Stable isotope geochemistry of the Creede hydrothermal system: U.S. Geol. Surv. Open-File Report 88-365, 40 p.

Rye, R.O., Stoffregen, R.E., and Bethke, P.M., 1990, Stable isotope systematics and magmatic hydrothermal processes in the Summitville, Co, gold deposit: U.S. Geol. Surv. Open-File Report 90-626, 31 p.

Rytuba, J.J., Arribas, A. Jr., Cunningham, C.G., Podwysocki, M.H., McKee, E.H., Castroviejo, R., 1988, Rodalquilar deposits (S.E. Spain), first example of caldera-related epithermal gold mineralization in Europe: part I caldera evolution (abst.): Geological Society of America Abstracts with Programs, v. 19, p. A351.

Sander, M.V., 1988, Geologic setting and the relation of epithermal gold-silver mineralization to wall rock alteration at the Round Mountain mine, Nye County Nevada: in Shaefer, R.W., Cooper, J.J., and Vikre, P.G., eds. Bulk mineable precious metal deposits of the western United States. Geological Society of Nevada, Reno, p. 375-416.

Savin, S.M. and Epstein, S., 1970, The oxygen and hydrogen isotope geochemistry of clay minerals: Geochim. Cosmochim Acta, v. 34, p. 43-64.

Savin, S.M. and Lee, M., 1988, Isotopic studies of phyllosilicates, *in* Reviews in Mineralogy v. 19, Bailey, S.W., ed. p. 189-219.

Schoen, R. and Rye, R.O., 1970, Sulfur isotope distributions in solfataras, Yellowstone National Park: Science, v. 170, p. 1082-1084.

Schoen, R., White, D.E., and Hemley J.J., 1974, Argillization by descending acids at Steamboat Springs, Nevada: Clays and Clay Minerals, v. 22, p. 1-22.

Sheppard, S.M.F. and Gustafson, L.B., 1976, Oxygen and hydrogen isotopes in the porphyry copper deposit at El Salvador, Chile: Econ. Geol., v. 71, p. 1549-1559.

Sillitoe, R.H., 1973, The tops and bottoms of porphyry copper deposits: Econ. Geol., v. 68, p. 799-815.

Sillitoe, R.H., 1983, Enargite-bearing massive sulfide deposits high in porphyry copper systems: Econ. Geol. v. 78, p. 348-352.

Sillitoe, R,H., and Bonham, H. F., 1984, Volcanic landforms and ore deposits: Econ. Geol, v. 79, p. 1286-1298.

Smith, A., 1941, The geochemistry and paragenesis of the ores of the Cactus mine, Kern County, California: Unpub. Ph.D. thesis, California Inst. of Technology, 44 p.

Steven, T.A., Cunningham, C.G., Naeser, C.W., and Mehnert, H.H., 1979, Revised stratigraphy and radiometric ages of volcanic rocks and mineral deposits in the Marysvale area, west-central Utah: U.S. Geol. Surv. Bull. 1469, 40 p.

Steven, T.A. and Ratte, J.C., 1960, Geology and ore deposits of the Summitville district, San Juan Mountains, Colorado: U.S. Geol. Survey Prof. Paper 343, 70 p.

Steven, T.A. and Eaton, G.P., 1975, Environment of ore deposition in the Creede mining district, San Juan Mountains Colorado: Part I: Geologic, hydrologic, and geophysical setting: Econ. Geol. v., 70, p. 1023-1037.

Stoffregen, R.E., 1987, Genesis of acid-sulfate alteration and Au-Cu-Ag mineralization at Summitville, Colorado: Econ. Geol., v. 82, p. 1575-1591.

Stoffregen, R.E. and Cygan, G., 1990, An experimental study of Na-K exchange between alunite and aqueous sulfate solutions: Am. Mineral. v. 75, p. 209-220.

Stoffregen, R.E., Rye, R.O., and Wasserman, D.M., 1989, Experimental determination of ^{18}O(sulfate-site) and D fractionations between alunite and water at 250 to 450°C (abst.): Geological Society of America Abstracts with Programs v. 21, p. A155.

Stoffregen, R.E., Rye, R.O., and Wasserman, D.M., 1990, Rates of alunite-water alkali and isotope exchange: Geological Society of America Abstracts with Programs, v. 22, no. 7, p. A162.

Taylor, R.B., 1975, Neogene tectonism in south-central Colorado: Geol. Soc. London Jour. v. 133, p. 509-558.

Taylor, B.E., Wheeler, M.C., and Nordstrom, D.K., 1984, Stable isotope geochemistry of acid mine drainage: Experimental oxidation of pyrite: Geochim. Cosmochim. Acta, v. 48, p. 2669-2678.

Taylor, H.P. Jr., 1979, Oxygen and hydrogen isotope relationships in mineral deposits: in Barnes, H.L. (ed.), Geochemistry of hydrothermal ore deposits, Holt Rinehart, and Winston, New York, p. 236-277.

Tingley, J.V. and Berger, B.R., 1985, Lode gold deposits of Round Mountain, Nevada : Nevada Bureau of Mines and Geology Bulletin 100, 62 p.

Troxel, B.W., and Morton, P.K., 1962, Mines and mineral resource of Kern county, California: California Div. of Mines and Geology, County Report 1, 370 p.

van Everdingen, R.O. and Krouse, H.R., 1985, Isotope composition of sulphates generated by bacterial and abiological oxidation: Nature v. 315, p. 395-396.

Vikre, P.G., 1985, Precious mineral vein systems in the National district, Humbolt county, Nevada: Econ. Geol., v. 80, p. 360-393.

Vikre, P.G., 1987, Paleohydrology of Buckskin Mountain, National district, Humbolt, County, Nevada: Econ. Geol., v. 82, p. 934-950.

Vikre, P.G., 1989a, Fluid-mineral relations in the Comstock lode: Econ. Geol., v. 84, p. 1574-1613.

Vikre, P.G., 1989b, Ledge formation at the Sandstrom and Kendall gold mines, Goldfield, Nevada: Econ. Geol., v. 84, p. 2115-2138.

Vikre, P.G, McKee, E.H., and Silberman M.L., 1988, Chronology of Miocene hydrothermal and igneous events in the western Virginia Range, Washoe, Storey, and Lyon counties, Nevada: Econ. Geol., v. 83, p. 864-874.

Wallace, A.B., 1979, Possible signatures of buried porphyry-copper deposits in Middle to Late Tertiary volcanic rocks of western Nevada: Nevada Bur. Mines Geol. Rept. 33, p. 69-76.

Wasserman, M.D., Rye, R.O., Bethke, P.M., and Arribas, A., 1990, Methods for separation of alunite from associated minerals and subsequent analysis of D, $^{18}O_{OH}$, $^{18}O_{SO4}$, ^{34}S (abst.): Geological Society of America Abstracts with Programs, v. 22, no. 7, p. A134.

Whitney, J.A., 1984, Volatiles in magmatic systems : Rev. Econ. Geol., v. 1, p. 154-175.

Whitney, J.A., 1988, Composition and activity of sulfurous species in quenched magmatic gases associated with pyrrhotite-bearing silicic magmas: Econ. Geol., v. 83, p. 86-92

FIGURE CAPTIONS

Figure 1a-b Schematic diagrams of (a) volcano-related hydrothermal systems showing possible steam-heated, magmatic-hydrothermal, and magmatic-steam environments of acid-sulfate alteration, and (b) steam-heated environment of acid-sulfate alteration overlying a near-neutral hydrothermal system with adularia-sericite-type mineralization driven by a deep magmatic heat source. Bold arrows indicate fluid flow. Modified from Henley and Ellis (1983).

Figure 2a-b Predicted δD, $\delta^{18}O_{SO4}$, $\delta^{18}O_{OH}$ and $\delta^{34}S$ systematics of supergene alunite-kaolinite assemblages. Assumptions: $\delta^{34}S_{\Sigma S}$ = 0‰; δD_{H2O} of meteoric fluid = -110‰; $\delta^{18}O_{H2O}$ of meteoric fluid = -15‰. Changes in assumptions will change positions, but not relationships, of fields. Lines and fields in 2b repeated for reference in succeeding δD-$\delta^{18}O$ diagrams: 1) MWL = meteoric water line of Craig (1961); 2) PMW = primary magmatic water field of Taylor (1979). *Note, many magmatic waters lie outside this field and waters of different origin may lie within the field*; 3) Kaolinite lines of Savin, and Epstein (1970); 4) Supergene alunite SO_4 field (SASF); 5) Supergene alunite OH zone (SAOZ). See text for definitions of 4) and 5) and further explanations.

Figure 3a-b Predicted δD, $\delta^{18}O_{SO4}$, $\delta^{18}O_{OH}$ and $\delta^{34}S$ systematics of steam-heated alunite-kaolinite assemblages. Figure 3a: $\delta^{18}O$, $\delta^{34}S$ systematics for steam-heated, exchanged meteoric water. Figure 3b: δD, $\delta^{18}O$ systematics for both steam-heated exchanged and unexchanged meteoric waters. Assumptions: T = 150° to 90° C; $\delta^{34}S_{\Sigma S}$ = 0‰; δD_{H2O} of meteoric fluid = -110‰ and -80‰; $\delta^{18}O_{H2O}$ of meteoric fluid = -5‰ and -12‰ for exchanged and unexchanged fluids, respectively. Changes in assumptions will change positions, but not relationships, of fields. See text for explanation.

Figure 4a-b Predicted δD, $\delta^{18}O_{SO4}$, $\delta^{18}O_{OH}$ and $\delta^{34}S$ systematics of magmatic hydrothermal alunites. Assumptions: T = 400° to 200° C; H_2S/SO_4 = 1 to 8; $\delta^{34}S_{\Sigma S}$ = 0‰; δD_{H2O} of magmatic fluid = -60‰; δD_{H2O} of meteoric fluid = -110‰; $\delta^{18}O_{H2O}$ of magmatic fluid = 6‰; $\delta^{18}O_{H2O}$ of meteoric fluid = -5‰. In Figure 4b low $\delta^{18}O$ margins of OH and SO_4 fields are for 400°C, high $\delta^{18}O$ margins are for 200°C. Changes in assumptions will change positions, but not relationships, of fields. See text for explanation.

Figure 5a-b Predicted δD, $\delta^{18}O_{SO4}$, $\delta^{18}O_{OH}$ and $\delta^{34}S$ systematics of magmatic steam alunites. Assumptions: T = 250° to 350° C; $\delta^{34}S_{\Sigma S}$ = 0‰; δD_{H2O} of magmatic fluid = -60‰; $\delta^{18}O_{H2O}$ of fluid = 5 ‰. In Figure 5b low $\delta^{18}O$ margins of OH and SO_4 fields are for 350°C, high $\delta^{18}O$ margins are for 250°C. Changes in assumptions will change positions, but not relationships, of fields. See text for explanation.

Figure 6a-b $\delta^{34}S$ range of main stage sulfides; δD, $\delta^{18}O_{SO4}$, $\delta^{18}O_{OH}$ and $\delta^{34}S$ values of supergene alunite and δD and $\delta^{18}O$ values of halloysite from the upper levels of the Creede, Colorado Ag-base metal deposit.

Figure 7a-b $\delta^{34}S$ range of main stage pyrite; δD, $\delta^{18}O_{SO4}$, $\delta^{18}O_{OH}$ and $\delta^{34}S$ values of alunite from the upper portions of the Round Mountain, Nevada, gold deposit.

Figure 8a-b δD, $\delta^{18}O_{SO4}$, $\delta^{18}O_{OH}$ and $\delta^{34}S$ values of alunites, δD and $\delta^{18}O$ of halloysites and range of $\delta^{34}S$ of precursor pyrite from supergene zones of various ore deposits and sulfide occurrences at different latitudes. Note that for clarity the $\delta^{18}O_{OH}$ data are not shown in 8a, and individual occurrences are not indicated in 8b. δD and $\delta^{34}S$ data for Mount Leyshon and Kidston are from Bird et al. (1989). $\delta^{34}S$ data on Santa Rita and Mineral Park are from Field (1966). Dashed lines in 8b enclose data for Riaza

Figure 9a-b δD, $\delta^{18}O_{SO4}$, $\delta^{18}O_{OH}$ and $\delta^{34}S$ values of alunite, δD and $\delta^{18}O$ of associated kaolinite, $\delta^{34}S$ of pyrite, calculated δD_{H2O} and $\delta^{18}O_{H2O}$ of fluids and δD and $\delta^{18}O$ of modern spring water from the steam-heated acid-sulfate alteration at Tolfa district, Latium, Italy. The $\delta^{34}S$ data are from Field and Lombardi (1972). Isotope data on kaolinites and waters are from Lombardi and Sheppard (1977). In this and succeeding figures, tie lines connect $\delta^{18}O_{SO4}$ and

$\delta^{18}O_{OH}$ of the same alunite and associated numbers on hydrothermal alunites indicate temperatures calculated from the $\Delta^{18}O_{SO_4\text{-}OH}$ when those temperatures are deemed reasonable for the environment. Temperatures deemed unreasonable are not plotted but can be obtained from Table 1. Alunite waters in 9b are calculated using temperatures based on $\Delta^{18}O_{SO_4\text{-}OH}$.

Figure 10a-b δD, $\delta^{18}O_{SO_4}$, $\delta^{18}O_{OH}$ and $\delta^{34}S$ values of alunite, range of $\delta^{34}S$ of pyrite, and calculated δD_{H_2O} and $\delta^{18}O_{H_2O}$ of fluids from the steam-heated replacement alunite deposits at Marysvale, Utah. $\delta^{34}S$ data are from Cunningham et al. (1984). Alunite waters in 10b are calculated using temperatures $\Delta^{18}O_{SO_4\text{-}OH}$. Note high degree of exchange with wall rocks implied by large values of $\delta^{18}O$ for waters.

Figure 11a-b δD, $\delta^{18}O_{SO_4}$, $\delta^{18}O_{OH}$ and $\delta^{34}S$ values of alunite, δD and $\delta^{18}O$ of wall rock (WR) and later vein kaolinite, range of $\delta^{34}S$ of coeval pyrite, and calculated δD_{H_2O} and $\delta^{18}O_{H_2O}$ of fluids from the magmatic-hydrothermal acid-sulfate alteration at Julcani district, Peru.

Figure 12a-b δD, $\delta^{18}O_{SO_4}$, $\delta^{18}O_{OH}$ and $\delta^{34}S$ values of alunite, δD and $\delta^{18}O$ of wall rock (WR) and later vein kaolinite, range of $\delta^{34}S$ of pyrite coeval with alunite, and calculated δD_{H_2O} and $\delta^{18}O_{H_2O}$ of fluids from the magmatic-hydrothermal acid-sulfate alteration at Summitville, Colorado.

Figure 13a-b δD, $\delta^{18}O_{SO_4}$, $\delta^{18}O_{OH}$ and $\delta^{34}S$ values of alunite from the magmatic-steam alunite at Marysvale, Utah. $\delta^{34}S$ data are from Cunningham et al. (1984).

Figure 14a-b δD, $\delta^{18}O_{SO_4}$, $\delta^{18}O_{OH}$ and $\delta^{34}S$ values of alunite, δD and $\delta^{18}O$ of kaolinite, $\delta^{34}S$ of pyrite from the acid-sulfate alteration at Cactus, CA.

Figure 15a-b δD, $\delta^{18}O_{SO_4}$, $\delta^{18}O_{OH}$ and $\delta^{34}S$ values of stages 1, 2, 3, and 4 alunite, δD and $\delta^{18}O$ of wall rock (WR) kaolinites, range of $\delta^{34}S$ values of pyrite, and calculated δD_{H_2O} and $\delta^{18}O_{H_2O}$ of fluids for the magmatic-hydrothermal (stages 1 and 2) alunites at Red Mountain, Lake City, Colorado.

Figure 16a-b δD, $\delta^{18}O_{SO_4}$, $\delta^{18}O_{OH}$ and $\delta^{34}S$ values of alunite, δD and $\delta^{18}O$ of kaolinite, range of $\delta^{34}S$ of pyrite, δD and $\delta^{18}O$ of supergene kaolinite, and calculated δD_{H_2O} and $\delta^{18}O_{H_2O}$ of fluids for the magmatic-hydrothermal and later supergene acid-sulfate alteration assemblages at El Salvador, Chile. $\delta^{34}S$ data are from Field and Gustafson (1976). Isotope data on kaolinites and calculated compositions of ambient meteoric water are from Sheppard and Gustafson (1976).

Figure 17a-b δD, $\delta^{18}O_{SO_4}$, $\delta^{18}O_{OH}$ and $\delta^{34}S$ values of stage 1 and stage 2 alunite, δD and $\delta^{18}O$ of stage 1 and stage 2 kaolinite, range of $\delta^{34}S$ of stage 1 pyrite, and calculated δD_{H_2O} and $\delta^{18}O_{H_2O}$ of fluids from the stage 1 magmatic-hydrothermal (MH) and later stage 2 supergene (SG) assemblages at Rodalquilar gold deposit, Almeria, Spain. Composition of present day meteoric water is also shown.

Figure 18a-b δD, $\delta^{18}O_{SO_4}$, $\delta^{18}O_{OH}$ and $\delta^{34}S$ values of alunite, δD and $\delta^{18}O$ of kaolinite, and range of $\delta^{34}S$ values of pyrite, from acid-sulfate alteration assemblages from Goldfield (GF) and Buckskin (BS) mining districts and from the western Virginia Range near and to the north of the Comstock mining district. $\delta^{34}S$ data of pyrite and isotope data on kaolinite are from Vikre (1987) and Vikre et al. (1988).

Figure 19a-b Fields of measured $\Delta^{34}S_{SO_4\text{-}OH}$ versus (a) temperature of formation for various types of acid-sulfate or alunite-forming environments as indicated by stable isotope data presented in this paper and (b) predicted equilibrium fractionations based on independently measured or presumed temperatures of deposition. Equilibrium values will fall along the line labelled Stoffregen et al. (1989) in 19a and the 1:1 line through the origin in 19b.

Figure 20a-b Fields of measured $\Delta^{34}S_{alun\text{-}py}$ or $\Delta^{34}S_{alun\text{-}H_2S}$ (20a) and $\Delta^{34}S_{SO_4\text{-}H_2O}$ (20b) versus predicted equilibrium fractionations. Topology as in Figure 19b.

STEAM-HEATED ACID-SULFATE AND MAGMATIC-STEAM ENVIRONMENTS OVER MAGMATIC-HYDROTHERMAL ENVIRONMENTS

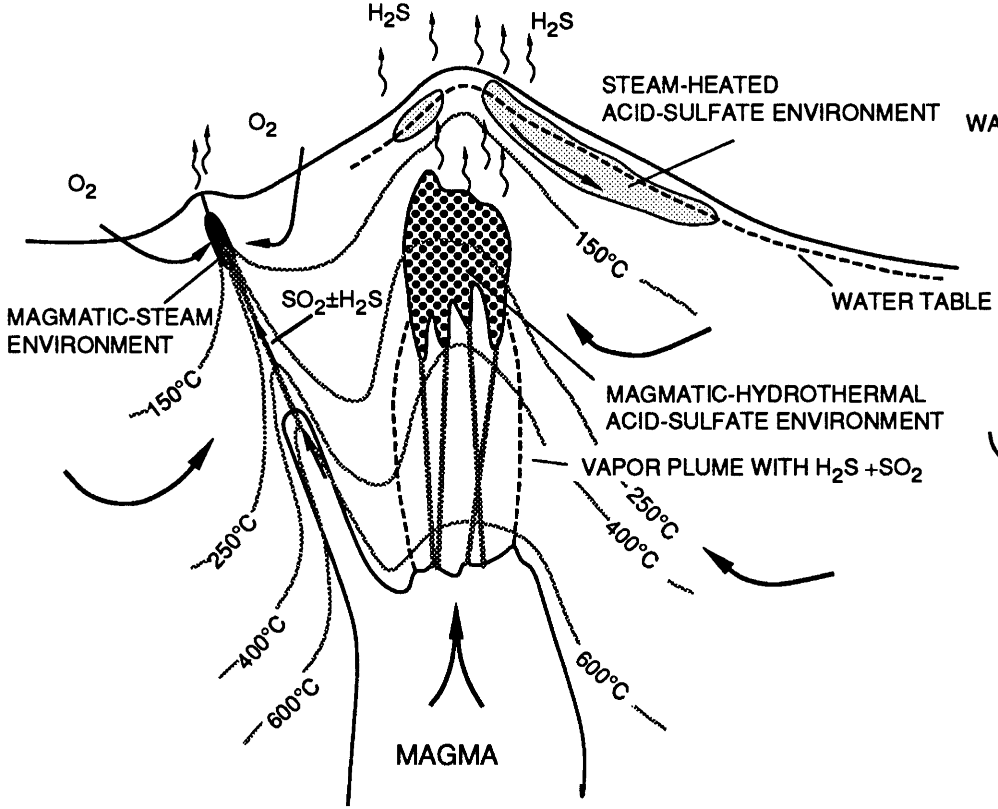

FIGURE 1a

STEAM-HEATED ACID-SULFATE ENVIRONMENT ABOVE ADULARIA-SERICITE EPITHERMAL SYSTEM

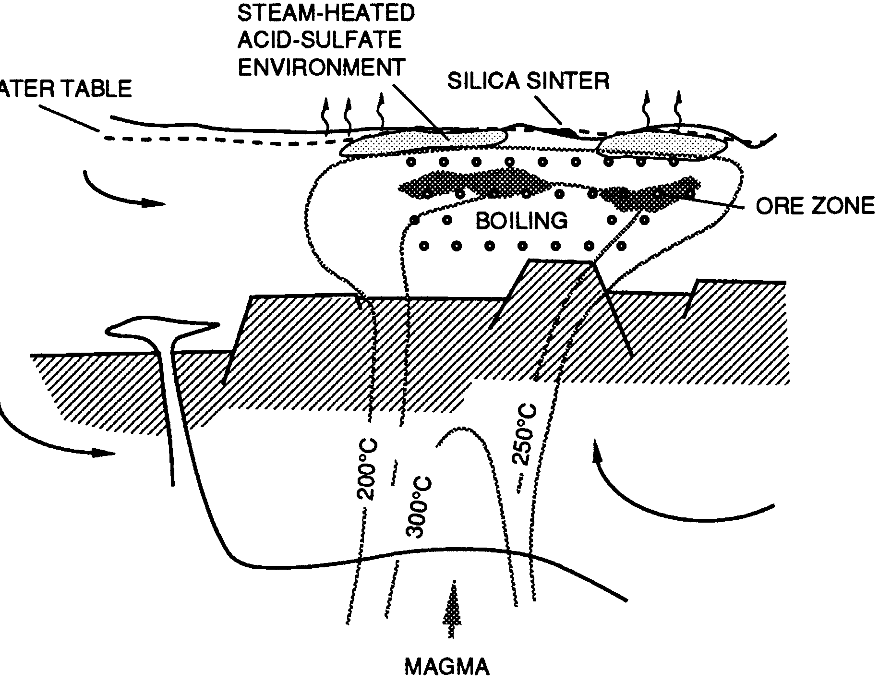

FIGURE 1b

PREDICTED δD - $\delta^{18}O_{SO4}$ - $\delta^{18}O_{OH}$ - $\delta^{34}S$ OF SUPERGENE ALUNITE

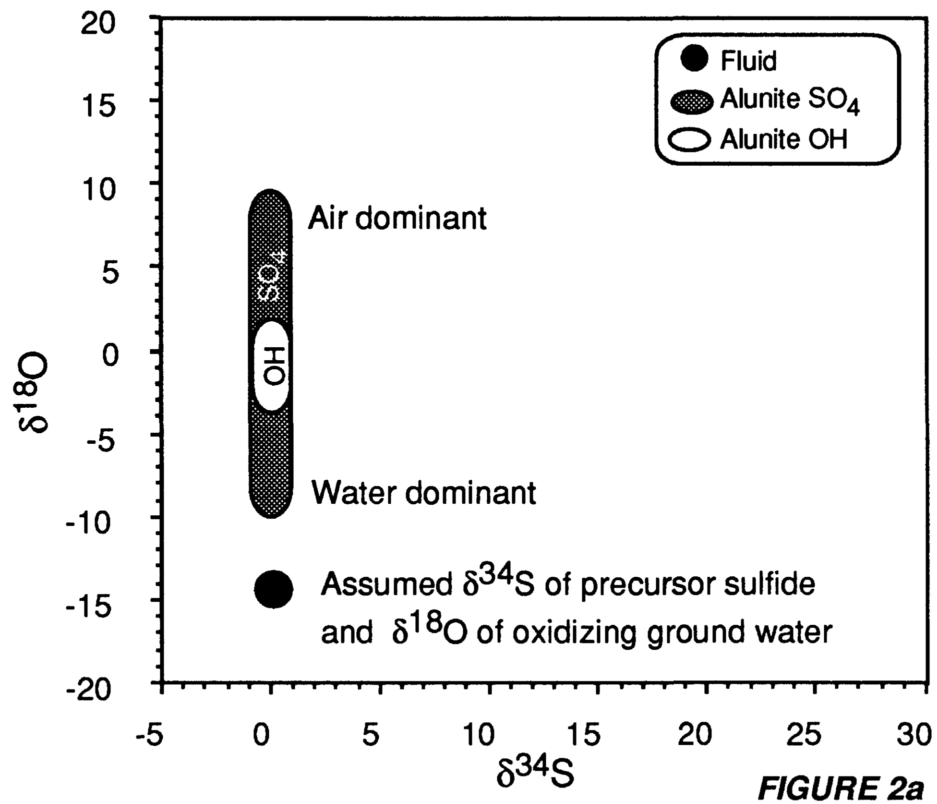

FIGURE 2a

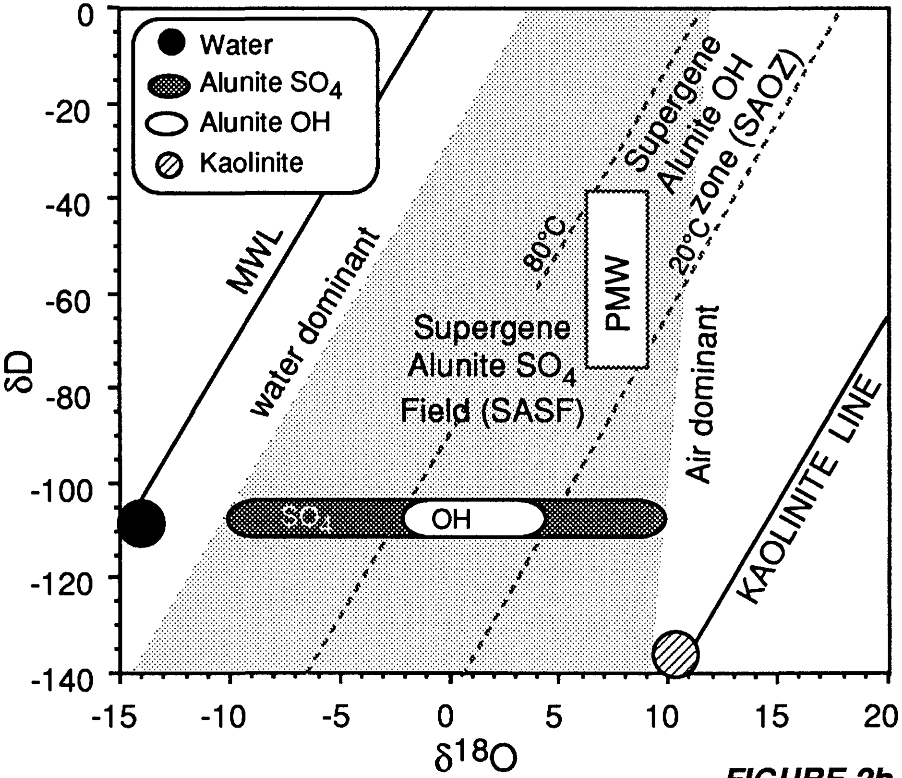

FIGURE 2b

PREDICTED δD - $\delta^{18}O_{SO4}$ - $\delta^{18}O_{OH}$ - $\delta^{34}S$ OF STEAM-HEATED ALUNITE

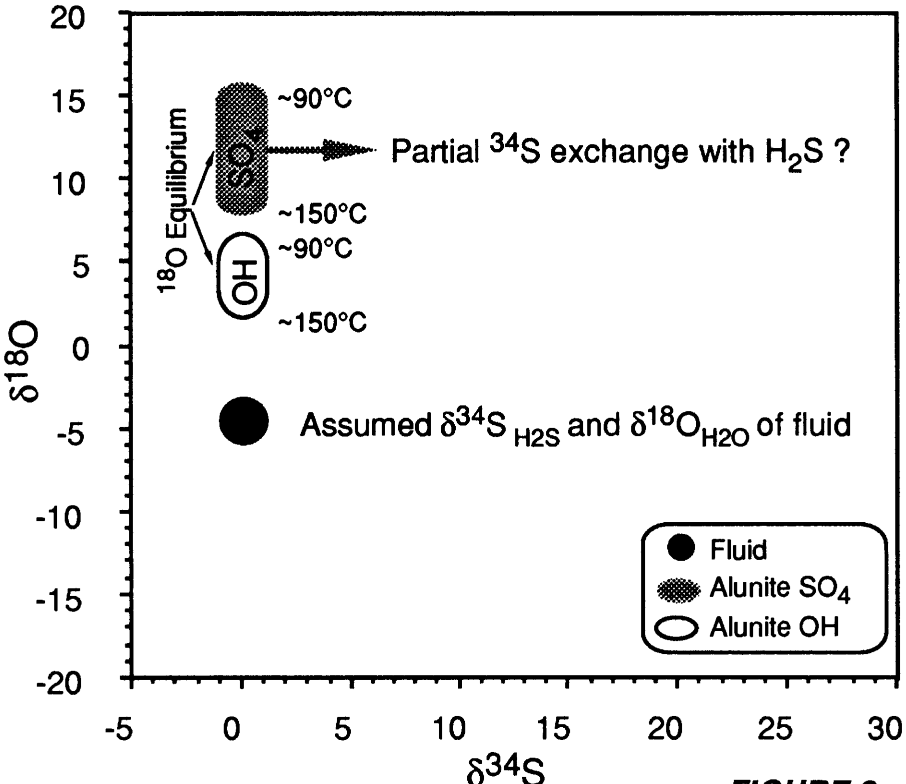

FIGURE 3a

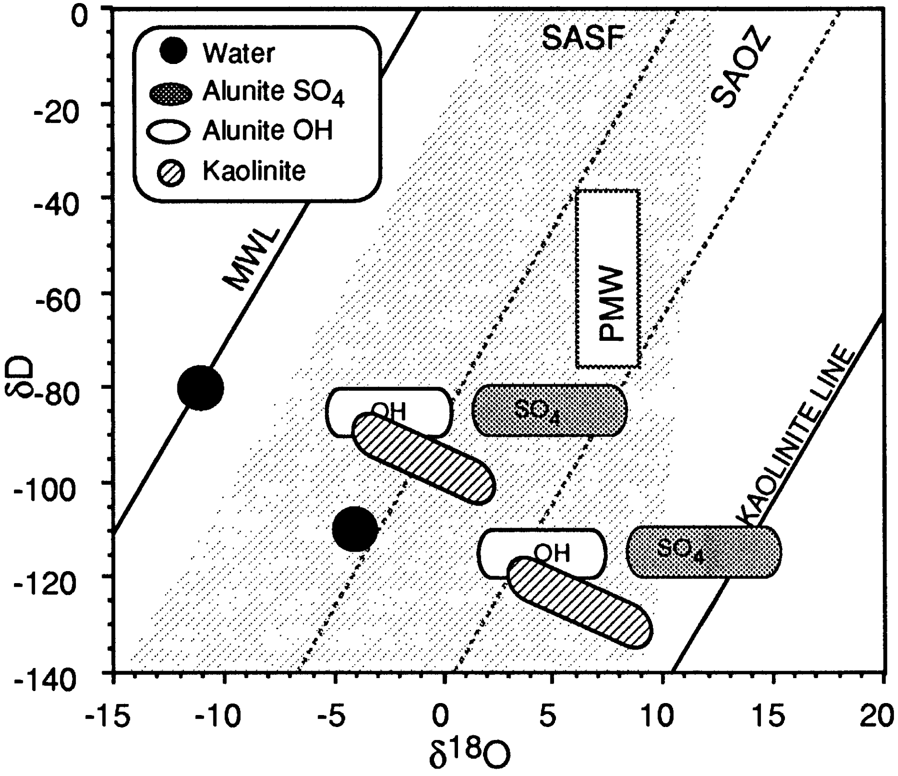

FIGURE 3b

PREDICTED δD - $\delta^{18}O_{SO4}$ - $\delta^{18}O_{OH}$ - $\delta^{34}S$ FOR MAGMATIC-HYDROTHERMAL ALUNITE

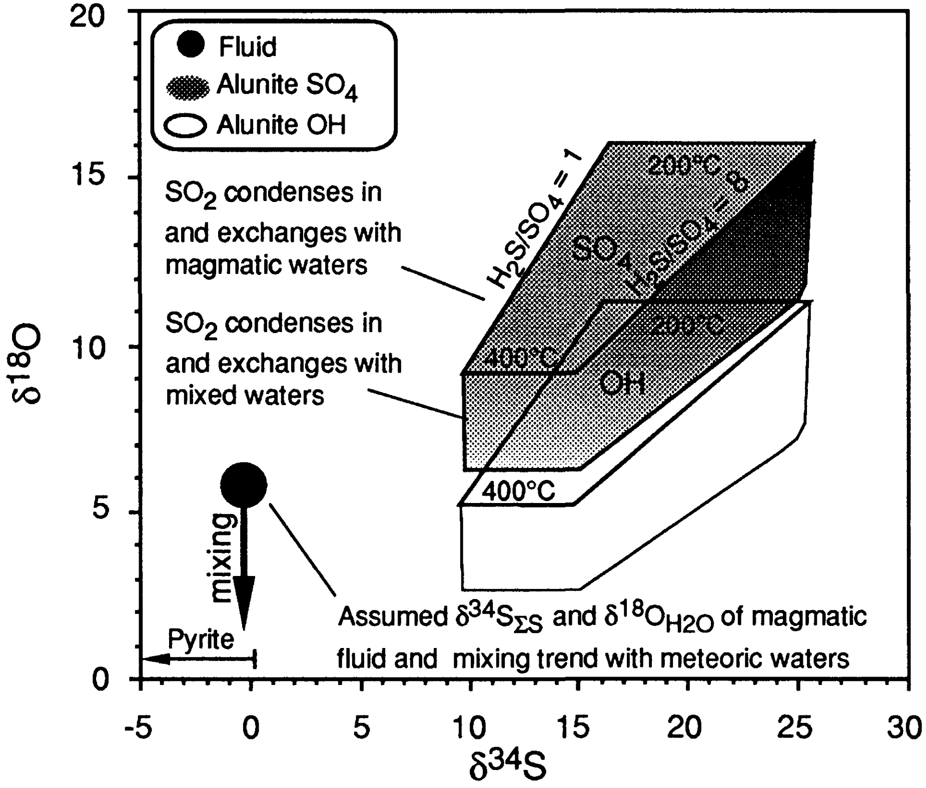

FIGURE 4a

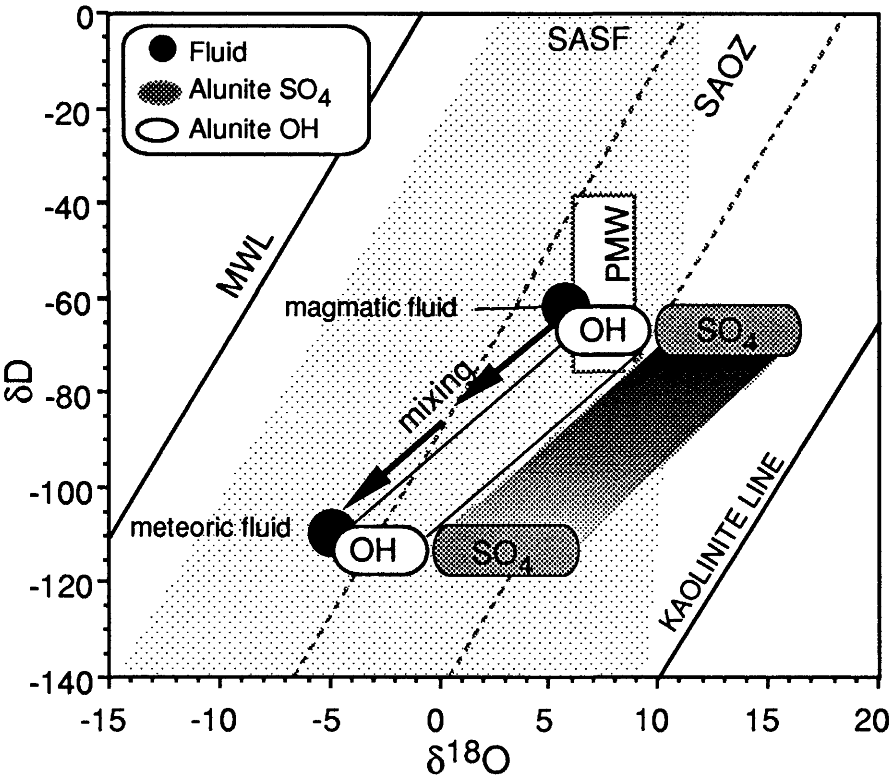

FIGURE 4b

PREDICTED δD - $\delta^{18}O_{SO4}$ - $\delta^{18}O_{OH}$ - $\delta^{34}S$ OF MAGMATIC-STEAM ALUNITE

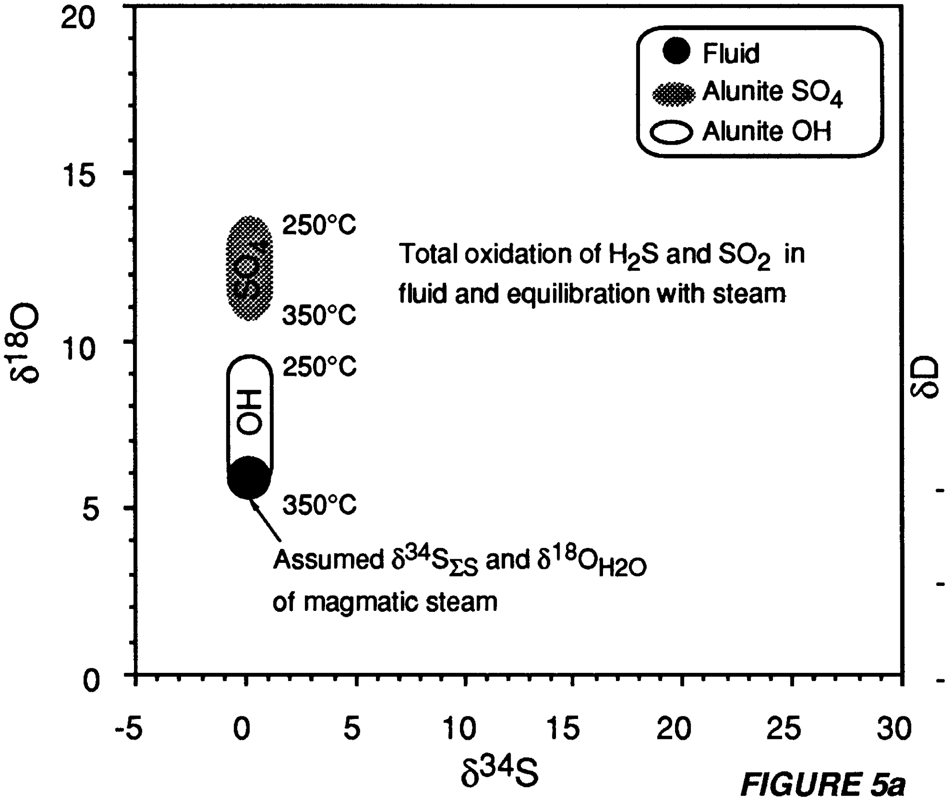

FIGURE 5a

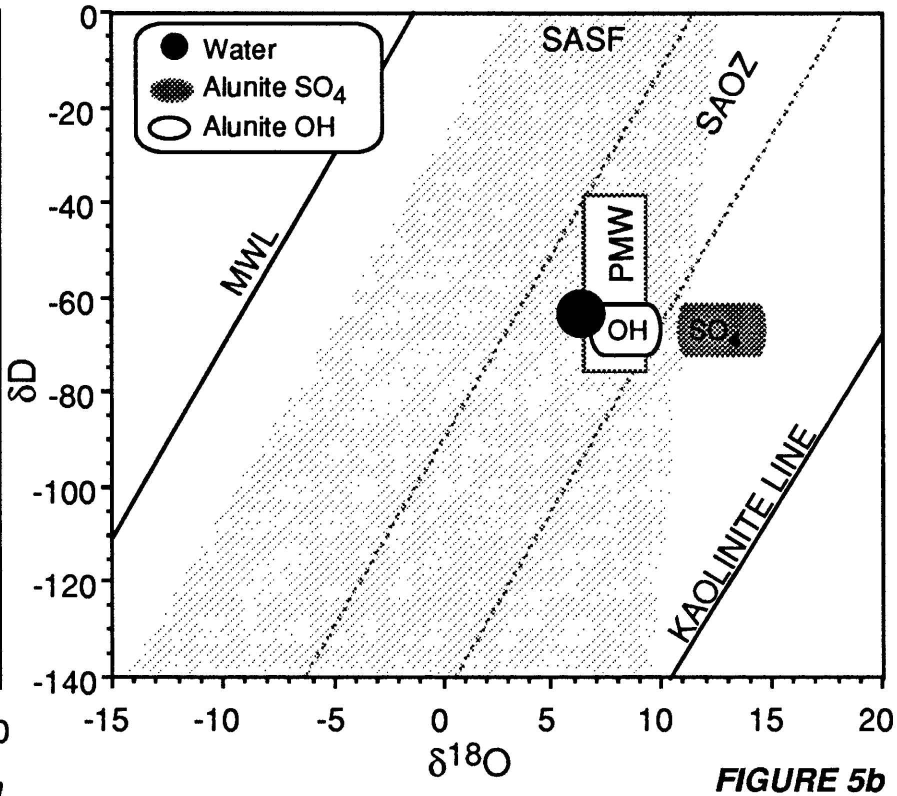

FIGURE 5b

δD - $\delta^{18}O_{SO4}$ -$\delta^{18}O_{OH}$ - $\delta^{34}S$ OF ALUNITE AT CREEDE, CO: AN EXAMPLE OF SUPERGENE ACID-SULFATE ALTERATION OVERLYING ADULARIA-SERICITE MINERALIZATION

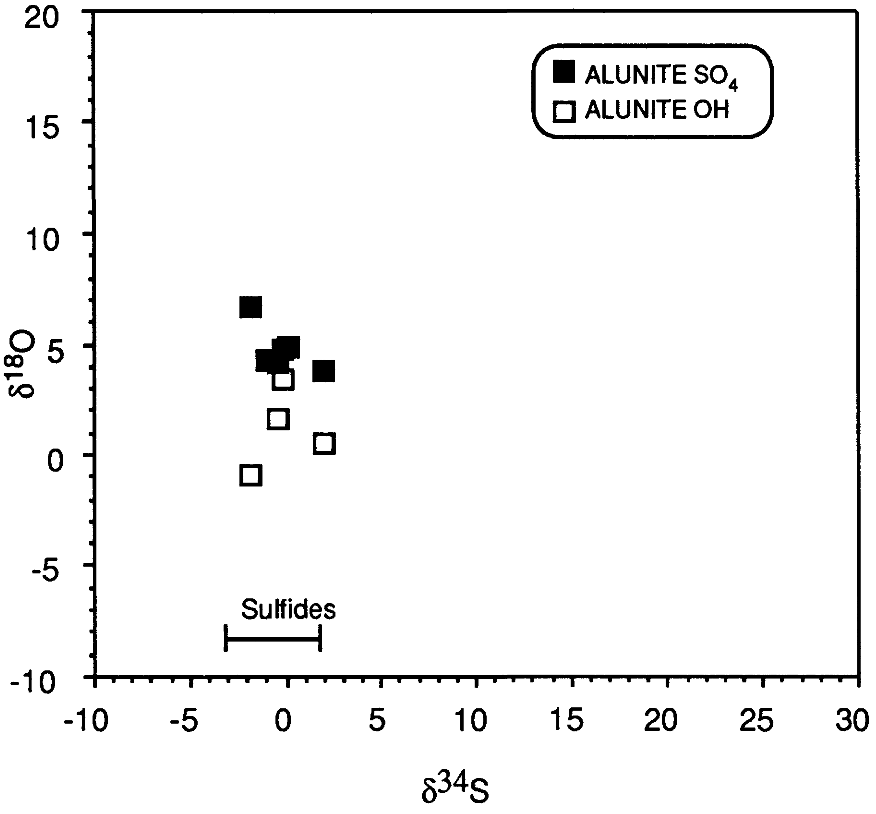

FIGURE 6a

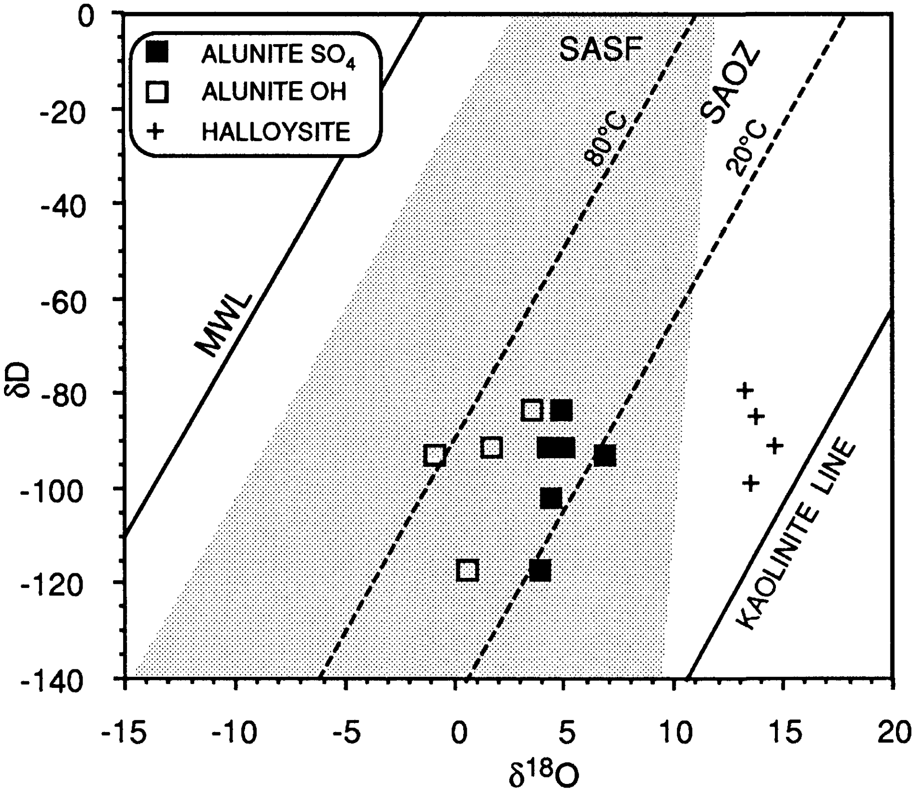

FIGURE 6b

δD-$\delta^{18}O_{SO4}$-$\delta^{18}O_{OH}$-$\delta^{34}S$ OF ALUNITES FROM ROUND MOUNTAIN, NV: AN EXAMPLE OF SUPERGENE ACID SULFATE ALTERATION OVERLYING ADULARIA-SERICITE-TYPE GOLD MINERALIZATION

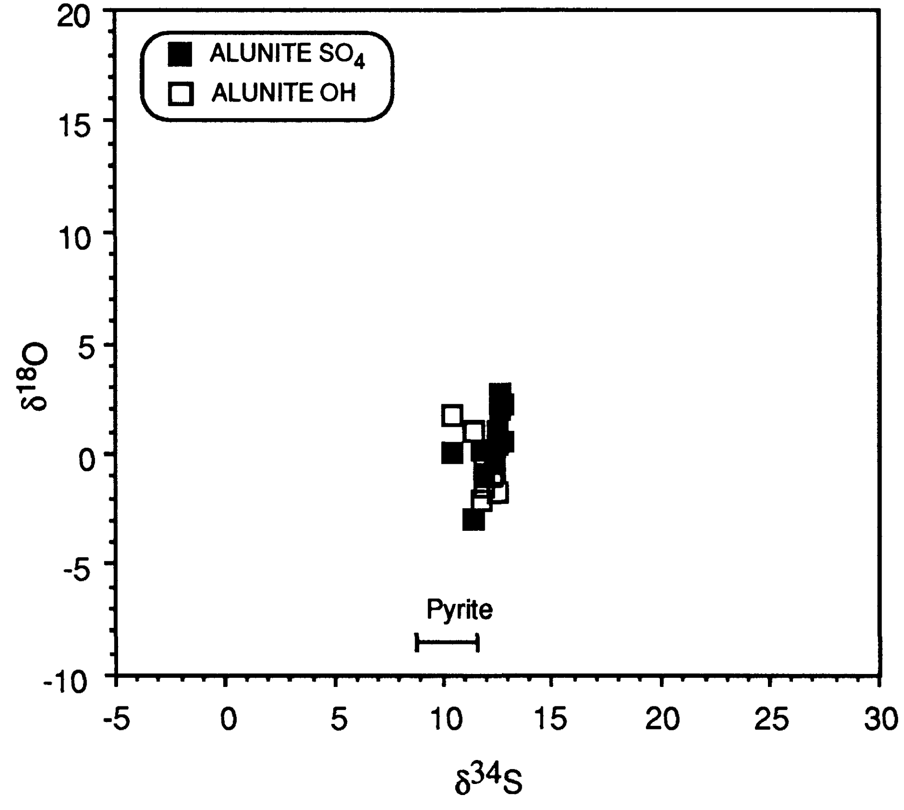

FIGURE 7a

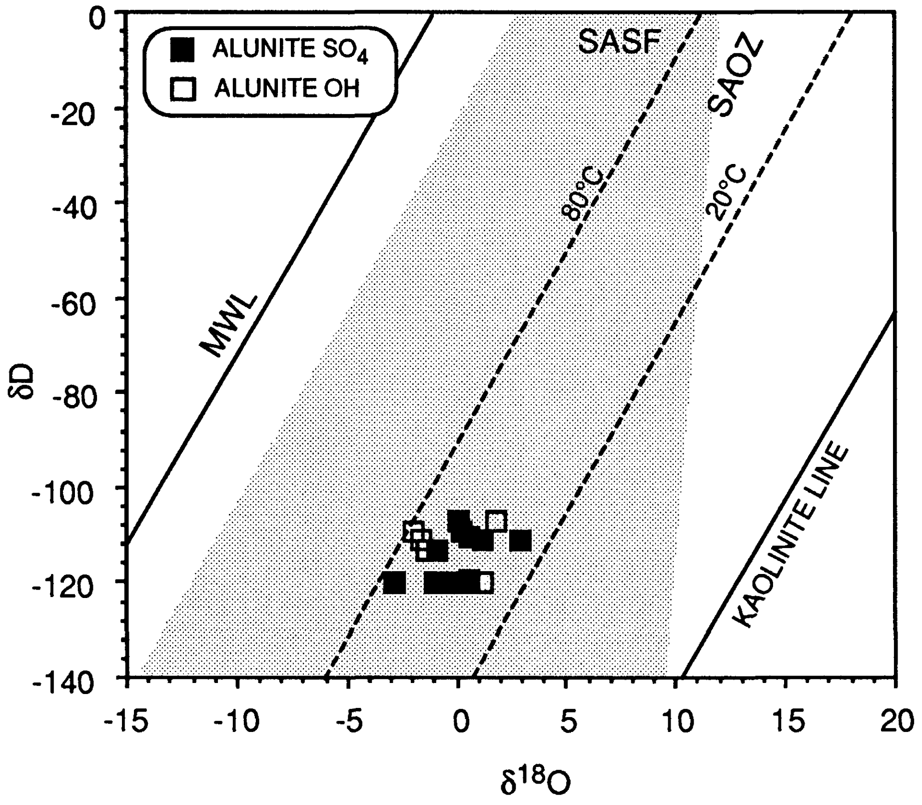

FIGURE 7b

δD - $\delta^{18}O_{SO4}$ - $\delta^{18}O_{OH}$ - $\delta^{34}S$ OF SUPERGENE ALUNITE, δD - $\delta^{18}O$ OF ASSOCIATED HALLOYSITE AND $\delta^{34}S$ OF PRECURSOR SULFIDES FOR DEPOSITS FROM A RANGE OF LATITUDES

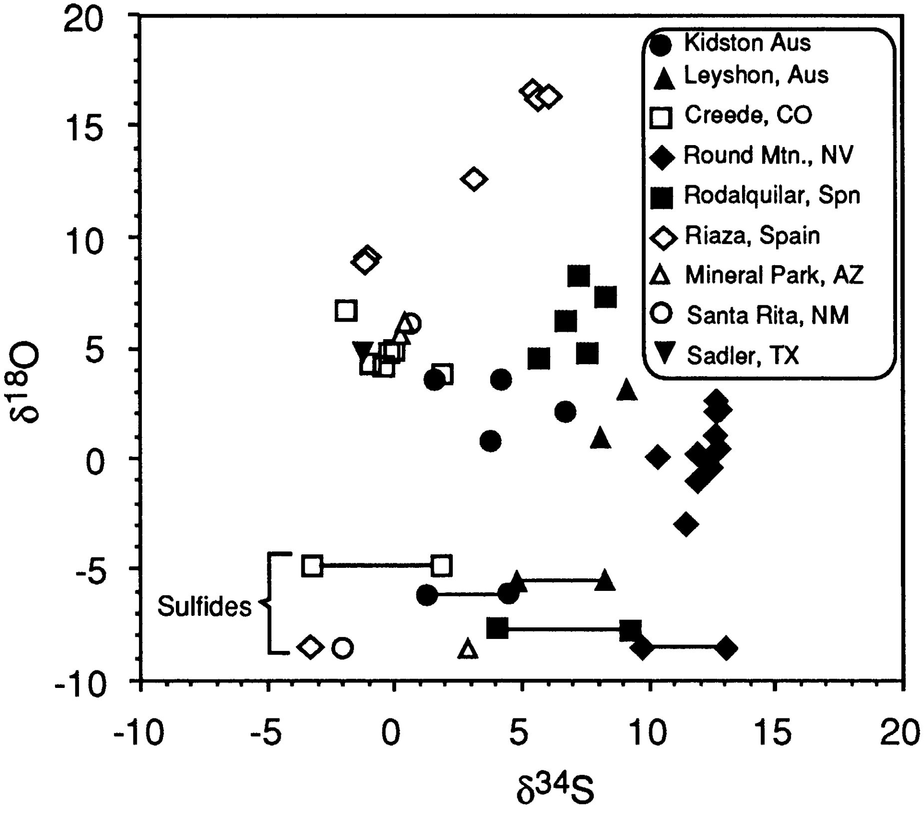

FIGURE 8a

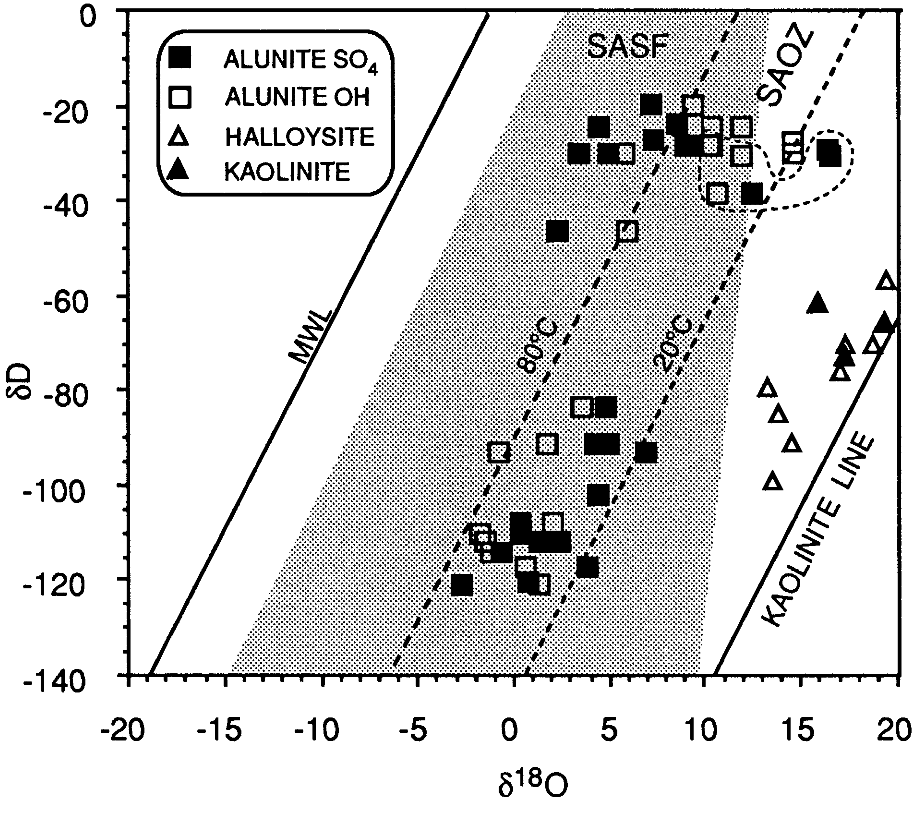

FIGURE 8b

δD-$\delta^{18}O_{SO4}$-$\delta^{18}O_{OH}$-$\delta^{34}S$ OF ALUNITE, δD-$\delta^{18}O$ OF KAOLINITE, AND δD_{H2O}-$\delta^{18}O_{H2O}$ OF FLUIDS FROM TOLFA DISTRICT, ITALY: AN EXAMPLE OF STEAM-HEATED ACID SULFATE ALTERATION

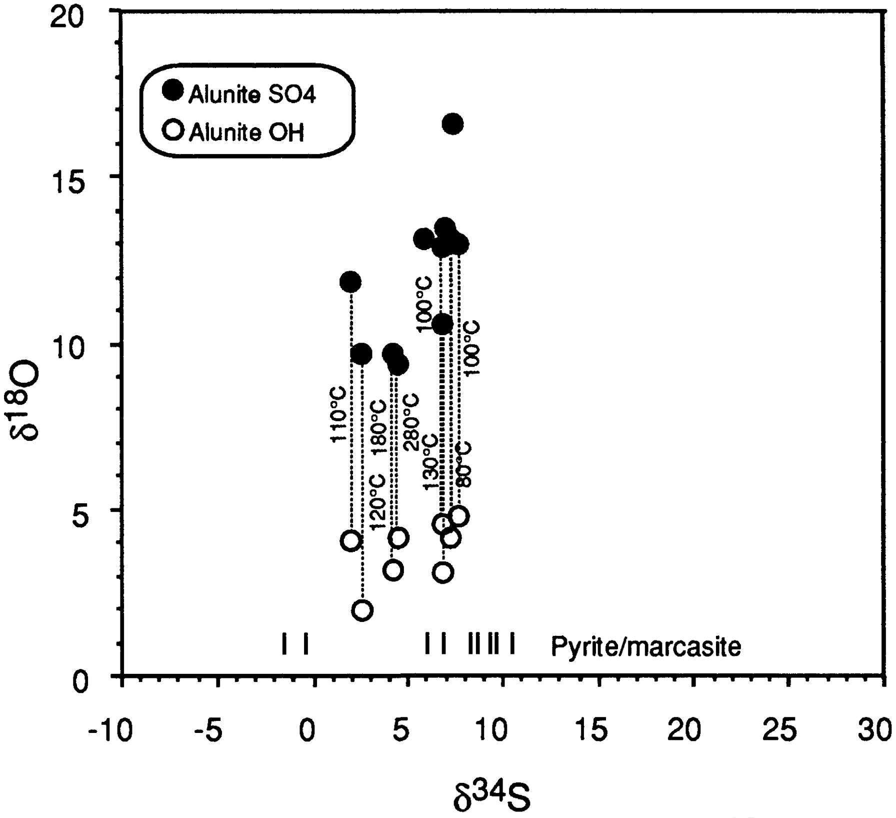

FIGURE 9a

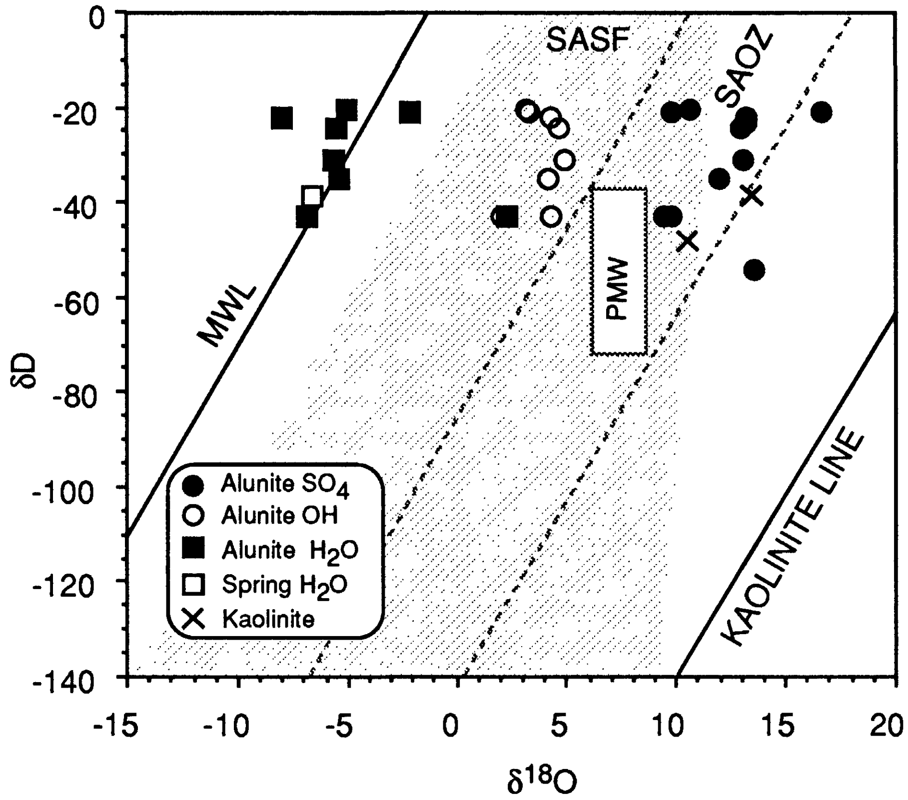

FIGURE 9b

δD - $\delta^{18}O_{SO4}$ -$\delta^{18}O_{OH}$ - $\delta^{34}S$ OF REPLACEMENT ALUNITE AND δD_{H2O} -$\delta^{18}O_{H2O}$ OF FLUIDS AT MARYSVALE, UT: AN EXAMPLE OF STEAM HEATED ACID SULFATE ALTERATION

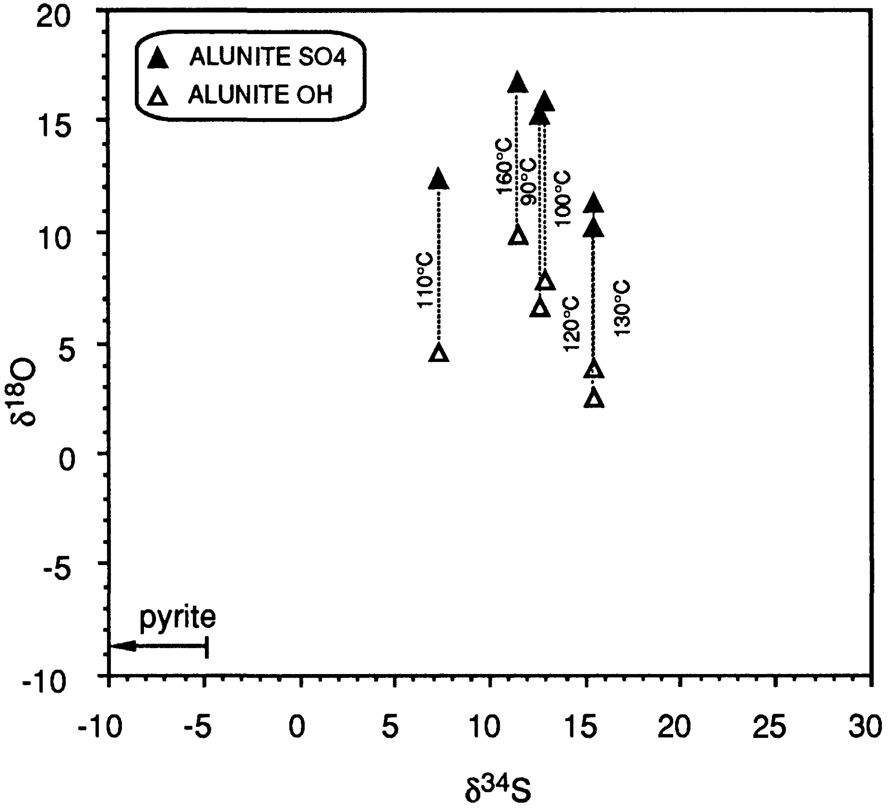

FIGURE 10a

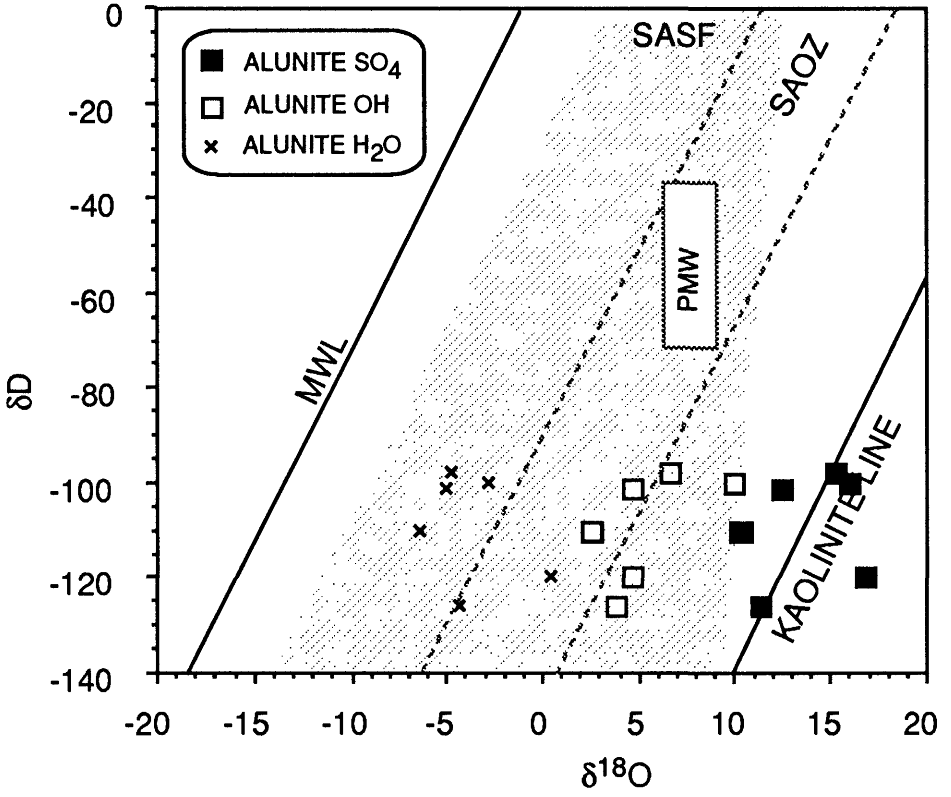

FIGURE 10b

δD - $\delta^{18}O_{SO4}$ - $\delta^{18}O_{OH}$ - $\delta^{34}S$ OF ALUNITE AND δD - $\delta^{18}O$ OF KAOLINITE FROM JULCANI DISTRICT, PERU: AN EXAMPLE OF A PURE MAGMATIC-HYDROTHERMAL SYSTEM

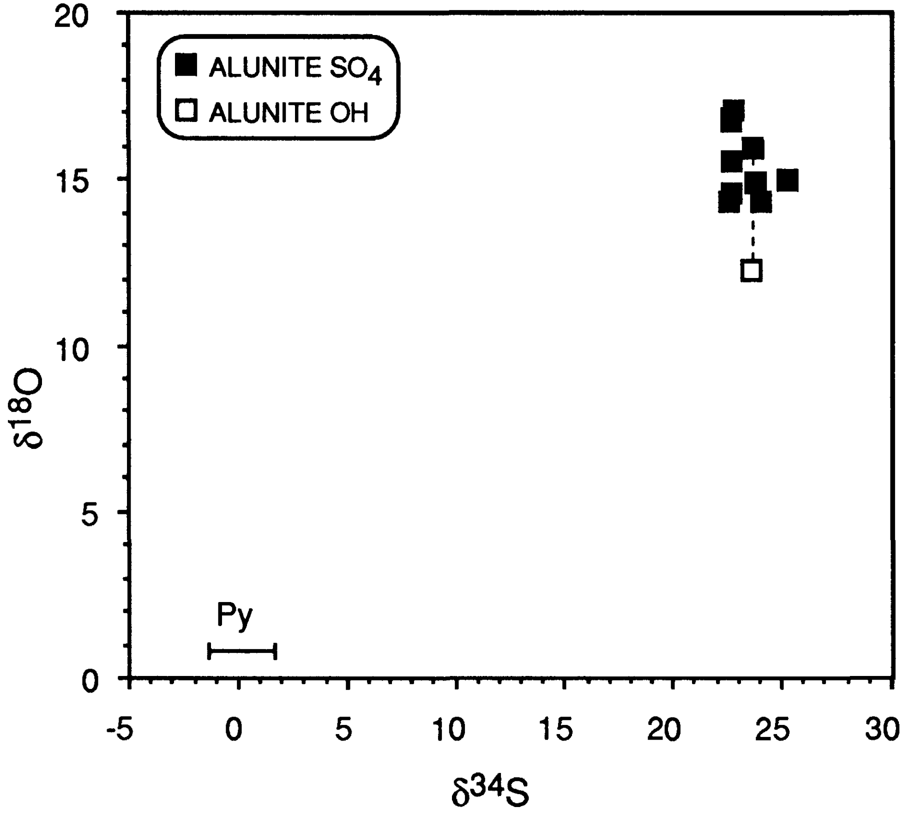

FIGURE 11a

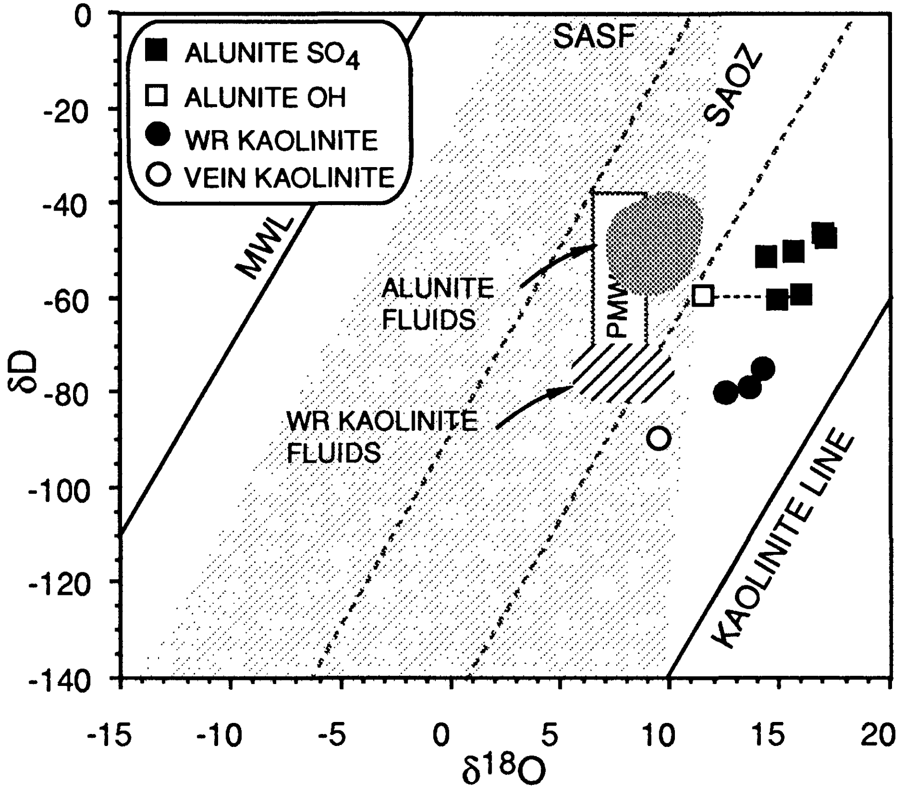

FIGURE 11b

δD - $\delta^{18}O_{SO4}$ - $\delta^{18}O_{OH}$ - $\delta^{34}S$ OF ALUNITE AND δD - $\delta^{18}O$ OF KAOLINITE FROM SUMMITVILLE, CO: AN EXAMPLE OF A MIXED MAGMATIC-METEORIC ACID SULFATE SYSTEM:

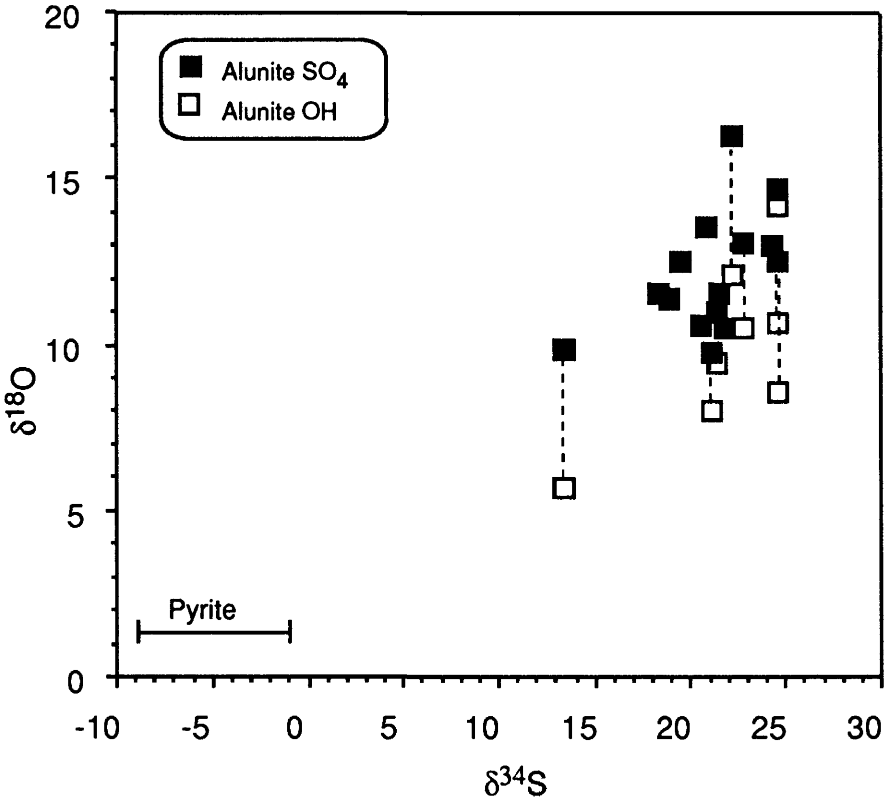

FIGURE 12a

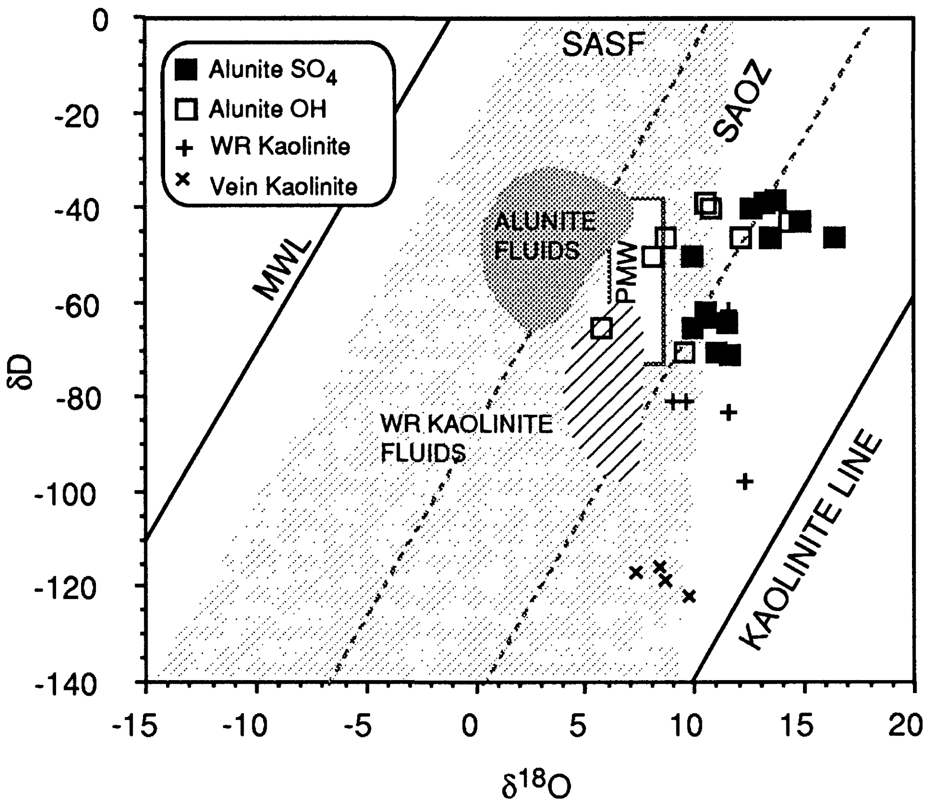

FIGURE 12b

δD - $\delta^{18}O_{SO4}$ - $\delta^{18}O_{OH}$ - $\delta^{34}S$ OF ALUNITE FROM ALUNITE RIDGE VEIN DEPOSITS NEAR MARYSVALE, UT: AN EXAMPLE OF MAGMATIC-STEAM ALUNITE:

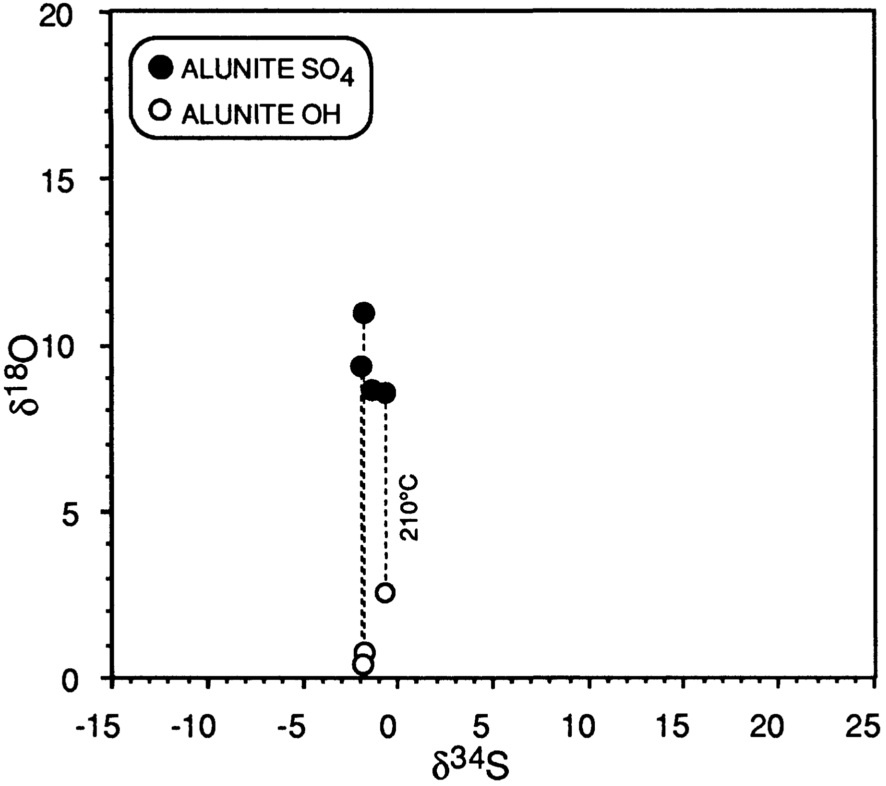

FIGURE 13a

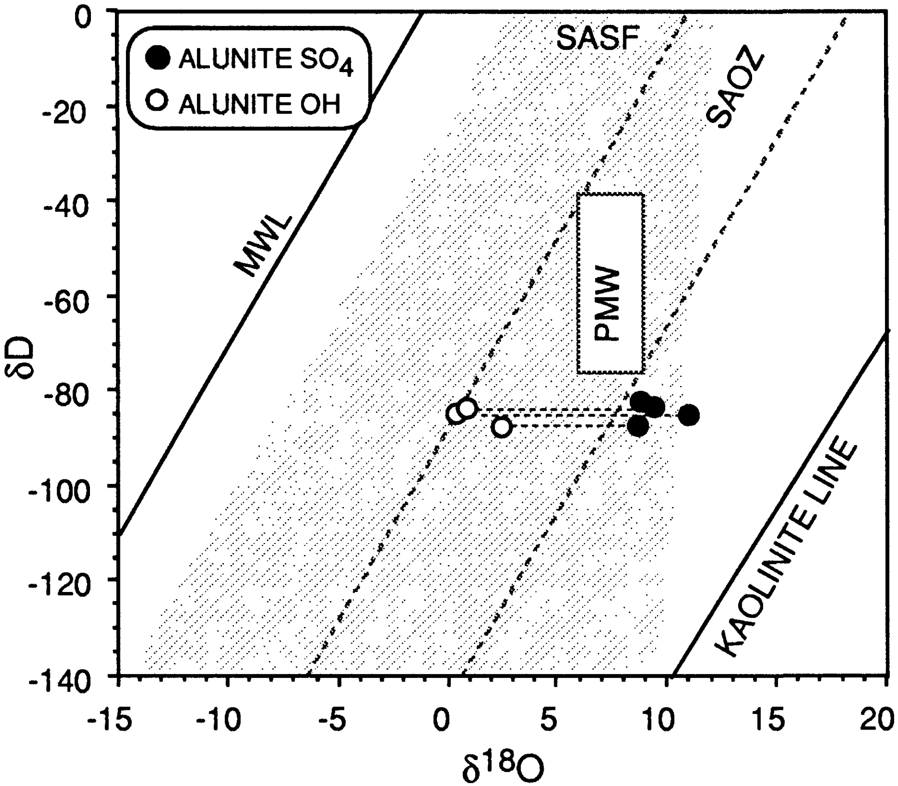

FIGURE 13b

δD-$\delta^{18}O_{SO4}$-$\delta^{18}O_{OH}$-$\delta^{34}S$ OF ALUNITE AND δD-$\delta^{18}O$ OF KAOLINITE FROM CACTUS GOLD DEPOSIT, CA: AN EXAMPLE OF ACID-SULFATE ALTERATION IN A VOLCANIC-DOME FIELD

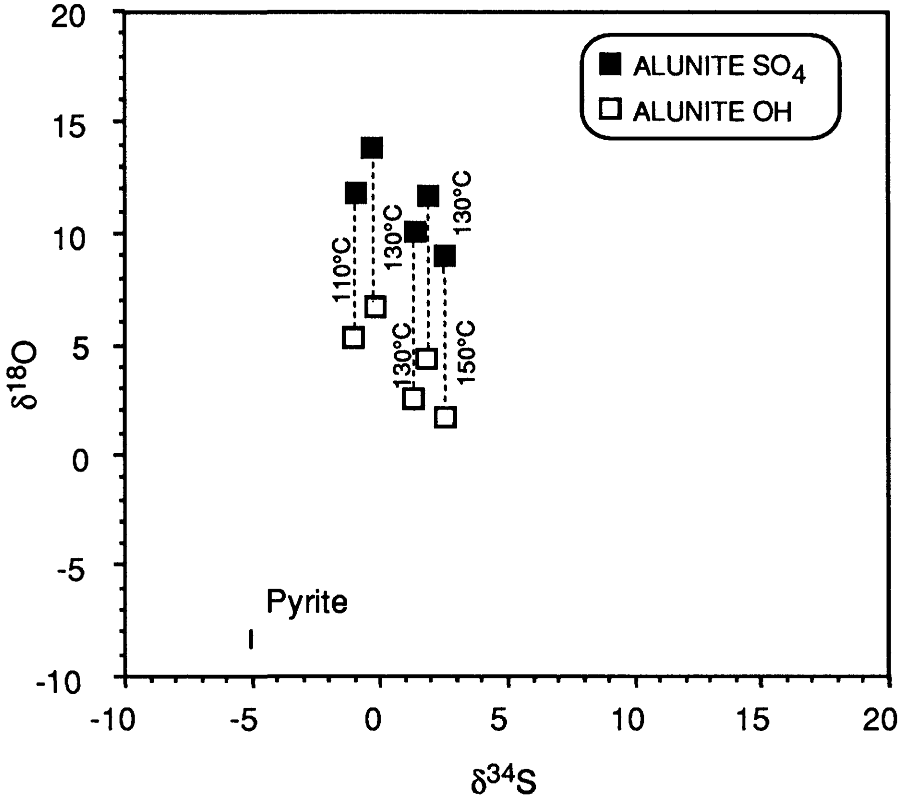

FIGURE 14a

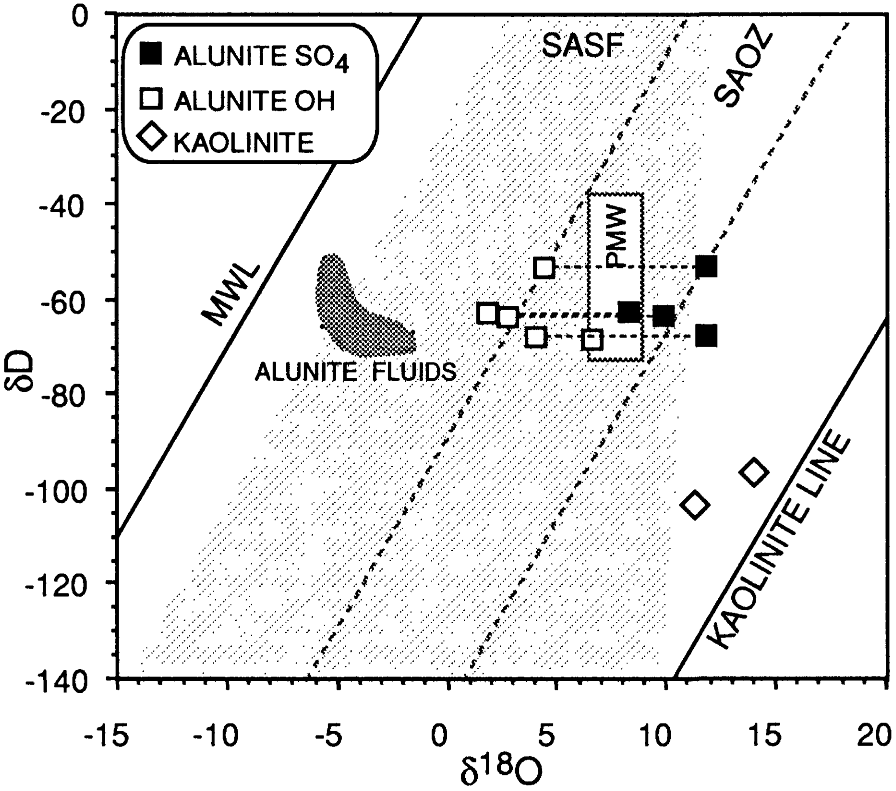

FIGURE 14b

δD-$\delta^{18}O_{SO4}$-$\delta^{18}O_{OH}$-$\delta^{34}S$ OF ALUNITES FROM RED MOUNTAIN, CO: AN EXAMPLE OF MULTIPLE STAGE MAGMATIC-HYDROTHERMAL ACID-SULFATE ALTERATION AND LATER MAGMATIC-STEAM ALUNITE

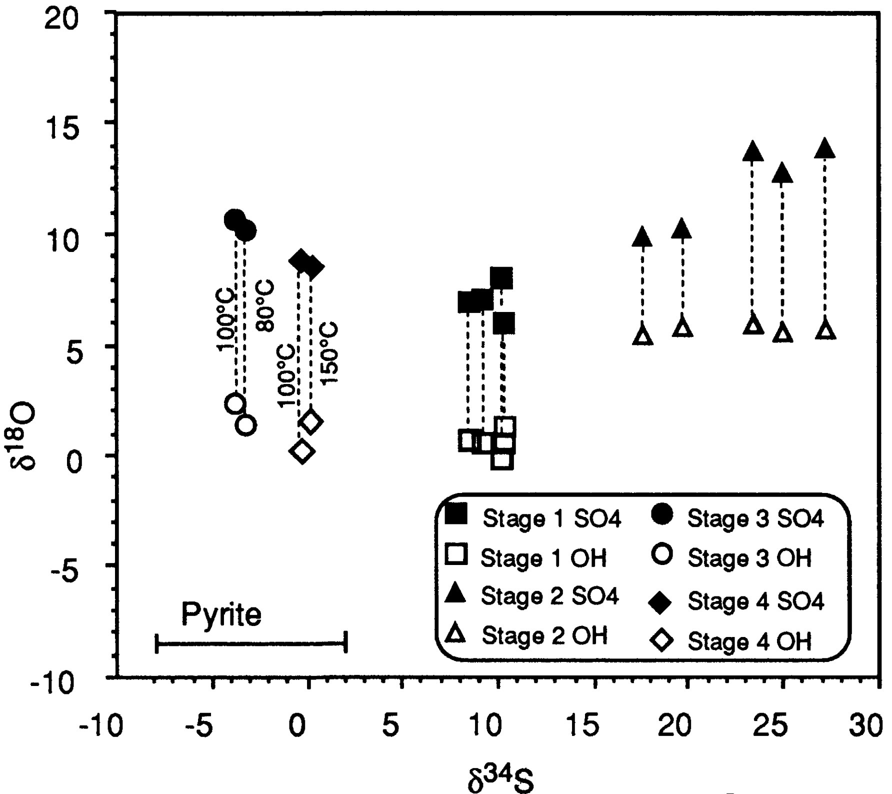

FIGURE 15a

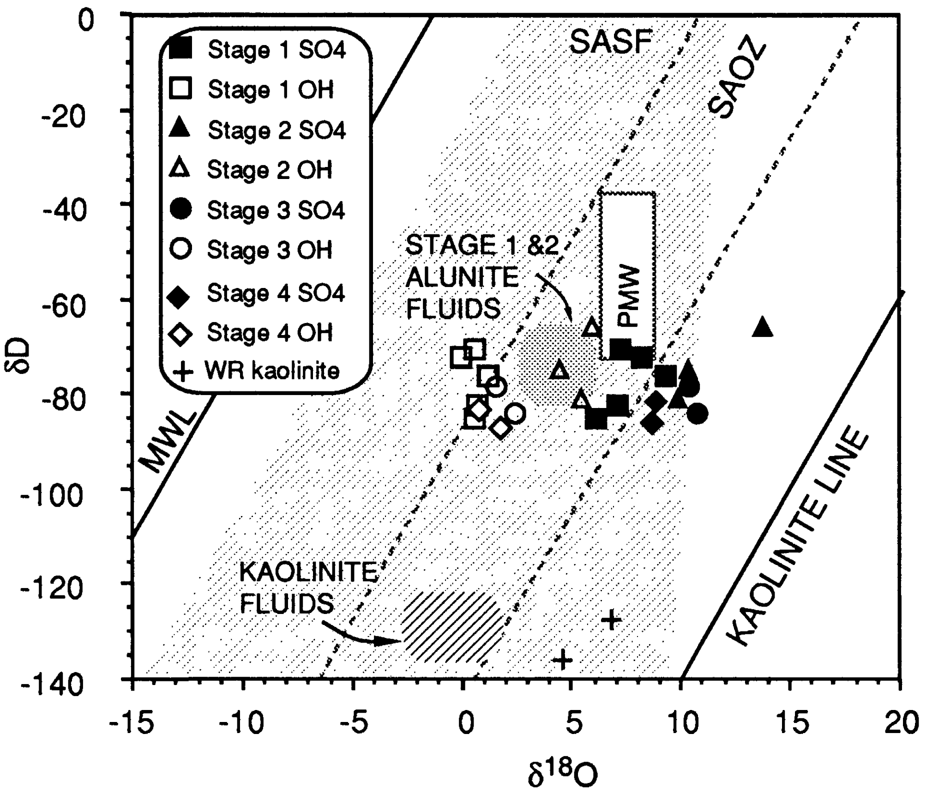

FIGURE 15b

δD-$\delta^{18}O_{SO4}$-$\delta^{18}O_{OH}$-$\delta^{34}S$ OF ALUNITE FROM EL SALVADOR, CHILE: AN EXAMPLE OF SUPERGENE ACID-SULFATE ALTERATION AND MAGMATIC-HYDROTHERMAL ALUNITE

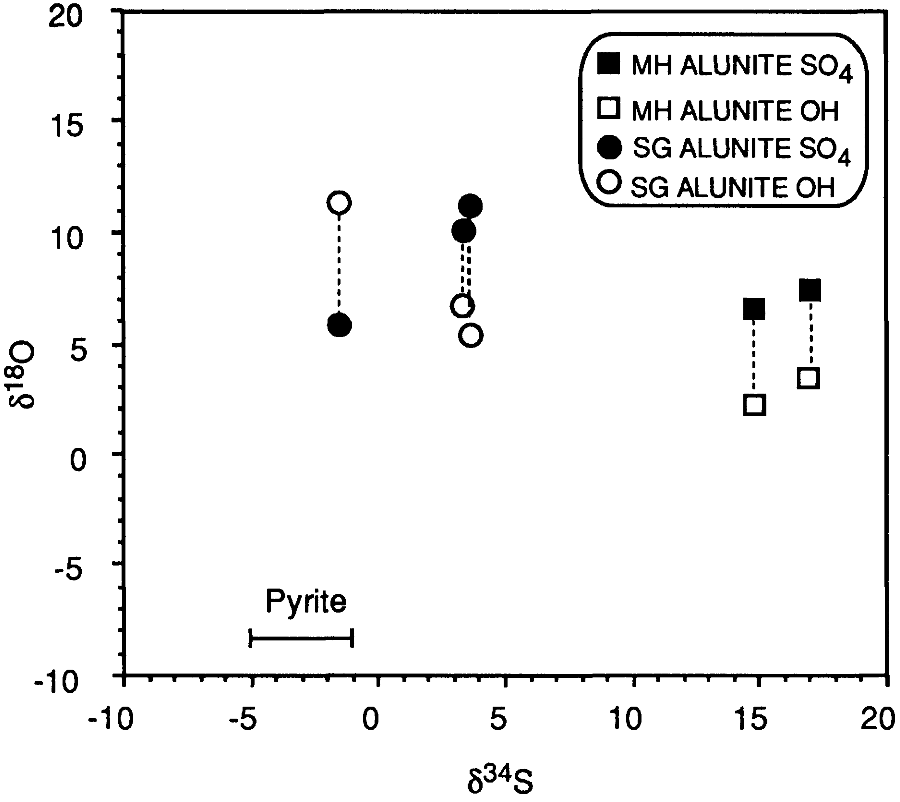

FIGURE 16a

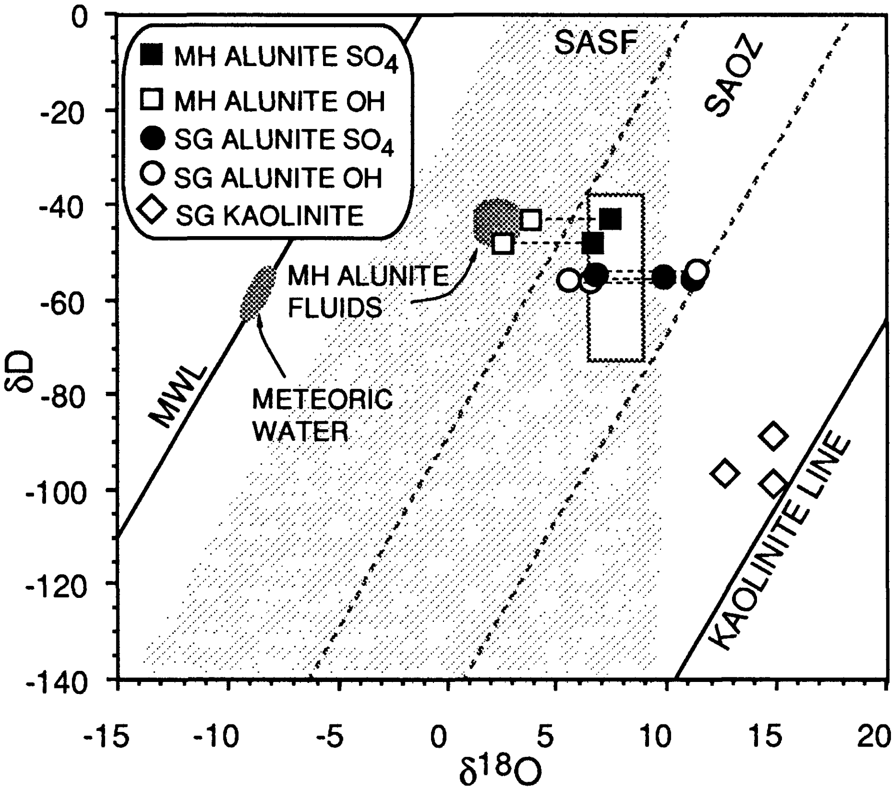

FIGURE 16b

δD - $\delta^{18}O_{SO4}$ - $\delta^{18}O_{OH}$ - $\delta^{34}S$ OF ALUNITE AND δD - $\delta^{18}O$ OF KAOLINITE AT RODALQUILAR, ALMERIA, SPAIN: AN EXAMPLE OF SUPERGENE AND MAGMATIC-HYDROTHERMAL ACID-SULFATE ALTERATION

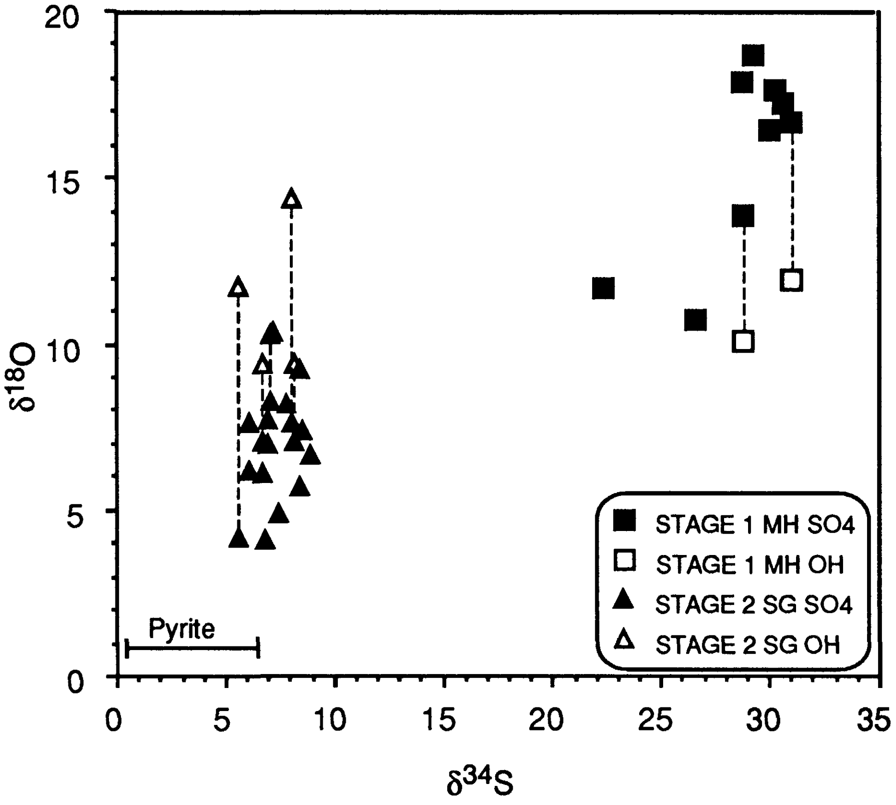

FIGURE 17a

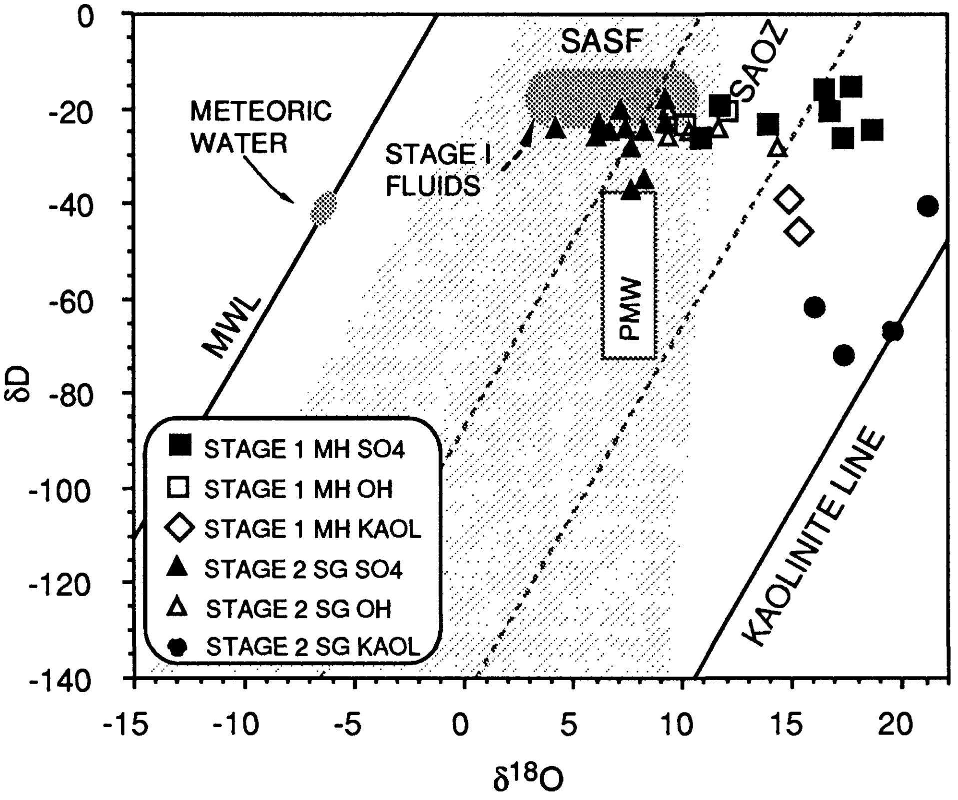

FIGURE 17b

δD - $\delta^{18}O_{SO4}$ - $\delta^{18}O_{OH}$ - $\delta^{34}S$ OF ALUNITE AND δD - $\delta^{18}O$ OF KAOLINITE FROM NEVADA TERTIARY DEPOSITS: EXAMPLES OF ACID-SULFATE ALTERATION IN DIVERSE SYSTEMS

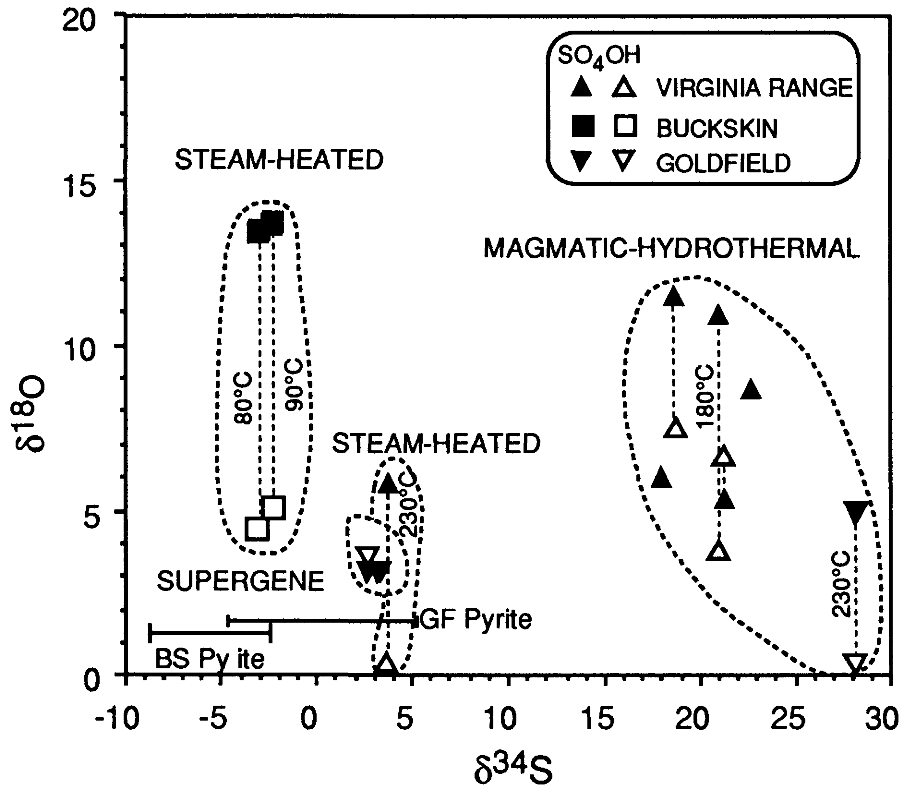

FIGURE 18a

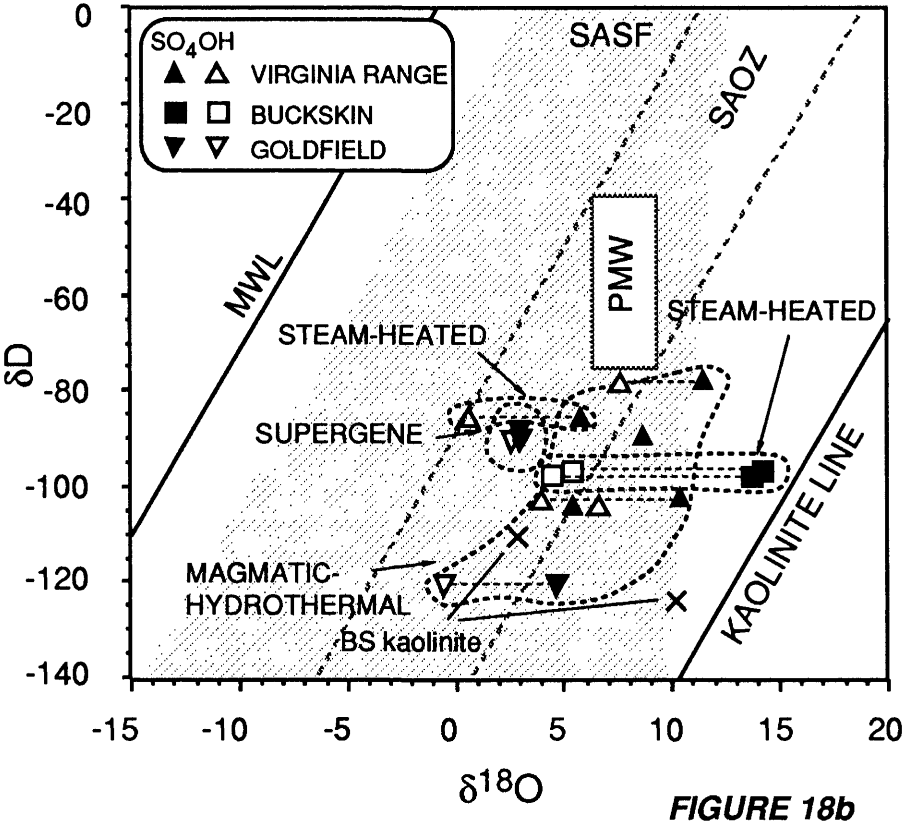

FIGURE 18b

$\Delta^{18}O_{SO4\text{-}OH}$ IN ALUNITE FROM VARIOUS ENVIRONMENTS PLOTTED AGAINST DEPOSITIONAL TEMPERATURE AND EQUILIBRIUM FRACTIONATIONS

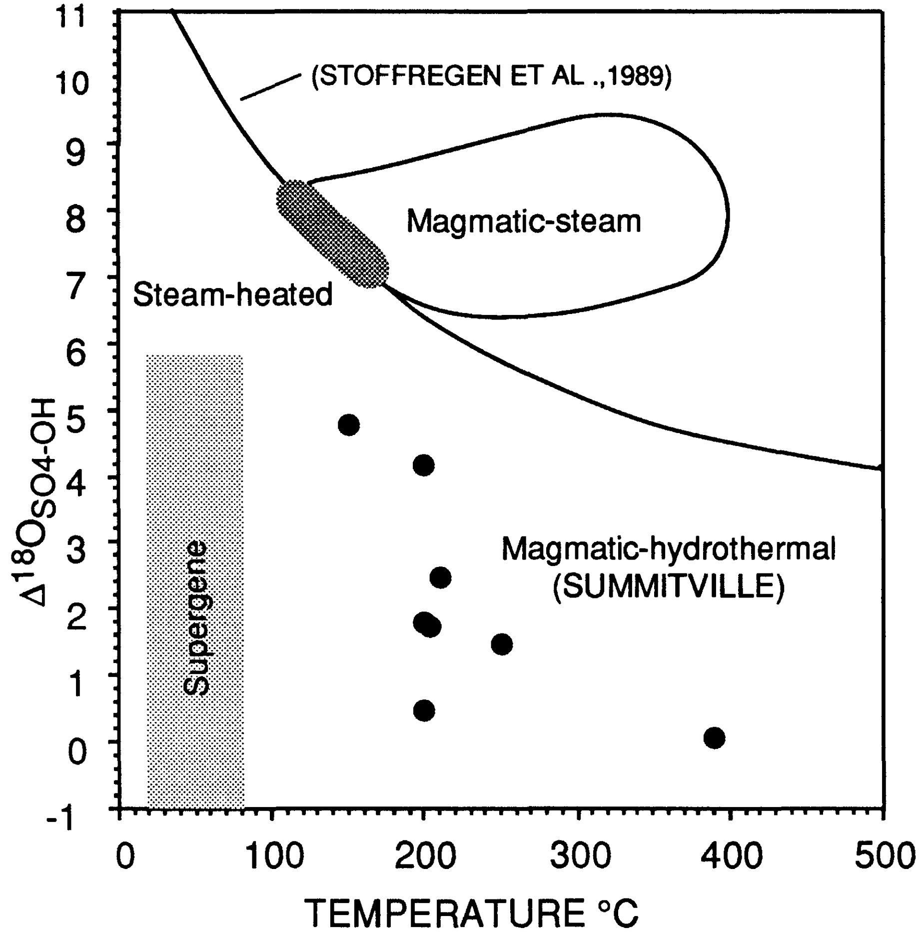

FIGURE 19a

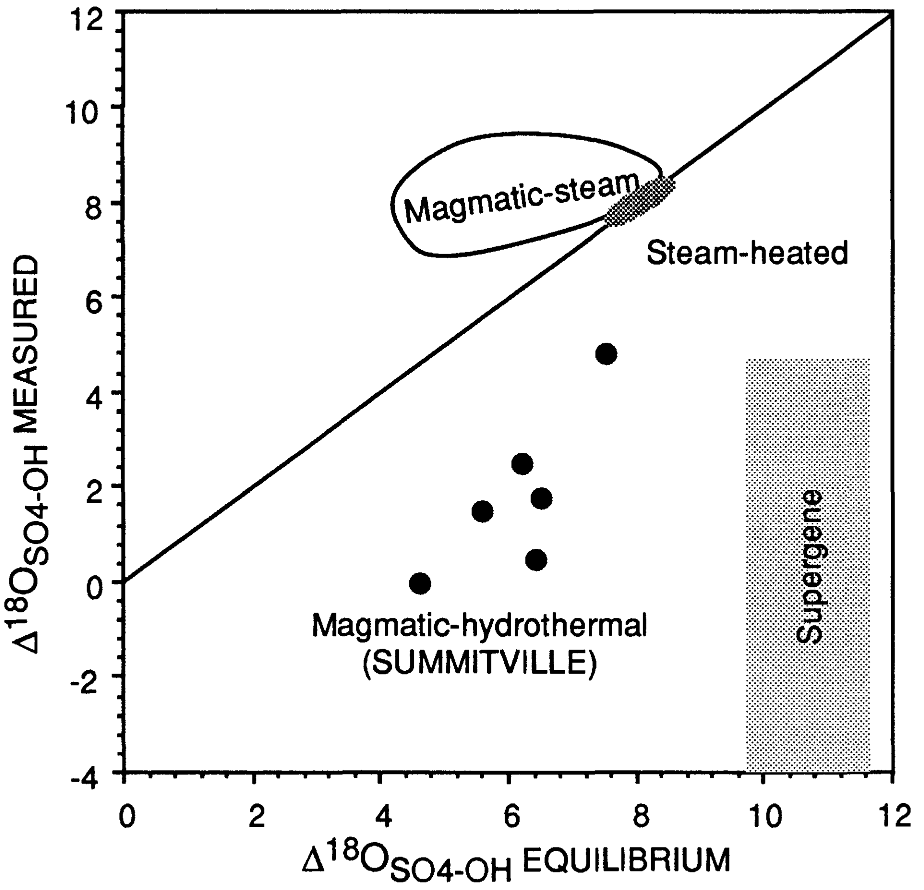

FIGURE 19b

MEASURED $\Delta^{34}S_{Alun-Py/H2S}$ AND $\Delta^{18}O_{SO4-H2O}$ VERSUS PREDICTED EQUILIBRIUM FRACTIONATIONS

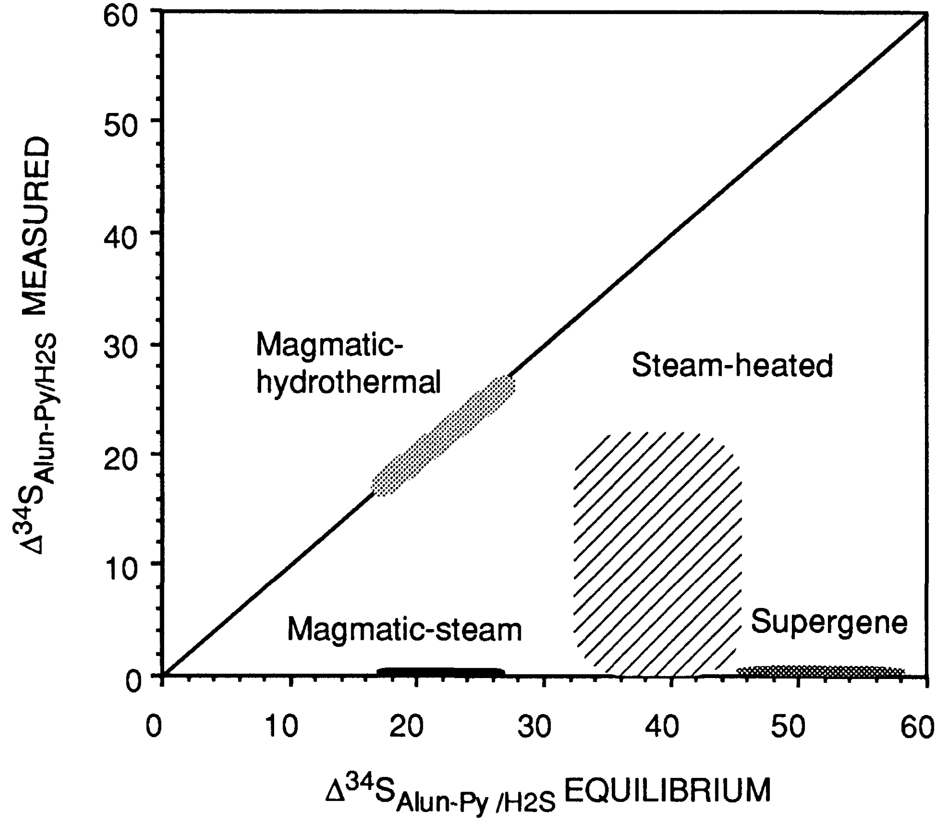

FIGURE 20a

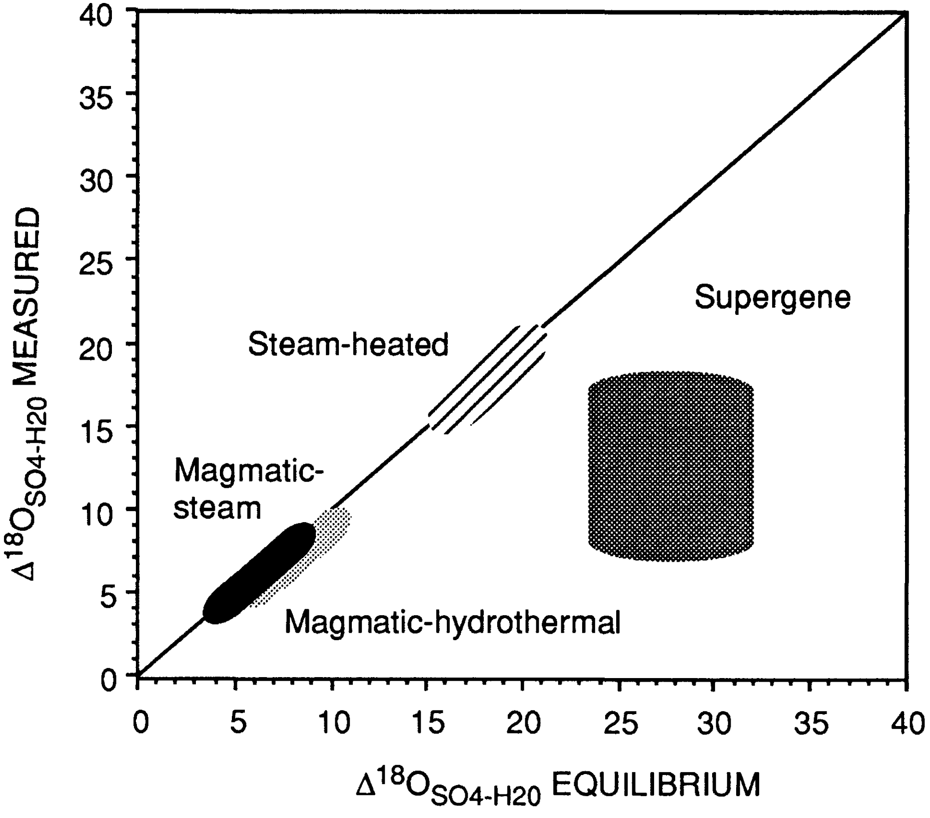

FIGURE 20b

TABLE 1
Stable isotope data of alunite and associated minerals

SAMPLE	DISTRICT	LOCATION	MINERAL	TYPE	COLLECTOR/REFERENCE	δD	$\delta^{18}O_{SO4}$	$\delta^{18}O_{OH}$	$\delta^{34}S$	$\delta^{18}O$	TEMP
PMB-ZI-1054	Creede, CO	Amethyst vein	alunite	SG	P.M. Bethke	-91	4.2	1.7	-.5		
PMB-ZI-1055	Creede, CO	Amethyst vein	alunite	SG	P.M. Bethke	-83	4.8	3.5	-.2		
PMB-ZP-1071	Creede, CO	Amethyst vein	alunite	SG	P.M. Bethke	-117	3.8	.6	1.9		
PMB-ZP-1070	Creede, CO	Amethyst vein	alunite	SG	P.M. Bethke	-104			1.9		
PMB-YC-1009	Creede, CO	Amethyst vein	alunite	SG	P.M. Bethke	-93	6.8	-.9	-1.9		
PMB-YF-1012	Creede, CO	Amethyst vein	alunite	SG	P.M. Bethke	-91	4.9		.0		
PMB-YG-1013	Creede, CO	Amethyst vein	alunite	SG	P.M. Bethke	-102	4.3		-1.0		
chance dump #26	Creede, CO	Amethyst vein	alunite	SG	P.M. Bethke	-84					
PMB-TQ-847	Creede, CO	Amethyst vein	alunite	SG	P.M. Bethke	-86					
PMB-154-5-76F	Creede, CO	Amethyst vein	alunite	SG	P.M. Bethke	-84					
PMB-TP-845A	Creede, CO	Amethyst vein	alunite	SG	P.M. Bethke	-85					
PMB-ZP-1071-79	Creede, CO	Amethyst vein	alunite	SG	P.M. Bethke	-101					
PMB-TR-84B-76	Creede, CO	Amethyst vein	alunite	SG	P.M. Bethke	-86					
PMB-T-28D-75	Creede, CO	Amethyst vein	alunite	SG	P.M. Bethke	-88					
PMB-ZP-1041-79	Creede, CO	Amethyst vein	halloysite	SG	P.M. Bethke	-99				13.5	
PMB-UD-867(c)	Creede, CO	Amethyst vein	halloysite	SG	P.M. Bethke	-85				13.8	
PMB-XO-985-79	Creede, CO	Amethyst vein	halloysite	SG	P.M. Bethke	-79				13.3	
PMB-TE-825	Creede, CO	Amethyst vein	halloysite	SG	P.M. Bethke	-91				14.6	
RM 6325P+75	Round Mtn., NV	Round Mtn. deposit	alunite	SG	R.A. Fifarek	-119	.6		12.7		
RM 6325 PE	Round Mtn., NV	Round Mtn. deposit	alunite	SG	R.A. Fifarek		2.1		12.6		
RM 6325P-30	Round Mtn., NV	Round Mtn. deposit	alunite	SG	R.A. Fifarek	-111	2.3		12.7		
RM 6325P+10C	Round Mtn., NV	Round Mtn. deposit	alunite	SG	R.A. Fifarek	-111	1.1	-1.7	12.5		
SH 6430-33POR	Round Mtn., NV	Round Mtn. deposit	alunite	SG	R.A. Fifarek		.3	-1.0	12.3		
SH 6430-33POW	Round Mtn., NV	Round Mtn. deposit	alunite	SG	R.A. Fifarek	-120	-2.9	1.1	11.4		
JT 32	Round Mtn., NV	Round Mtn. deposit	alunite	SG	R.A. Fifarek	-107	.1	1.8	10.4		
JT 900L	Round Mtn., NV	Round Mtn. deposit	alunite	SG	R.A. Fifarek	-109	.2	-2.0	11.8		
JT 27	Round Mtn., NV	Round Mtn. deposit	alunite	SG	R.A. Fifarek		2.8		12.6		
SH 6360-11	Round Mtn., NV	Round Mtn. deposit	alunite	SG	R.A. Fifarek		-.9	-1.4	11.9		
SH 6430-82	Round Mtn., NV	Round Mtn. deposit	alunite	SG	R.A. Fifarek		-1.0	-.2	11.9		
SH 6465-113	Round Mtn., NV	Round Mtn. deposit	alunite	SG	R.A. Fifarek		.5	.5	12.5		
SH 6360-18	Round Mtn., NV	Round Mtn. deposit	alunite	SG	R.A. Fifarek		-.4	-.9	12.4		
1E	Kidston, Australia	Kidston Au dep.	alunite	SG	Bird et al., 1989	*-46*	2.2	5.9	*6.7*		
1F	Kidston, Australia	Kidston Au dep.	alunite	SG	Bird et al., 1989	*-50*	.9		*3.7*		
1H	Kidston, Australia	Kidston Au dep.	alunite	SG	Bird et al., 1989	*-46*	3.6		*1.5*		
1 J	Kidston, Australia	Kidston Au dep.	alunite	SG	Bird et al., 1989	*-44*	3.6		*4.2*		
LEY 1A	Leyshon, Australia	Mt Leyshon Au dep	alunite	SG	Bird et al., 1989	*-29*	3.3		*9.1*		
LEY 5C	Leyshon, Australia	Mt Leyshon Au dep	alunite	SG	Bird et al., 1989	*-28*	.8	5.8	*8.0*		
Sadler	Sadler, TX	Woodbine Fm.	alunite	SG	R.E. Stoffregen	-30	4.9	14.6	-1.1		
AAR1	Riaza, Spain	Villacort	alunite	SG	A. Arribas	-32	16.4	11.7	6.0		
AAR2	Riaza, Spain	Villacort	alunite	SG	A. Arribas	-31	16.4	11.4	5.9		
AAR3	Riaza, Spain	Villacort	alunite	SG	A. Arribas	-32	16.6	10.9	5.2		

AAR4	Riaza, Spain	Madrigurera	alunite	SG	A. Arribas	-38	12.4	10.6	3.0		
AAR5	Riaza, Spain	Madrigurera	halloysite	SG	A. Arribas	-70				17.4	
AAR6	Riaza, Spain	Madrigurera	halloysite	SG	A. Arribas	-76				17.0	
AAF7	Riaza, Spain	Madrigurera	halloysite	SG	A. Arribas	-57				19.4	
AAR11	Riaza, Spain	Negredo	halloysite	SG	A. Arribas	-70				18.7	
AAR12	Riaza, Spain	Negredo	alunite	SG	A. Arribas	-28	9.0	10.3	-1.2		
AAR13	Riaza, Spain	Negredo	alunite	SG	A. Arribas	-28	9.2	10.2	-1.1		
C-6	Santa Rita, NM	Chino Mine	alunite	SG	Field, 1966	-54	6.1	8.9	.6		
MP-10b	Wallapai, Dist., AZ	Mineral Park	alunite	SG	Field, 1966	-65	5.7	5.5	.2		
33	Tolfa, Italy	Le Cave Vecchie	alunite	SH	Field and Lombardi, 1972	-21	9.7	3.2	*4.1*		180
51	Tolfa, Italy	Le Cave Vecchie	alunite	SH	Field and Lombardi, 1972	-43	9.4	4.2	*4.4*		280
17	Tolfa, Italy	Le Cave Vecchie	alunite	SH	Field and Lombardi, 1972	-31	13.0	4.8	*7.6*		100
26	Tolfa, Italy	Le Cave Vecchie	alunite	SH	Field and Lombardi, 1972	-22	13.2	4.2	*7.2*		80
56	Tolfa, Italy	Le Cave Vecchie	alunite	SH	Field and Lombardi, 1972	-20	10.6	3.1	*6.8*		100
31	Tolfa, Italy	La Gavaccia	alunite	SH	Field and Lombardi, 1972	-24	12.9	4.6	*6.8*		130
64A	Tolfa, Italy	Allumiere	alunite	SH	Field and Lombardi, 1972	43	9.7	2.0	*2.5*		120
65A	Tolfa, Italy	Allumiere	alunite	SH	Field and Lombardi, 1972	-35	11.9	4.1	*6.9*		110
H 12	Tolfa, Italy	La Cave Vecchie	kaolinite	SH	Lombardi and Sheppard, 1977	*-37*				*13.4*	
H28	Tolfa, Italy	Allumiere	kaolinite	SH	Lombardi and Sheppard, 1977	*-44*				*10.4*	
H43	Tolfa, Italy	Allumiere	kaolinite	SH	Lombardi and Sheppard, 1977	*-45*				*10.5*	
M765	Marysvale, UT	Mary's Lamb	alunite	SH	Cunningham et al., 1984	-110	10.2	2.5	*15.4*		120
M30	Marysvale, UT	White Horse	alunite	SH	Cunningham et al., 1984	-98	15.3	6.6	*12.6*		90
M47B	Marysvale, UT	Yellow Jacket	alunite	SH	Cunningham et al., 1984	-100	15.9	10.0	*12.9*		100
M53	Marysvale, UT	Winkleman	alunite	SH	Cunningham et al., 1984	-120	16.8	4.6	*11.5*		160
M804	Marysvale, UT	Al Kee Mee	alunite	SH	Cunningham et al., 1984	-101	12.4	4.6	*7.4*		110
M764	Marysvale, UT	White Hills	alunite	SH	Cunningham et al., 1984	-126	11.3	3.8	*15.4*		130
390 V 14-198	Julcani, Peru	Herminia	alunite	MH	J.A. Deen		16.8		22.7		
390 V 14-198	Julcani, Peru	Herminia	pyrite	MH	J.A. Deen				-1.2		
420 V DOC CR	Julcani, Peru	Herminia	alunite	MH	J.A. Deen		14.4		24.0		
420 V DOC CR	Julcani, Peru	Herminia	pyrite	MH	J.A. Deen				1.9		
420 V 2NW G	Julcani, Peru	Herminia	alunite	MH	J.A. Deen	-47	17.1		22.8		
420 V 2NW G	Julcani, Peru	Herminia	pyrite	MH	J.A. Deen				1.6		
JAD-49	Julcani, Peru	Lucrecia	alunite	MH	J.A. Deen		14.6		22.6		
JAD-50	Julcani, Peru	Lucrecia	alunite	MH	J.A. Deen		15.0		25.2		
JAD-51	Julcani, Peru	Lucrecia	alunite	MH	J.A. Deen	-51	14.4		22.5		
JAD-51	Julcani, Peru	Lucrecia	pyrite	MH	J.A. Deen				0.8		
300 LUC BY PASS	Julcani, Peru	Lucrecia	alunite	MH	J.A. Deen	-59	16.0	12.3	23.6		590
300 LUC BY PASS	Julcani, Peru	Lucrecia	pyrite	MH	J.A. Deen				0.5		
500 Esperanza	Julcani, Peru	Herminia	alunite	MH	J.A. Deen	-60	14.9		23.8		
500 Esperanza	Julcani, Peru	Herminia	pyrite	MH	J.A. Deen				-0.4		
420 RAMPA 1	Julcani, Peru	Herminia	alunite	MH	J.A. Deen	-46	16.9		22.7		
420 RAMPA 1	Julcani, Peru	Herminia	pyrite	MH	J.A. Deen				0.2		
420 RAMPA 5	Julcani, Peru	Herminia	alunite	MH	J.A. Deen	-50	15.6		22.6		
420 RAMPA 5	Julcani, Peru	Herminia	pyrite	MH	J.A. Deen				1.8		
420 2NW T	Julcani, Peru	Herminia	alunite	MH	J.A. Deen				28.1		

420 2NW T	Julcani, Peru	Herminia	pyrite	MH	J.A. Deen				1.6		
630 Doc 245-30E	Julcani, Peru	Herminia	WR kaolinite	MH	J.A. Deen	-75				12.6	
420 R. 340 v.14-198	Julcani, Peru	Herminia	WR kaolinite	MH	J.A. Deen	-75				13.4	
420 v. 2NW T34W	Julcani, Peru	Herminia	WR kaolinite	MH	J.A. Deen	-70				14.8	
300 Pozo 258-20	Julcani, Peru	Herminia	kaolinite	vein	J.A. Deen	-90				7.8	
266-629	Summitville, CO	Chandler	alunite	MH	R.E. Stoffregen		10.5		21.8		
255-692	Summitville, CO	Chandler	pyrite	MH	R.E. Stoffregen				-3.0		
266-716	Summitville, CO	Cu-Hill	alunite	MH	R.E. Stoffregen		11.6		21.4		
266-716	Summitville, CO	Cu-Hill	pyrite	MH	R.E. Stoffregen				-8.1		
281-401	Summitville, CO	Del Norte	alunite	MH	R.E. Stoffregen	-70	11.0	9.5	21.3		>600
281-401	Summitville, CO	Del Norte	pyrite	MH	R.E. Stoffregen				-3.6		
289-406	Summitville, CO	W. End	alunite	MH	R.E. Stoffregen	-46	16.3	12.1	22.1		440
289-406	Summitville, CO	W. End	pyrite	MH	R.E. Stoffregen				-7.6		
328-108	Summitville, CO	Annie	alunite	MH	R.E. Stoffregen	-65	9.9	5.7	13.4		440
332-126	Summitville, CO	N. Tweks.	alunite	MH	R.E. Stoffregen	-39	13.1	10.5	22.7		>600
14-2667	Summitville, CO	Iowa	alunite	MH	R.E. Stoffregen	-63	10.5	10.5	13.5		>600
14-2667	Summitville, CO	Iowa	pyrite	MH	R.E. Stoffregen				-2.2		
84-2	Summitville, CO	Annie	alunite	MH	R.E. Stoffregen	-64	11.4		18.8		
257-163	Summitville, CO	Annie	alunite	MH	R.E. Stoffregen		8.0				
293-40	Summitville, CO	N. Tewks.	alunite	MH	R.E. Stoffregen		13.6		20.7		
293-175	Summitville, CO	N. Tewks.	alunite	MH	R.E. Stoffregen		12.5		19.4		
84-9-014	Summitville, CO	Del Norte	alunite	MH	R.E. Stoffregen	-43	14.7	14.2	24.5		>600
84-9-050	Summitville, CO	Del Norte	alunite	MH	R.E. Stoffregen		11.6		18.2		
Sum 12	Summitville, CO	Dump	alunite	MH	R.E. Stoffregen		10.6		20.5		
Sum 1	Summitville, CO	Dump	alunite	MH	R.E. Stoffregen		13.0		24.2		
SUM D W(88)(4)	Summitville, CO	Science	alunite	MH	P.M. Bethke and R.O. Rye	-50	9.8	8.0	21.0		>600
SUM D W(88)(6)	Summitville, CO	Science	alunite	MH	P.M. Bethke and R.O. Rye	-40	12.5	10.7	24.6		>600
1-88A	Summitville, CO	Science	alunite	MH	P.M. Bethke and R.O. Rye	-46	13.4	8.6			320
SUM G W 88 (1)	Summitville, CO	Science	kaolinite	MH	P.M. Bethke and R.O. Rye	-62					
SUM D W 88 (3)	Summitville, CO	Science	kaolinite	MH	P.M. Bethke and R.O. Rye	-60					
SUM D W 88 (5)	Summitville, CO	Science	kaolinite	MH	P.M. Bethke and R.O. Rye	-62				11.5	
SUM F W 88 10MIC	Summitville, CO	Science	kaolinite	MH	P.M. Bethke and R.O. Rye	-62					
SUM G W 88 (2)	Summitville, CO	Science	kaolinite	MH	P.M. Bethke and R.O. Rye	-61					
SUM I W 88 (1)	Summitville, CO	Science	kaolinite	MH	P.M. Bethke and R.O. Rye	-64					
SUM I W 88 (2)	Summitville, CO	Science	kaolinite	MH	P.M. Bethke and R.O. Rye	-83				11.6	
84-9-227	Summitville, CO	Del Norte	pyrite	MH	R.E. Stoffregen				-3.0		
86-SC-14A	Rodalquilar, Spain	Caldera complex	alunite 1	MH	A. Arribas	-16	16.5		30.0		
86-SC-14B	Rodalquilar, Spain	Caldera complex	alunite 1	MH	A. Arribas		17.9		28.7		
87A150	Rodalquilar, Spain	Caldera complex	alunite 1	MH	A. Arribas	-20	16.7	12.0	31.0		350
87A150	Rodalquilar, Spain	Caldera complex	pyrite 1	MH	A. Arribas				5.9		
87A237	Rodalquilar, Spain	Caldera complex	alunite 1	MH	A. Arribas	-24	18.7		29.3		
87A111	Rodalquilar, Spain	Caldera complex	alunite 1	MH	A. Arribas	-23	13.9	10.1	28.8		530
87A111	Rodalquilar, Spain	Caldera complex	pyrite 1	MH	A. Arribas				5.7		
87A110	Rodalquilar, Spain	Caldera complex	alunite 1	MH	A. Arribas	-26	10.8		26.5		
87A110	Rodalquilar, Spain	Caldera complex	pyrite 1	MH	A. Arribas				6.5		

87A225	Rodalquilar, Spain	Caldera complex	alunite 1	MH	A. Arribas	-15	17.7		30.2		
87A187	Rodalquilar, Spain	Caldera complex	alunite 1	MH	A. Arribas	-26	17.3		30.6		
87A120	Rodalquilar, Spain	Caldera complex	alunite 1	MH	A. Arribas	-19	11.7		22.3		
87A120	Rodalquilar, Spain	Caldera complex	pyrite 1	MH	A. Arribas				4.9		
88A06	Rodalquilar, Spain	Caldera complex	alunite 1	MH	A. Arribas		15.2	10.5			350
87A254	Rodalquilar, Spain	Caldera complex	kaolinite 1	MH	A. Arribas	-39				15.6	
87A165	Rodalquilar, Spain	Caldera complex	kaolinite 1	MH	A. Arribas	-36				14.9	
88A20	Rodalquilar, Spain	Caldera complex	alunite 2	SG	A. Arribas		8.2	8.7			
87A83	Rodalquilar, Spain	Caldera complex	alunite 2	SG	A. Arribas		7.0		7.0		
87A84	Rodalquilar, Spain	Caldera complex	alunite 2	SG	A. Arribas		7.6		6.1		
87A67	Rodalquilar, Spain	Caldera complex	alunite 2	SG	A. Arribas	-23	9.2		8.5		
87A36f	Rodalquilar, Spain	Caldera complex	alunite 2	SG	A. Arribas	-18	9.2		8.4		
87A363	Rodalquilar, Spain	Caldera complex	alunite 2	SG	A. Arribas	-37	7.7		7.0		
87A373	Rodalquilar, Spain	Caldera complex	alunite 2	SG	A. Arribas	-26	6.1	9.4	6.7		
87A111.2	Rodalquilar, Spain	Caldera complex	alunite 2	SG	A. Arribas	-25	8.3	10.3	7.1		
87A97	Rodalquilar, Spain	Caldera complex	alunite 2	SG	A. Arribas	-20	7.1	9.4	8.2		
87A298	Rodalquilar, Spain	Caldera complex	alunite 2	SG	A. Arribas	-20	7.1		6.7		
87A82	Rodalquilar, Spain	Caldera complex	alunite 2	SG	A. Arribas	-24	7.4				
87A380	Rodalquilar, Spain	Caldera complex	alunite 2	SG	A. Arribas	-35	8.2		7.8		
86A32	Rodalquilar, Spain	Caldera complex	alunite 2	SG	A. Arribas	-24	4.2	11.7	5.6		
S1m47	Rodalquilar, Spain	Caldera complex	alunite 2	SG	A. Arribas	-23	6.2		6.1		
87A31A	Rodalquilar, Spain	Caldera complex	alunite 2	SG	A. Arribas	-25	6.7		8.9		
87A40	Rodalquilar, Spain	Caldera complex	alunite 2	SG	A. Arribas		4.8				
87A21	Rodalquilar, Spain	Caldera complex	alunite 2	SG	A. Arribas	-28	7.6	14.4	8.1		
86-SC-12A	Rodalquilar, Spain	Caldera complex	alunite 2	SG	A. Arribas	-48	7.4		8.6		
86-SC-12B	Rodalquilar, Spain	Caldera complex	alunite 2	SG	A. Arribas		4.9		7.5		
1985 RR 1	Rodalquilar, Spain	Caldera complex	alunite 2	SG	A. Arribas		5.7		8.4		
1985 RR 2	Rodalquilar, Spain	Caldera complex	alunite 2	SG	A. Arribas		10.4		7.2		
1985 RR 3	Rodalquilar, Spain	Caldera complex	alunite 2	SG	A. Arribas		4.1		6.8		
87A51	Rodalquilar, Spain	Caldera complex	kaolinite 2	SG	A. Arribas	-72				17.2	
88BA40	Rodalquilar, Spain	Caldera complex	kaolinite 2	SG	A. Arribas	-66				19.5	
88A43	Rodalquilar, Spain	Caldera complex	kaolinite 2	SG	A. Arribas	-61				16.0	
88A61	Rodalquilar, Spain	Caldera complex	kaolinite 2	SG	A. Arribas	-41				21.2	
88A63b	Rodalquilar, Spain	Caldera complex	kaolinite 2	SG	A. Arribas	-42					
ES-7486V	El Salvador, Chile	Vug in pyroclastic	alunite	SG	Field and Gustafson, 1976	-56	10.1	6.4	*3.3*		
ES-1450	El Salvador, Chile	Pebble dike	alunite	SG	Field and Gustafson, 1976	-56	11.3	5.6	*3.6*		
ES-8233	El Salvador, Chile	"X" porphyry	alunite	SG	Field and Gustafson, 1976	-57	5.8	11.5	*-1.5*		
ES-6573	El Salvador, Chile	Pebble dike	alunite	MH	Field and Gustafson, 1976	-48	6.6	2.3	*14.8*		400
ES-5827	El Salvador, Chile	Rhyolite	alunite	MH	Field and Gustafson, 1976	-43	7.5	3.8	*17.0*		590
ES-1855	El Salvador, Chile	Andesite	kaolinite	SG	Sheppard and Gustafson, 1976	*-96*				*12.4*	
ES-6	El Salvador, Chile	"L" Porphyry	kaolinite	SG	Sheppard and Gustafson, 1976	*-99*				*15.1*	
ES-8	El Salvador, Chile	"L" Porphyry	kaolinite	SG	Sheppard and Gustafson, 1976	*-87*				*15.0*	
BN-2-268	National Dist. NV	Buckskin Mine	alunite	SH	Vikre, 1987	-99	13.8	5.1	-2.8		90
BN-2-297	National Dist. NV	Buckskin Mine	alunite	SH	Vikre, 1987	-97	13.7	4.5	-2.9		80
CN-82-62A	Viriginia Range, NV	Occidental Lode	alunite	MH	Vikre et al., 1988	-104	10.6	4.1	21.0		180

CNS-84-7	Viriginia Range, NV	Comstock Lode	alunite	MH	Vikre et al., 1988	-105	5.2	6.9	21.0		>600
VC-84-5B	Viriginia Range, NV	Geiger Grade	alunite	MH	Vikre et al., 1988	-78	11.9	7.4	18.7		370
VC-85-17	Viriginia Range, NV	Up Lousetown Ck.	alunite	MH	Vikre et al., 1988	-83	6.0		18.0		
VC-84-11A	Viriginia Range, NV	Long Valley	alunite	MH	Vikre et al., 1988	-86	5.9	.2	3.7		230
RC-84-3	Viriginia Range, NV	Ramsey	alunite	MH	Vikre et al., 1988	-90	8.6		22.4		
G7-38.2	GoldField, NV	Main district	alunite	SG	R. Ashley	-91	3.2	3.2	2.8		
P3-15	GoldField, NV	Main district	alunite	SG	R. Ashley	-90	3.2		2.9		
R9-25	GoldField, NV	Main district	alunite	MH	R. Ashley	-122	4.9	.8	28.1		230
LC-1-214k	Lake City, CO	Red Mtn.	alunite 1	MH	D.J. Bove	-72	8.1	-.1	10.2		100
LC-1-214a	Lake City, CO	Red Mtn.	alunite 1	MH	D.J. Bove	-82	7.0	.7	8.4		190
LC-1-72b	Lake City, CO	Red Mtn.	alunite 1	MH	D.J. Bove	-70	7.1	.6	9.2		180
LC-1-72a	Lake City, CO	Red Mtn.	alunite 1	MH	D.J. Bove	-85	6.0	1.3	10.3		350
Tqr2#1	Lake City, CO	Red Mtn.	alunite 1	MH	D.J. Bove	-76	9.2	.9	8.9		100
LC 448	Lake City, CO	Red Mtn.	pyrite 1	MH	D.J. Bove				-8.1		
LC-3-119	Lake City, CO	Red Mtn.	alunite 2	MH	D.J. Bove	-75	10.3	4.5	19.7		370
LC-3-120	Lake City, CO	Red Mtn.	alunite 2	MH	D.J. Bove		12.8	5.5	24.9		130
LC-2-129a	Lake City, CO	Red Mtn.	alunite 2	MH	D.J. Bove	-66	13.7	5.9	23.4		110
LC-2-129c	Lake City, CO	Red Mtn.	alunite 2	MH	D.J. Bove		13.9	5.7	27.2		100
LC-1-95	Lake City, CO	Red Mtn.	alunite 2	MH	D.J. Bove	-81	9.9	5.4	17.6		370
LC-2-448	Lake City, CO	Red Mtn.	pyrite 2	MH	D.J. Bove				-5.8		
LC-2-475	Lake City, CO	Red Mtn.	pyrite 2	MH	D.J. Bove				-7.0		
LC-3-154	Lake City, CO	Red Mtn.	alunite 3	MS	D.J. Bove	-78	10.3	1.5	-3.3		80
LC-3-0-20	Lake City, CO	Red Mtn.	alunite 3	MS	D.J. Bove	-84	10.7	2.4	-3.9		100
LC-3-191	Lake City, CO	Red Mtn.	alunite 4	MS	D.J. Bove	-81	8.7	.5	.1		100
LC-3-198A	Lake City, CO	Red Mtn.	alunite 4	MS	D.J. Bove	-86	8.7	1.7	.1		150
LC-4-1207	Lake City, CO	Red Mtn.	kaolinite	MH	D.J. Bove	-130					
LC-4-1380	Lake City, CO	Red Mtn.	kaolinite	MH	D.J. Bove	-137					
LC-4-470	Lake City, CO	Red Mtn.	sericite	MH	D.J. Bove	-115					
LC 4-1910-20	Lake City, CO	Red Mtn.	sericite	MH	D.J. Bove	-108					
M-341	Alunite Ridge, UT	Christmas mine	alunite	MS	Cunningham et al., 1984	-83	9.4	.6	*-2.1*		80
M938A	Alunite Ridge, UT	L&N	alunite	MS	Cunningham et al., 1984	-82	11.0	.2	*-1.9*		40
M938B	Alunite Ridge, UT	L&N	alunite	MS	Cunningham et al., 1984	-85	8.7		*-1.5*		
M939	Alunite Ridge, UT	Mineral Products	alunite	MS	Cunningham et al., 1984	-87	8.6	2.6	*.8*		200
CAC 001	Cactus, CA	Winkler pit	kaolinite	SH	P.M. Bethke and R.O. Rye	-112					
CAC Box Car	Cactus, CA	Box Car Canyon	alunite	MS	P.M. Bethke and R.O. Rye		14.0	6.5	-.3		130
CAC 017	Cactus, CA	Box Car Canyon	alunite	MS	P.M. Bethke and R.O. Rye	-67	11.9	4.1	-1.0		110
CAC 035-1	Cactus, CA	Winkler Undergrnd.	alunite	MS	P.M. Bethke and R.O. Rye	-63	10.0	2.7	1.4		130
CAC 025	Cactus, CA	Winkler Undergrnd.	alunite	MS	P.M. Bethke and R.O. Rye	-62	8.7	1.7	2.7		150
CAC 027	Cactus, CA	Winkler Undergrnd.	kaolinite	SH	P.M. Bethke and R.O. Rye	-95				14.0	
CAC 037	Cactus, CA	Winkler Undergrnd.	kaolinite	SH	P.M. Bethke and R.O. Rye	-103				11.2	
CAC 037 fine	Cactus, CA	Winkler Undergrnd.	alunite	MS	P.M. Bethke and R.O. Rye		9.5	5.2			400
CAC 038B	Cactus, CA	Eagle Mountain	alunite	MS	P.M. Bethke and R.O. Rye	-54	11.8	4.3	2.1		130

SG = supergene; MH = magmatic-hydrothermal; SH = steam-heated; MS magmatic-steam; Italics indicate data from published sources
Temperatures (°C) calculated from $\Delta^{18}O_{SO4\text{-}OH}$ values using experimentally derived equation, $1000\ln\alpha_{\text{alunite } SO4\text{-}OH} = 0.8\times10^6T^{-2} + 2.8$ (Stoffregen et al., 1989)